

UHABS-6

Critical Design Review

Team Makahiki Wai

CDR-F18-S2-P1

Department of Mechanical Engineering
University of Hawaii at Manoa
December 3, 2018



MEMBERS & Participation %

Christian Feria [CF] 6.31%

Ian Fujitani [IF] 9.01%

Bryson Inafuku [BI] 11.71%

Jacob Keomaka [JK] 25.23%

Austin Quach [AQ] 9.01%

Trevor Shimokusu [TS] 11.71%

Reginald Tolentino [RT] 15.32%

Akira Yokoyama [AY] 11.71%

Submitted To:

Dr. Trevor C. Sorensen

Department of Mechanical Engineering, University of Hawaii at Manoa

ACKNOWLEDGEMENTS

- ❖ Dr. Trevor C. Sorensen
- ❖ Dr. A Zachary Trimble
- ❖ Dr. Zhuoyuan Song
- ❖ Dr. Marvin Young
- ❖ Saeed Karimi
- ❖ Hawaii Space Flight Laboratory
- ❖ University of Hawaii at Manoa - Dept. of Mechanical Engineering



CDR Scoring Table

Section	Max	Score
Executive Summary	5	
Introduction	3	
Technical Overview	60	
Management & Cost Overview	10	
Conclusion	2	
Appendices	10	
Overall Quality, Conciseness, and Effectiveness	5	
Compliance	5	
Total	100	

EXECUTIVE SUMMARY

[JK]

The University of Hawaii Advance Balloon Satellite 6 (UHABS-6) will be the second BalloonSat project to be executed as an ME 481/482 senior design project. The UHABS-6 team consists of seven mechanical engineering students and one electrical engineering student. Dissimilar from the 3-month time frame in the ME 419 Astronautics BalloonSat project, the UHABS-6 team shall have a full academic year to design, build, test, and launch a fully functional BalloonSat. With the UHABS-6 team's increased time frame to complete the project, the University of Hawaii at Manoa (UHM) BalloonSat Program has made an additional requirement for this year's BalloonSat team to incorporate a reliable autonomous recovery system to help ensure safe recovery of the BalloonSat modules if it were to land in either Oahu's ocean or mountainous terrain.

The success of the UHABS-6 mission relies heavily on the recovery of the BalloonSat modules after launch as specified in the mission statement:

“The UHABS-6 team will successfully develop a high altitude BalloonSat system capable of carrying small payloads in a near-space environment, while flight testing the Comprehensive Solution for Mission Operations Systems (COSMOS) mission operations software, and return safely to Earth for intact recovery. A recovery system will be incorporated into the BalloonSat system that upon landing in the ocean will be programmed to autonomously propel itself to a designated recovery site for recovery.”

Due to the importance of the recovery, the UHAB-6 team must ensure that the design, operations, and capabilities of the autonomous recovery system meet the objectives and success criteria of the mission. To fulfill these requirements and constraints, the design concept of UHABS-6 primarily focuses on the recovery vehicle and propulsion system. The major trade studies to develop the design concept for the recovery vehicle and propulsion system involved researching successfully developed and water-related unmanned autonomous vehicles (UAV). Using systems engineering techniques, such as pugh matrix analyses, to compare the different designs of UAVs, the UHABS-6 team will be able to develop an autonomous recovery vehicle with a wave-power propulsion system design concept.

The major subsystems of UHABS-6 are: Balloon/C&C Module (BCCM), Recovery Vehicle & Propulsion System (RVP), and Ground Station (GS). The BCCM subsystem is responsible for the electronics and sensors being interfaced in the autonomous recovery vehicle, and also is responsible for the flight system of the BalloonSat. These electronics and sensors will allow the BalloonSat module, or autonomous recovery vehicle, to perform autonomous navigation, collecting environmental & engineering data, collect images, and stream live-video to the GS. The RVP subsystem is responsible for recovery vehicle, propulsion/steering system, and power system. The GS subsystem is responsible for communications, COSMOS integration, and launch operations. These components will allow the GS to receive data/video from BCCM, and uplink commands to the BCCM through the use of COSMOS. Base off their component selection, the current system budget for mass, volume, and power are: 6.8 lbs, 45 in³, and 22 watts.

The internal interfaces of the UHABS-6 subsystems is centralized by the BCCM subsystem. The BCCM subsystem physically interfaces with the RVP subsystem, and wirelessly interfaces with the GS subsystem. Through physical interfacing, the BCCM subsystem mounts all avionics to the internal housing of the autonomous recovery vehicle design of the RVP subsystem, and also interfaces the flight system components such as the balloon, parachute, and FTMs to the

autonomous recovery vehicle. In addition, the RVP subsystem provides electrical power to the electrical components of the BCCM subsystem. The wirelessly interface of the BCCM and GS subsystem involves the communication relay of data, video, and command signals. The primary external interfaces affecting the UHABS-6 subsystem is centralized by the GS subsystem. The external interfaces affecting the GS subsystem are user input, predicted winds and ocean currents, and providing mission results to Hawaii Space Flight Laboratory (HSFL).

Since the Preliminary Design Review (PDR), the conceptual design of the autonomous recovery vehicle has evolved and changed to better meet the technical, operational, and behavior requirements of the mission. The key components that were changed from the conceptual design of the autonomous recovery vehicle were the hull and the propulsion system.

For the hull, the RVP altered the flat-hull design to a catamaran shape. The catamaran hull shape allows the recovery vehicle to be more mobile as the double-hull structure cuts through the water better than a flat-hull, while maintaining the necessary wave pitch required to produce forward-thrust with the oscillating fin. To protect the oscillating fin and rudder from landing impact, the catamaran hull shape is adjusted to be more rounded to make the recovery vehicle to be self-righting, or resistant to capsizing, so the recovery vehicle can be landed on its side, shielding both the rudder and oscillating fin during landing impact. In this report, the principles of the oscillating fin are proven and test show that the oscillating fin generates enough thrust to overcome waves. Furthermore, the auxiliary propulsion from the conceptual design was removed to improve weight and reduce power consumption.

The BCCM subsystem has finalized their electrical components to meet the operational requirements during both flight and recovery phases of the mission. The BCCM subsystem team was able to determine the required high-altitude balloon and parachute size through kinematic analysis. As mentioned above, the RVP subsystem have modified the hull and propulsion system to improve the overall performance of the recovery vehicle. The RVP subsystem team finalized the layout of internal and external C&C module components, and finalized hardware necessary to assemble the propulsion and steering system to the recovery vehicle. Also, the team conducted analyses on the oscillating fin, solar panels, batteries, rudder, and the hull. The Ground Station has finalized their components for their communications and identified how the COSMOS integrates and interacts with the BCCM subsystem. A RF analysis was conducted the proposed-on RF and video transmitter and receiver sets, and prove that in the perfect conditions, the Ground Station will be able to maintain communications with the BalloonSat during the entire mission.

Based off of the subsystem's final component selection, the total financial budget with 20% margin is \$2,370. With the current source of funding from UHM Mechanical Engineering Department at \$2000, the difference comes out to be \$370, which must be covered from other forms of funding. The all UHABS-6 team members agreed and plans to personally fund the remaining \$370 by splitting the cost amongst the 8 members.

TABLE OF CONTENTS

1.0 Introduction	1
2.0 Technical Overview	3
2.1 Objectives and Requirements	3
2.1.1 Mission Statement	3
2.1.2 Objectives and Success Criteria	3
2.2 Conceptual and Basic Designs	4
2.3 Detailed Design	9
2.3.1 Top Level System	9
2.3.1.1 System Architecture	9
2.3.1.2 Concept of Operations (CONOPs)	10
2.3.1.3 Top-level Functional Flow Block Diagram	11
2.3.1.4 Overall configuration	12
2.3.1.5 Performance Analyses	15
2.3.1.6 System FMECA	16
2.3.1.7 Safety Engineering	17
2.3.1.8 Fabrication Plan	17
2.3.1.9 Integration & Test Plan	18
2.3.1.10 Human Factors Engineering/Accessibility & Maintainability	20
2.3.1.11 System Weight & Volume Budgets	21
2.3.1.12 System Level Power Budget and Power Profile	21
2.3.2 Subsystems	22
2.3.2.1 Balloon and Command & Control Module	22
2.3.2.1.1 Subsystem Team Roles & Responsibilities	22
2.3.2.1.2 Changes in subsystem design since PDR	23
2.3.2.1.3 BCCM Functional (Flow) Block Diagram	23
2.3.2.1.4 Subsystem Weight & Volume Budgets	24
2.3.2.1.5 Subsystem Power Budget	24
2.3.2.1.6 Description	26
2.3.2.1.6.1 Parts Description	26
2.3.2.1.6.2 Component layout	28
2.3.2.1.6.3 Software Description	29
2.3.2.1.7 Results of Technical Analyses	31
2.3.2.1.7.1 High Altitude Balloon Analysis	31
2.3.2.1.7.2 Parachute Size Analysis	33
2.3.2.1.7.3 FTM Analysis	34
2.3.2.1.8 Risk Analysis	34
2.3.2.1.9 Subsystem FMECA and Fault Tree	35
2.3.2.1.10 Detailed Test Plan	36
2.3.2.1.11 Subsystem WBS	38

2.3.2.1.12 Subsystem Schedule WBS and Gantt Chart	38
2.3.2.1.13 Requirements vs. Implementation	39
2.3.2.1.14 Remaining Issues and Concerns	39
2.3.2.2 Recovery Vehicle and Propulsion	40
2.3.2.2.1 Subsystem Team Roles & Responsibilities	40
2.3.2.2.2 Changes in subsystem design since PDR	40
2.3.2.2.3 RVP Functional (Flow) Block Diagram	41
2.3.2.2.4 Subsystem Weight & Volume Budgets	41
2.3.2.2.5 Subsystem Power Budget	42
2.3.2.2.6 Description	42
2.3.2.2.7 Results of Technical Analyses	44
2.3.2.2.7.1 Hull Thermal Analyses	44
2.3.2.2.7.2 Hull Stability	45
2.3.2.2.7.3 Structures and Fin FEA	46
2.3.2.2.7.4 Propulsion and Steering Analysis	50
2.3.2.2.7.5 Battery Operation Time	53
2.3.2.2.7.6 Solar Panel Analysis	55
2.3.2.2.8 Risk Analysis	56
2.3.2.2.9 Subsystem FMECA and Fault Tree	57
2.3.2.2.10 Detailed Test Plan	59
2.3.2.2.11 Subsystem WBS	60
2.3.2.2.12 Subsystem Schedule WBS and Gantt Chart	60
2.3.2.2.13 Requirements vs. Implementation	61
2.3.2.2.14 Remaining Issues and Concerns	61
2.3.2.3 Ground Station	62
2.3.2.3.1 Subsystem Team Roles & Responsibilities	62
2.3.2.3.2 Ground Segment Architecture	62
2.3.2.3.3 Changes in subsystem design since PDR	63
2.3.2.3.4 GS Functional (Flow) Block Diagram	63
2.3.2.3.5 Detailed description	64
2.3.2.3.6 Subsystem Integration Plan	64
2.3.2.3.7 Software flowchart	65
2.3.2.3.8 COSMOS Architecture	66
2.3.2.3.9 Results of Analyses - Signal Reliability	66
2.3.2.3.10 Risk Analysis	69
2.3.2.3.11 Results of FMECA and Reliability Analysis	70
2.3.2.3.12 Site Selection	71
2.3.2.3.13 Flight Path Estimations	72
2.3.2.3.14 Detailed Testing Plan	73
2.3.2.3.15 Requirements vs Implementation Table	74

2.3.2.3.16 Subsystem WBS	74
2.3.2.3.17 Subsystem Schedule WBS and Gantt Chart	75
2.3.2.3.18 Remaining Issues and Concerns	75
3.0 Management and Cost Overview	75
3.1 Team Organizational Chart	75
3.2 Project Work Breakdown Structure	76
3.3 System-level Schedule	77
3.4 Hardware Acquisition Status/Plan	78
3.5 Risks Management	79
3.6 Configuration and Change Management	80
3.7 Financial Budget	80
3.8 Documentation List	82
3.9 Remaining Issues and Concerns	83
4.0 Conclusion	84
References	85
Appendices	A

LIST OF FIGURES AND TABLES

Figures

Figure 1	Conceptual Design of Autonomous Recovery Vehicle	7
Figure 2	Current Design of Autonomous Recovery Vehicle	8
Figure 3	Mission Operational System Architecture	9
Figure 4	Concept of Operations	10
Figure 5	Overall System Functional Flow Block Diagram	11
Figure 6	System Level External View	12
Figure 7	System Level Internal View	13
Figure 8	Camera Angle Views	13
Figure 9	Autonomous Vehicle Dimensions	14
Figure 10	Exploded View of Recovery Vehicle	15
Figure 11	System Level Safety Engineering	17
Figure 12	System Level Integration Plan	18
Figure 13	System Accessibility/Human Factor Engineering	20
Figure 14	System Maintainability	20
Figure 15	Power Profile of UHABS-6	22
Figure 16	BCCM Functional Flow Block Diagram	23
Figure 17	Power and energy usage for flight and recovery during a simulated operation	25
Figure 18	Internal layout of C&C module inside the recovery vehicle	28
Figure 19	External view of C&C parts on the recovery vehicle	29
Figure 20	C&C Module Programming Flow Diagram	30
Figure 21	Programming Flow of Balloon Release FTM	31
Figure 22	Programming Flow of Parachute Release FTM	31
Figure 23	Kaymont 1200g Initial Volume to Burst Altitude	32
Figure 24	Kaymont 1200g Initial Volume to Ascent Velocity	33
Figure 25	BCCM Flight Fault Tree	36
Figure 26	BCCM Recovery Fault Tree	36
Figure 27	WBS of BCCM	38
Figure 28	BCCM Combined WBS and Gantt Chart with progress	38
Figure 29	RVP Functional Flow Block Diagram	41
Figure 30	Power System Diagram	43
Figure 31	Center of gravity location on recovery vehicle	45
Figure 32	Center of buoyancy location on recovery vehicle with water-line indicator	45
Figure 33	FEA Drop Test Simulation on Front Face	46
Figure 34	FEA Drop Test Simulation on Side Face	46
Figure 35	FEA Drop Test Simulation on Corner Face	47
Figure 36	FEA Drop Test Simulation on Bottom Face	47
Figure 37	FEA results of the fin during a bottom impact	49

Figure 38	FEA results of the fin during a side impact	49
Figure 39	Illustration of the oscillating fin during a wave upstroke	51
Figure 40	Predicted speeds of advance for a sea state 2 and sea state 6	52
Figure 41	Image of the servo linkage that will control steering	53
Figure 42	Fault tree analysis for RVP	58
Figure 43	WBS for RVP	60
Figure 44	Gantt Chart with integrated WBS	60
Figure 45	Ground Segment Architecture	62
Figure 46	Ground Station Functional Flow Block Diagram	63
Figure 47	Ground Station Software Flowchart	65
Figure 48	Ground Station COSMOS Architecture	66
Figure 49	Ground Station Fault Tree	70
Figure 50	Possible Site Selections	71
Figure 51	Possible Wind & Ocean Current Simulator	71
Figure 52	Flight Path Estimation for Kokololio Beach Park	72
Figure 53	Flight Path Estimation for Hukilau Beach Park	72
Figure 54	Flight Path Estimation for Swanzy Beach Park	72
Figure 55	Ground Station WBS	74
Figure 56	Gantt Chart with integrated WBS	75
Figure 57	UHABS-6 Team Organizational Chart	76
Figure 58	UHABS-6 Work Breakdown Structure	77
Figure 59	UHABS-6 System Level Gantt Chart	78
Figure 60	System Financial Budget	81

Tables

Table 1	Second Pugh matrix of Design Concepts (UAV)	6
Table 2	System FMECA	16
Table 3	System Test Plan for Autonomous Recovery Vehicle	19
Table 4	System Test Plan for Data Transmission	19
Table 5	System Weight & Volume Budget	21
Table 6	Power Budget	21
Table 7	Changes in BCCM Subsystem Design Since PDR	23
Table 8	BCCM Mass and Volume Budget	24
Table 9	BCCM Power Requirements	25
Table 10	BCCM Break down of Power, Energy, and Duration of Simulated Operation	26
Table 11	Parts list for C&C	26
Table 12	Parts List for Flight System and FTM	27
Table 13	BCCM Subsystem Risk Management	34
Table 14	FMECA of BCCM subsystem	35
Table 15	Mass and volume budget for RVP	41

Table 16	Parts list for RVP	42
Table 17	Summary of maximum heat losses during flight	44
Table 18	Von Mises Stress and Displacement Summary FEA Drop Test Simulation	47
Table 19	Electrical Power Consumption During Each Operational Phase	54
Table 20	Risk Analysis for RVP	56
Table 21	FMECA for RVP	57
Table 22	Detailed testing plan for RVP	59
Table 23	Parts list for Ground Station	64
Table 24	XTend 900 RF Signal Reliability Under Ideal Conditions and Ideal Gain	67
Table 25	Video Transmitter Signal Reliability Under Ideal Conditions and Ideal Gain	67
Table 26	Risk Analysis for Ground Station	69
Table 27	FMECA for Ground Station	70
Table 28	Detailed Testing Plan for Ground Station	73
Table 29	Component List Per Subsystem	79
Table 30	Project Management Risk Analysis	79
Table 31	Change Management Log	80
Table 32	Financial Summary	81

GLOSSARY

BCCM	Balloon/Command & Control Module
COSMOS	Comprehensive Open-Architecture Solution for Mission Operations Systems
C&C	Command and Control
FAA	Federal Aviation Administration
FEA	Finite Element Analysis
FMECA	Failure Mode, Effects & Criticality Analysis
FTM	Flight Termination Mechanism
HSFL	Hawaii Space Flight Laboratory
GS	Ground Station
IMU	Inertial Measurement Unit
MPPT	Maximum Power Point Tracking
PM	Project Manager
PA	Project Administrator
RF	Radio Frequency
RPN	Risk Priority Number
RVP	Recovery Vehicle & Propulsion System
SI	System Integrator
UAV	Unmanned Autonomous Vehicle
UHABS-6	University of Hawaii Advance Balloon Satellite 6
UHM	University of Hawaii at Manoa
WBS	Work Breakdown Structure

1.0 Introduction

[JK]

BalloonSat launches have become a means for many organizations to quickly deploy low-cost instrumented vehicles to collect data, test hardware & software, and perform other miscellaneous tasks in the near-space environment. The HSFL at UHM has taken interest in BalloonSat projects to test their components, sub-assemblies, instrumentation, software, and procedures to aid their missions, and has requested the help of the UHM BalloonSat Program, initiated by Dr. Sorensen, to develop a reliable BalloonSat system. However, unlike the past BalloonSat launches that Dr. Sorensen has conducted in Kansas, BalloonSat launches in Oahu have a high probability of landing in the ocean or mountainous terrain. This factor causes the retrieval of the BalloonSat modules to be difficult and costly especially if the BalloonSat module becomes damaged and/or is not recovered. Therefore, there is not only a need for a reliable BalloonSat that can perform their specific duties and survive the entire flight intact but also a need for a reliable recovery system that enables ocean landing and autonomous unmanned capabilities for efficient recovery.

With the addition of meeting the design requirements of the HSFL and UHM BalloonSat Program, BalloonSat launches and designs must adhere to the rules and regulations of the Federal Aviation Administration (FAA). The rules and regulations for an unmanned balloon-satellite system can be found in Title 14, Chapter 1, Subchapter F, Part 101, Subpart D [1]. These rules and regulations are placed by the FAA to create a safe, efficient airspace. Violation of these laws and regulations may result in damage to equipment and/or civilians, therefore the design of the balloon-satellite system will need to adhere to those designated constraints.

The predecessors of UHABS projects all shared a similar mission of developing a reliable high altitude BalloonSat to carry a small payload to the near-space environment and ensure intact recovery. These UHABS projects usually consist of a styrofoam enclosure payload, except UHABS-3 with a carbon fiber enclosure, and were all equipped with temperature and atmospheric sensors, an onboard camera, and GPS. However, only UHABS-3 and UHABS-5 had to incorporate an autonomous recovery system to enable landings on the ocean and autonomously propel itself to a designated recovery site. These missions had to include additional software and hardware, such as motors, propellers, etc.

The general operation procedure of past UHABS missions was to use helium-filled high-altitude balloons to lift the payload to a specific altitude or until balloon rupture. The payload modules then descended, at a specific speed, to ground level by a deployed parachute. The team would track and follow the payload module to the landing site, via GPS, for retrieval. In the case for UHABS-3 and UHABS-5, if the payload module should land in the ocean, the payload would autonomously propel itself to the designated recovery site. According to their final reports, only UHABS-1 and UHABS-4 successfully launched, but neither of those featured autonomous recovery [2][3].

The autonomous recovery systems of the two previous UHABS missions will influence the autonomous recovery system of UHABS-6. UHABS-3 created a single carbon fiber payload enclosure and applied a paddle wheel system to propel itself through the water [4]. UHABS-5 designed a catamaran styrofoam boat as their single payload enclosure and implemented propeller thrusters to propel itself through the water. Unfortunately, both of these UHABS mission was unsuccessful with their mission and were unable to create a reliable recovery system [4][5]. UHABS-3 proved to be a poor design as water was able to leak into the payload module, and was unable to perform necessary repairs on their broken paddle wheel system as the

enclosure could not be reopened after sealing it [4]. UHABS-5 was unable to perform their mission as time ran out due to being unable to fix or replace their electrical motor, which caused the boat/module to vibrate aggressively to the point that the payload module would not propel itself effectively [8]. In addition, these projects mention difficulty with communications between their payload and ground station and had difficulty with integrating COSMOS [4][5].

The UHABS program is not the only university program, or individual, seeking to develop autonomous recovery systems for BalloonSats. While working on his Ph.D. at Oklahoma State University in 2004, Dr. Seong-Jin Lee conducted intensive research to develop an autonomous recovery of BalloonSats through the use of parafoils to aid the Atmospheric and Space Threshold Research Oklahoma (ASTRO) program [6]. Dr. Lee's mission was to develop a cost-effective, simple, and reliable autopilot system which can be applied to the payload used in the ASTRO project [6]. The final report places a heavy focus on analyzing and modeling the dynamics of parafoils and developing a dynamic program, based on wind predictions, to optimize path-finding during flight [6]. To verify the application of the autonomous parafoil recovery system, Dr. Lee conducted flight simulations using a MatLab/Simulink program [6]. The results of the flight simulations were that the vehicle was able to track the desired path very well under no windy conditions [6]. However, the system took a few seconds to calculate the next waypoint and adjust itself to the correct path [6]. Under windy conditions, the vehicle exhibited signs of noisy movements but was able to stay on the desired pathways [6].

Similarly, other university BalloonSat programs are looking into developing an autonomous parafoil recovery system. Under the Stanford Student Space Initiative, Team Balloonerang from Stanford University has dedicated a parafoil team to fully develop a novel system that can steer the payload to a specified GPS location in hopes to facilitate ease of payload retrieval [7]. The Space Hardware Club from the University of Alabama Huntsville is currently working on multiple BalloonSat projects with one of them being their autonomous recovery system called RAPTOR [8]. From their website, Project RAPTOR is summarized as, "The Ram-Air Parafoil Targeted Object Return (RAPTOR) system is a payload designed for the simplification of high-altitude balloon payload recovery. The objective of the project is to minimize recovery costs for any high-altitude ballooning flight through autonomous targeted landings. RAPTOR is a low-cost, low-weight addition to any payload line, utilizing basic control algorithms, electronics, and commercially available parafoils [8]."

Unfortunately, an autonomous parafoil recovery system is not feasible to develop for the UHABS-6 team. The team lacks time and manpower to develop such a complex recovery system. From reading Dr. Seong-Jin Lee report on autonomous parafoil recovery systems, analyzing and modeling the dynamics of parafoils requires intense research and testing. In addition, to develop a dynamic program taking into account predicted winds would probably a dedicated team in itself, larger than the current 8-member UHABS-6 team. Also, it's not within the scope of the UHABS-6 mission.

With the likelihood of BalloonSats launches landing in the ocean of Oahu, the UHABS-6 team will research and develop autonomous underwater vehicles (AUV) or unmanned autonomous vehicles (UAV), such as boats, drones, and submarines, to use as a design concept for the autonomous recovery vehicle for the BalloonSat module.

2.0 Technical Overview

2.1 Objectives and Requirements

2.1.1 Mission Statement

[JK]

The UHABS-6 team will successfully develop a high altitude BalloonSat system capable of carrying small payloads in a near-space environment, while flight testing the Comprehensive Solution for Mission Operations Systems (COSMOS) mission operations software, and return safely to Earth for intact recovery. A recovery system will be incorporated into the BalloonSat system that upon landing in the ocean will be programmed to autonomously propel itself to a designated recovery site for recovery.

2.1.2 Objectives and Success Criteria

[JK]

ID	Primary Objectives
OBJ-01	To develop a reliable, high-altitude BalloonSat system capable of carrying small payloads to a near-space environment.
OBJ-02	To develop a recovery system which enables the BalloonSat module to safely land in the ocean or land.
OBJ-03	To develop a recovery system able to autonomously propel the payload to a designated recovery site if an ocean landing occurs.
OBJ-04	To utilize and test COSMOS as operations and flight software for the HSFL.
ID	Secondary Objectives
OBJ-05	To obtain images and video during the flight phase.
OBJ-06	To collect atmospheric and state-of-health data during the flight phase.

ID	Success Criteria
SC-01	UHABS-6 reaches and releases modules at the desired altitudes.
SC-02	The parachute deploys after module release to ensure a safe landing. The UHABS-6 modules are highly visible and labeled with contact information to improve recoverability.
SC-03	UHABS-6 modules are designed for ocean conditions and successfully test the autonomous recovery system in the ocean prior to launch.
SC-04	COSMOS successfully integrates the system of the UHABS-6 modules with the GS and perform mission operations.
SC-05	UHABS-6 modules successfully store on-board and transmit images and live-stream video to the GS.
SC-06	UHABS-6 modules successfully store data onboard and transmit data to GS.

2.2 Conceptual and Basic Designs

[JK]

The conceptual design of UHABS-6 primarily focused on the recovery vehicle and the propulsion system. UHABS-6 will meet all requirements and capabilities throughout the flight phase of the mission. However, the success of the UHABS-6 mission depends on the recovery of the BalloonSat module. Due to the importance of the recovery, the UHAB-6 team must ensure that the design, operations, and capabilities of the autonomous recovery system meets the all top-level system requirements and constraints. The major trade studies to develop the design concept for the recovery vehicle and propulsion system involved researching successfully developed and water-related unmanned autonomous vehicles (UAV).

While researching trades studies on UAVs, the UHABS-6 team held a dedicated team meeting to develop UAV criteria based on the customer's needs. Together, the team developed these UAV criteria to take into consideration when researching possible UAV designs:

- Lower cost: To minimize the budget required for developing the UAV.
- Complexity of code: The difficulty for the Ground Station team to program the UAV propulsion system to perform autonomous navigation.
- Power to Distance Ratio: The total distance traveled versus the amount of power consumption for the UAV.
- Weight: UAV weight approximation to meet the 6-lb module weight limit. Approximated by the major weight factors such as hull/structure design and number of required motors/propellers.
- Manufacturability: The difficulty to manufacture the UAV.
- Time to Manufacture: The required time to fully manufacture the UAV.
- Accessibility: The ability for the user to easily access any part in the UAV to conduct maintenance, fix, and/or replace in a timely manner.
- Travel Longevity: The durability of the UAV while traveling through the ocean environment.
- Survival Impact: The durability of the UAV to withstand the landing impact during the flight phase of the mission.
- Avionic Protection: The UAV ability to protect the avionics from water during the recovery phase of the mission.
- Resistance to Capsize: The UAVs ability to maintain upright orientation in the ocean environment.

With the list of criteria to consider for the design concept, the UHABS-6 team was able to filter the trades conducted by each member, which the team was able to narrow down their possible design concept to six choices:

1. Airboat: A airboat that propels through the water with the use of a large aircraft propeller above the water. The hull for airboats is usually flat-bottom. However, for the purpose of UHABS-6 mission, the team will consider other hull designs. An autonomous airboat was developed by a company called "Platypus, LLC." The UAV was designed for environmental monitoring, flood response, fish farming, and other applications [9].

2. Submarine: A long cylindrical, round-faced underwater vehicle shaped similar to a missile/torpedo. For the UHABS-6 mission, the submarine would be designed to only be half-submerged in the water. An autonomous underwater submarine was developed by Bluefin Robotics [10]. As described by a web article, the autonomous submarine would “perform military missions such as intelligence, surveillance and reconnaissance, anti-submarine warfare, mine countermeasures, port and harbor security, rapid environmental assessment, communications relay, mobile acoustic countermeasure and decoy, and unexploded ordnance discovery [10].”
3. Wave-Powered Boat: A surface vehicle that uses oscillating fins to convert vertical motion of waves into lift forces acting in the direction of advance. Many systems operating on this principle have been developed, such as the Wave Glider by Liquid Robotics and a Wave Devouring system by Tokai University [11] [12]. The boat propels through the water with underwater propellers on the main boat hull and an attached wave glider [12]. The wave glider is a separate boat-like structure with multiple oscillating fins, and remains a few feet below the boat [12]. These fins on the wave glider uses the ocean wave’s up-down motion to propel itself forward [12]. In addition, the wave glider has a propeller for extra thrust when needed [12]. The wave glider is attached, by a rubber-like tubing, to the bottom of the hull of the boat, and essentially pulls the boat forward [12]. Furthermore, when the boat depletes all battery power for the propellers, the wave glider can keep the boat moving while the solar panels recharge the batteries.
4. Seaplane: An aircraft which is able to land and takeoff on water. At the University of Michigan, their Autonomous Aerospace Systems Lab team successfully developed an autonomous seaplane called the Flying Fish [13].
5. Quadcopter with Landing Pad: A drone with 4 propellers designed to be light-weight and capable of carrying a payload. Similar to the “WaterStrider” from DroneRafts, the drone is equipped with a buoy-like land pads which allow the drone to safely land and takeoff in the water [14].

The UHABS-6 team decided that the best method to select a design concept was to conduct a Pugh selection method. The Airboat design was chosen as the baseline of comparison between the other possible design concepts due to its similarity to the UHABS-5 catamaran design. The rest of the possible designs stray away of a boat design and approaches ocean travel in a different way. The list of criteria was used to compare the baseline, the Airboat, to each of the other 5 possible designs. The UHABS-6 team discussed together how to weigh each criterion, and decided to use a 1-3-5 weighing scale.

The results of the Pugh matrix analysis (refer to Appendix) shows that the baseline, the Airboat, is the best design based on the current weightings and criteria. However, the UHABS-6 team decided to have their Pugh matrix analysis to be reviewed by Professor Marvin Young, a System Engineering course instructor at the University of Hawaii at Manoa. After reviewing the pugh matrix and providing a brief summary of the UHABS-6 mission, Professor Young suggested that there is missing a key criterion, Resistance to Capsizing. A second iteration of the Pugh matrix

analysis was conducted with the Resistance to Capsizing criteria with the appropriate weighting, as shown below in Table 1.

Table 1: Second Pugh matrix of Design Concepts (UAV)

Criteria	Weighting	Baseline (Airboat)	Submarine	Seaplane	Wave Power	Drone w/ Landing Pad
Lower Cost	1	0	-1	-1	-1	-1
Complexity of Code	5	0	0	0	0	-1
Power to Distance	3	0	-1	-1	1	-1
Weight	5	0	-1	-1	-1	1
Manufacturability	3	0	-1	-1	-1	-1
Time to Manufacture	5	0	-1	-1	-1	-1
Accessibility	3	0	-1	0	0	1
Travel Longevity	5	0	1	-1	1	0
Survival Impact	5	0	1	-1	0	-1
Avionic Protection	5	0	1	1	0	-1
Resistance to Capsizing	5	0	1	-1	1	-1
Total		0	0	-27	-1	-24

The second pugh matrix analysis reduces the score gap between the baseline (Airboat) and two possible designs: Submarine and Wave-power boat. The Submarine breaks even with the baseline with a zero score. The Wave-power boat design came up short compared to the baseline with a negative one score. However, the results of the Pugh matrix analysis were inconclusive.

The UHABS-6 team had a final discussion on developing a design concept. The UHABS-6 discussion can be summarized in two parts:

1. A wave-powered boat is just a boat with oscillating fins. The team could attach oscillating fins to a swamp boat or submarine design and use propellers as auxiliary propulsion, similar to the Wave Glider.
2. Taking advantage of conserving battery power with oscillating fins allows the autonomous recovery vehicle to travel further per battery charge before going into a recharge state.

Furthermore, the UHABS-6 team decided to select the best features from the possible design concepts to develop an autonomous recovery vehicle with a hybrid-pulsion system. First, use oscillating fins from the wave-powered boats as primary propulsion. Next, use the propulsion system of either airboat or submarine as auxiliary propulsion. Lastly, the flat-hull design of an airboat.

The hybrid-propulsion system relies on two types of propulsion systems, one that utilizes kinetic energy from ocean wave motion and the other utilizing electrical energy from batteries. of both a wave power boat and an airboat. As primary propulsion, the autonomous recovery vehicle uses an oscillating fin to take advantage of the ocean waves to create a forward thrust. The ocean waves cause the hull/structure of the BalloonSat module to heave upward and downward which the generates lift, upward and downward on the oscillating fin. The generated lifts interact with the fluid flow acting on the oscillating fin which combine to create a perpendicular thrust to the cord orientation of the oscillating fin. The oscillating fin is attached perpendicular to the hull/structure of the BalloonSat module by linkage, below and near the bow side of the hull/structure. The oscillating fin does not require power to operate, and allows for the autonomous recovery vehicle to operate for longer periods before reaching a recharge status. As auxiliary propulsion, the aircraft propeller and motor system are attached to the transom of the autonomous recovery vehicle hull/structure, and allows the autonomous recovery vehicle to propel forward in the absence of waves. To control the auxiliary propulsion, the built-in accelerometer in the inertial measurement unit (IMU) senses the heave on the hull/structure from the ocean waves. Furthermore, auxiliary propulsion activates in the absence of ocean waves and deactivates when ocean motion returns. With only a singular auxiliary propeller, the autonomous recovery vehicle will depend on rudders for steering.

A flat-hull design for the autonomous recovery vehicle will aid the primary propulsion, the oscillating fin, in generating forward thrust. The flat-hull rides the full upward and downward motion of the wave as the design does not reduce heave. Furthermore, more lift is generated on the oscillating fin to create forward thrust. The flat-hull can be easily manufactured and provides solar cells a suitable platform to mount on.

Figure 1 shows the Solidworks model of the conceptual design of the hybrid-propulsion autonomous recovery vehicle.

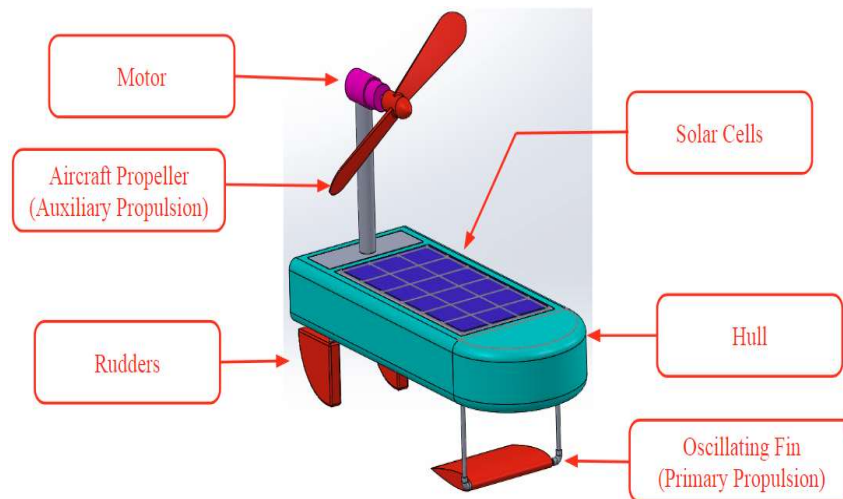


Figure 1: Conceptual Design of Autonomous Recovery Vehicle

Since the Preliminary Design Review (PDR), the conceptual design of the autonomous recovery vehicle has evolved and changed to better meet the technical, operational, and behavior

requirements of the mission. The key components that were changed from the conceptual design of the autonomous recovery vehicle were the hull and the propulsion system.

From the team meetings with Dr. Trevor Sorensen, who acts as both UHABS-6 Project Mentor & customer, Dr. Sorensen provided feedback and insight on the hull design and the propulsion system. These were the key takeaways:

1. The flat-hull design of the autonomous recovery vehicle will hinder the vehicle's ability to maneuver in the water.
2. The autonomous recovery vehicle does not need the auxiliary propulsion (aircraft propeller) if the principles of the oscillating fin (wave-power) can be proven and can produce enough thrust to overcome ocean current.
3. The exposed rudders and oscillating fin can be broken upon landing impact and needs to be addressed.

The provided feedback was taken into consideration and the RVP subsystem made the necessary adjustments to the hull and propulsion system. The current autonomous vehicle design is shown in Figure 2.

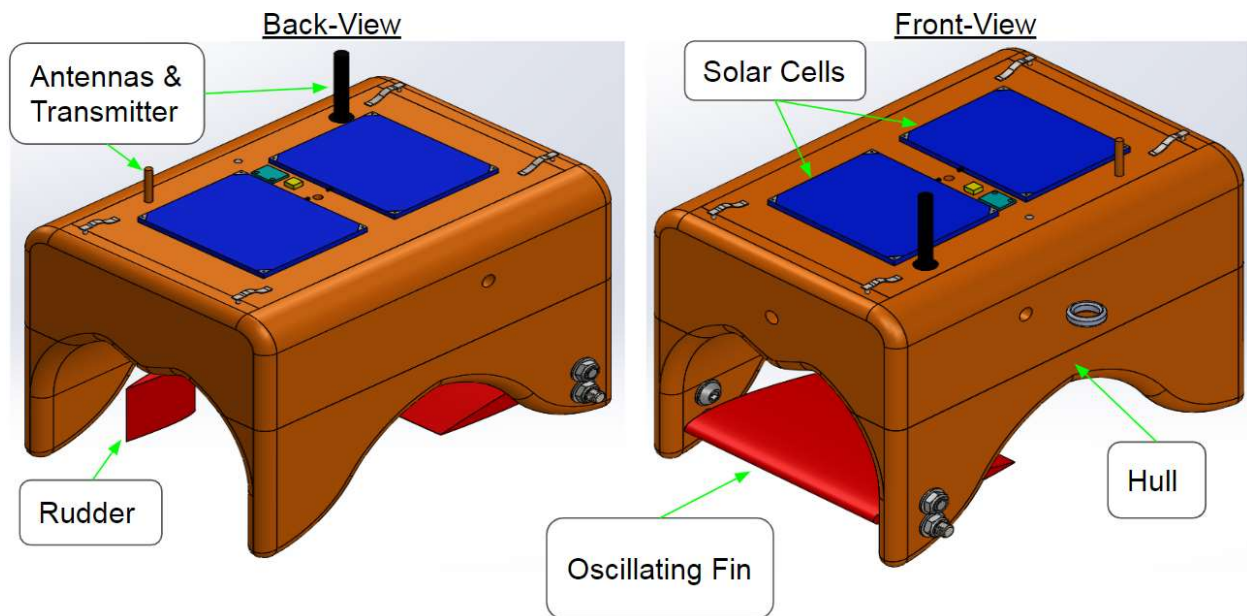


Figure 2: Current Design of Autonomous Recovery Vehicle

For the hull, the RVP altered the hull design to a catamaran shape. The catamaran hull shape allows the recovery vehicle to be more mobile as the double-hull structure cuts through the water better than a flat-hull, while maintaining the necessary wave pitch required to produce forward-thrust with the oscillating fin. To protect the oscillating fin and rudder from landing impact, the catamaran hull shape is adjusted to be more rounded to make the recovery vehicle to be self-

righting, or resistant to capsizing, so the recovery vehicle can be landed on its side, shielding both the rudder and oscillating fin during landing impact. In the Critical Design Review (CDR) report, the principles of the oscillating fin are proven and test show that the oscillating fin generates enough thrust to overcome waves. Furthermore, the auxiliary propulsion was removed to improve weight and reduce power consumption.

The engineering analyses performed on the autonomous recovery vehicle were finite element analysis (FEA) of the catamaran hull, oscillating fin, and rudders, and kinematic analysis of the oscillating fin and autonomous recovery vehicle. The FEA were conducted on the hull, fin, and rudder to study the effect of a landing impact at a velocity of 15 feet per second. The kinematic analysis was conducted on the oscillating fin to observe the relationship of wave amplitude to thrust and velocity produced by the fin. The kinematic analysis of the hull was to identify the waterline, center of mass, and center of buoyancy of a fully assembled recovery vehicle.

A bench level experiment was performed with a 3D printed model of the oscillating fin to prove the principles of wave-powered thrust. The 3D printed oscillating fin was attached to a styrofoam block, and was placed into a wave tank located at Holmes Hall Room 142. The 3D printed model was tested both against, with, across the waves generated in the tank.

2.3 Detailed Design

2.3.1 Top-Level System

2.3.1.1 System architecture

[JK]

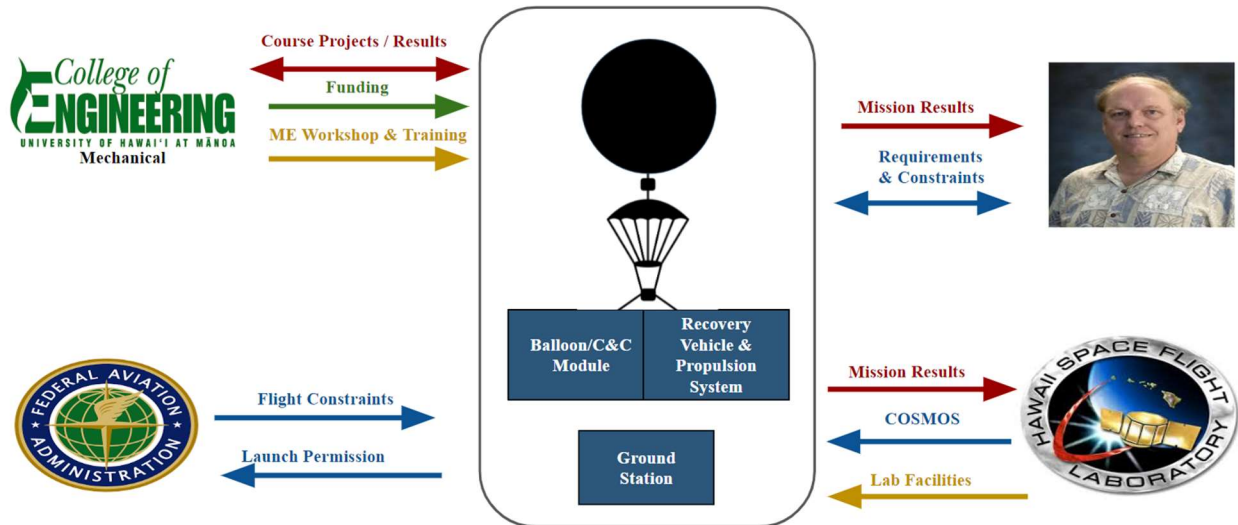
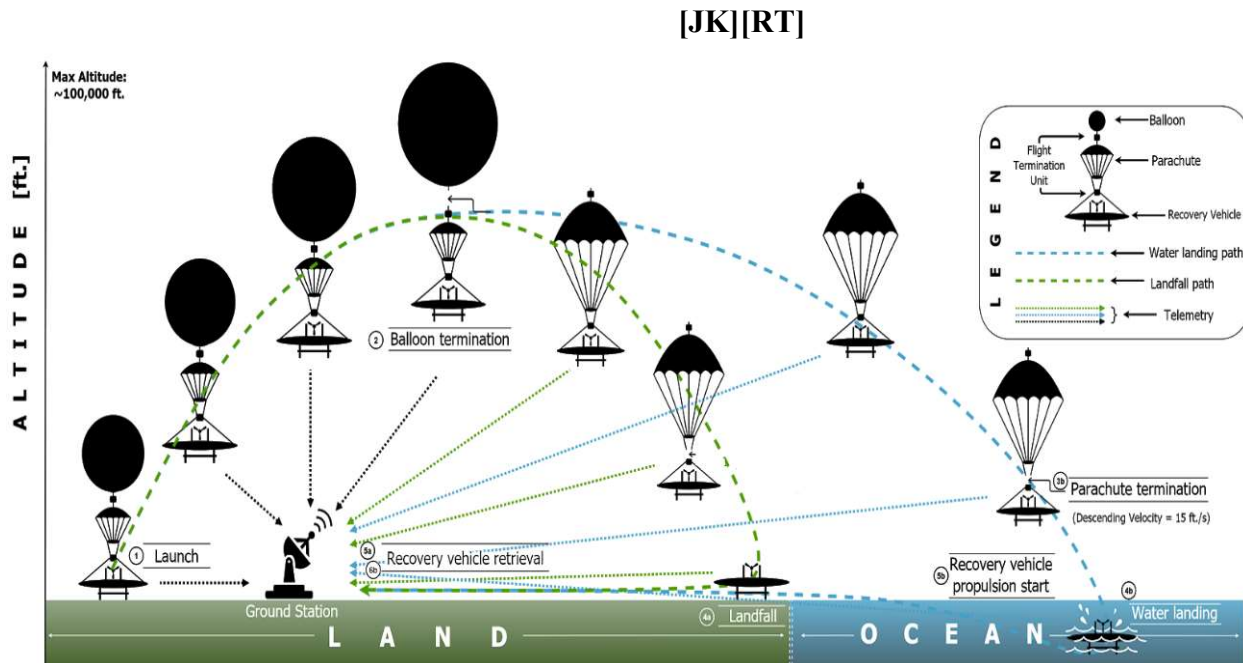


Figure 3: Mission Operational System Architecture [15] [16] [17] [18]

Figure 3 shows the external elements with their interfaces to UHABS-6. The UHM Mechanical Engineering Department provides UHABS-6 with funding and manufacturing facilities to develop the BalloonSat module structure, or recovery vehicle hull. In addition, the UHABS-6 mission is a project for both ME 481 and ME 491 which fall under the UHM Mechanical Engineering Department. The UHABS-6 mission receives requirements & constraints and provide mission results to both Dr. Trevor Sorensen and Hawaii Space Flight Laboratory (HSFL). HSFL also provides UHABS-6 with facilities and tools for assembling and testing the electrical components for the mission. The UHABS-6 mission must to the flight constraints of the Federal Aviation Administration and must request permissions, or notify, before launch.

2.3.1.2 Operations concept



The concept of operations (CONOPs), as shown in Figure 4, provides an overall visual of the UHABS-6 operation during the different phases of the mission. Starting at point 1, the GS goes through launch operation procedures, and prepare the BalloonSat module for launch. From leaving point 1, the BalloonSat module begins and continues to collect sensor data, images, and streams live-video to the GS for the duration of the flight phase of the mission. At point 2, the balloon will be released at the desired altitude below 100,000 feet from either burst or command of the payload or GS through the flight termination units (FTM). The parachute deploys and descends at a speed less than 15 ft/s. The BalloonSat module will descend and land within miles of Oahu, either onto land (green) line) or the ocean (blue). If landfall occurs, the audio beacon activates and will be tracked for recovery. If ocean landing occurs, the second FTM will release the parachute by payload or GS command before making contact with the ocean. Afterwards, the BalloonSat module will autonomously propel itself to a designated site for recovery.

2.3.1.3 Top-level Functional Flow Block Diagram

[JK]

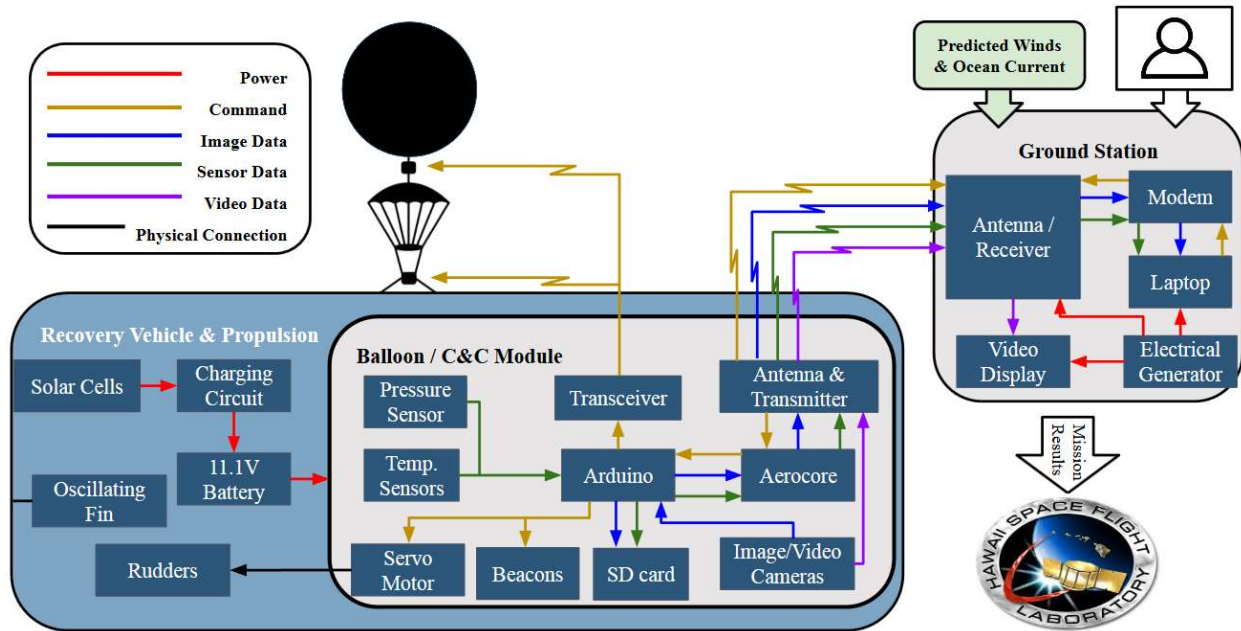


Figure 5: Overall System Functional Flow Block Diagram [16]

The overall system functional flow block diagram, shown in Figure 5, show all the interfaces between the UHABS-6 subsystems and the external interfaces that affect the system. The internal interfaces of the UHABS-6 subsystems is centralized by the BCCM subsystem. The BCCM subsystem physically interfaces with the RVP subsystem, and wirelessly interfaces with the GS subsystem. Through physical interfacing, the BCCM subsystem mounts all avionics to the internal housing of the autonomous recovery vehicle design of the RVP subsystem, and also interfaces the flight system components such as the balloon, parachute, and FTMs to the autonomous recovery vehicle. In addition, the RVP subsystem provides electrical power to the electrical components of the BCCM subsystem. The wirelessly interface of the BCCM and GS subsystem involves the communication relay of data, video, and command signals. The primary external interfaces affecting the UHABS-6 subsystem are centralized by the GS subsystem. The external interfaces affecting the GS subsystem are user input, predicted winds and ocean currents, and providing mission results to Hawaii Space Flight Laboratory (HSFL).

2.3.1.4 Overall configuration

[AQ]

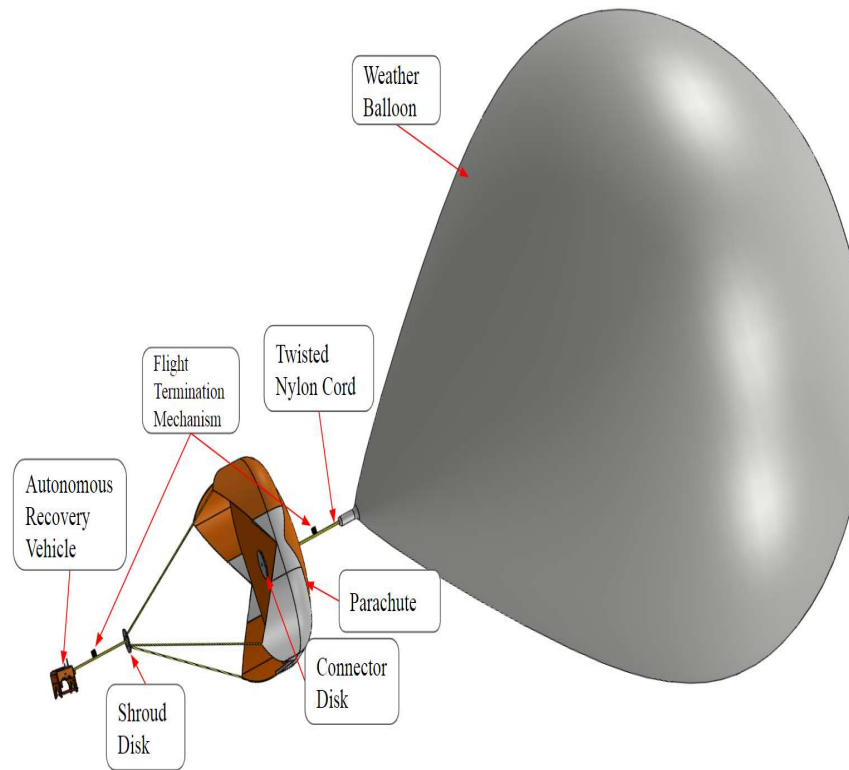


Figure 6: System Level External View

The external system is shown in Figure 6 which includes a 1200g weather balloon, a 6 ft diameter cruciform parachute, two flight termination mechanisms, an autonomous recovery vehicle, a shroud disk to deduce the chances of the parachute entangling, a connector disk for the connection between the balloon and the parachute, and a twisted nylon cord.

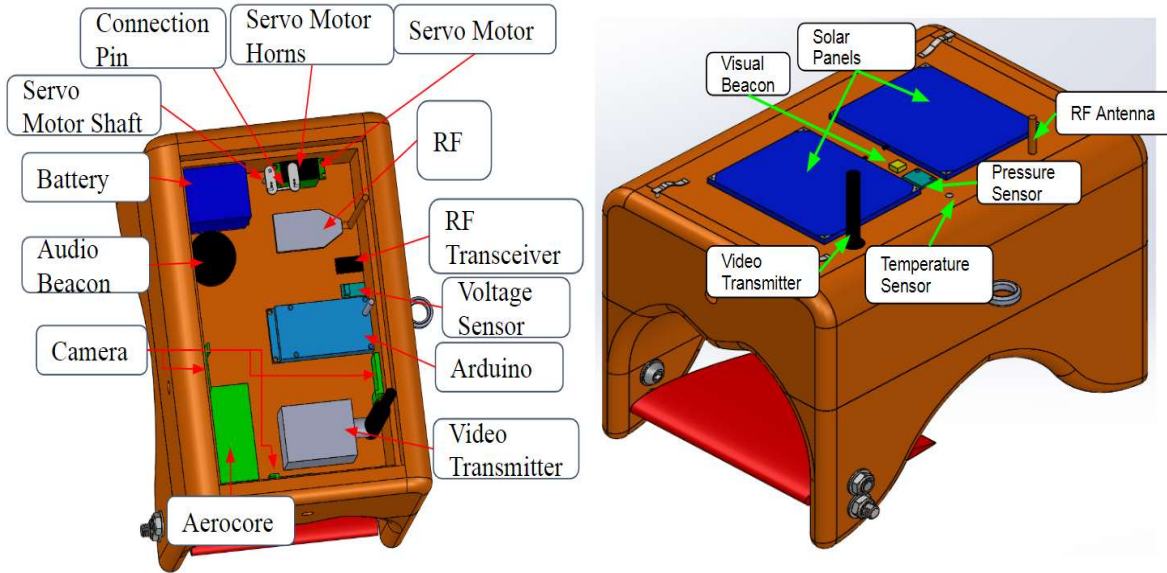


Figure 7: System Level Internal View

In Figure 7 the internal components are shown, on the left are instruments that are housed inside the recovery vehicle and on the right are instruments that are installed outside; however, will be wire connected inside.

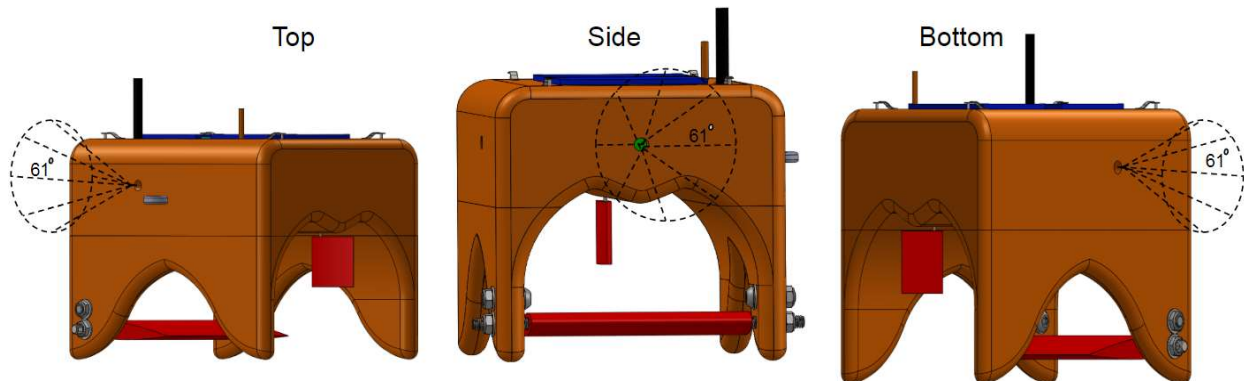


Figure 8: Camera Angle Views

In Figure 8 all three-camera viewing angle are shown, each camera has a viewing angle of 61 degrees because the lens of the camera is not flushed with the surface of the recovery vehicle. Due to the orientation of the recovery vehicle while ascension, the top viewing angle will be on the side of the boat, the bottom will be the opposite side, and the side view will be on the front of the vehicle.

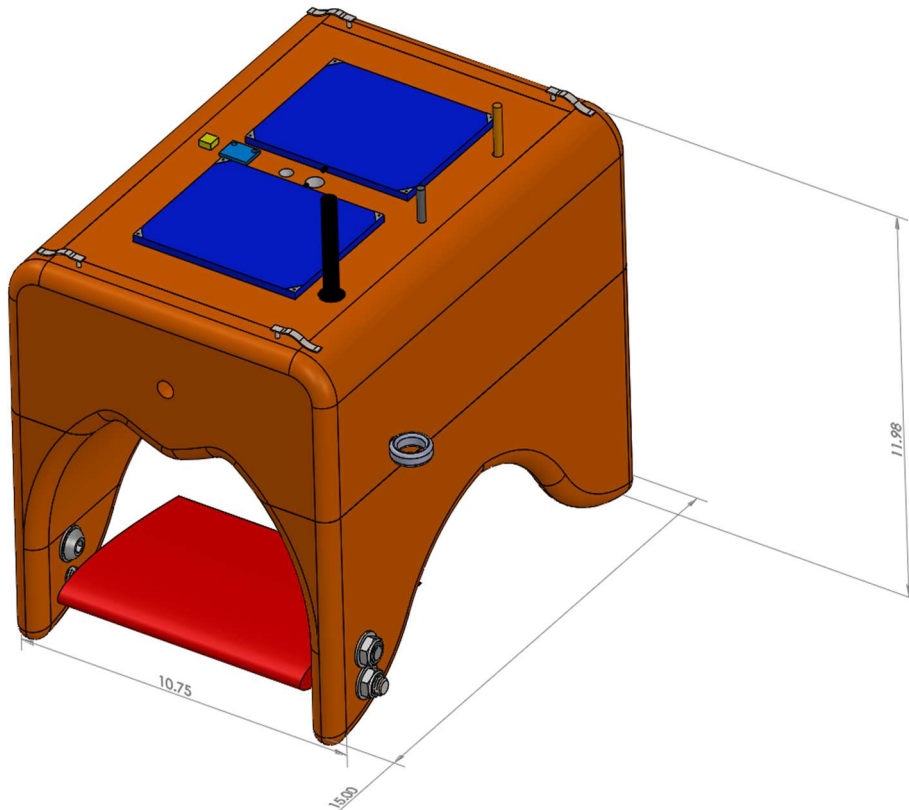


Figure 9: Autonomous Vehicle Dimensions

In Figure 9 the recovery vehicle's dimensions can be seen, the length is 15 inches, width is 10.75 inches, and the height is 11.98 inches. The dimensions were based off of the propulsion system as well as to accommodate the avionics configuration.

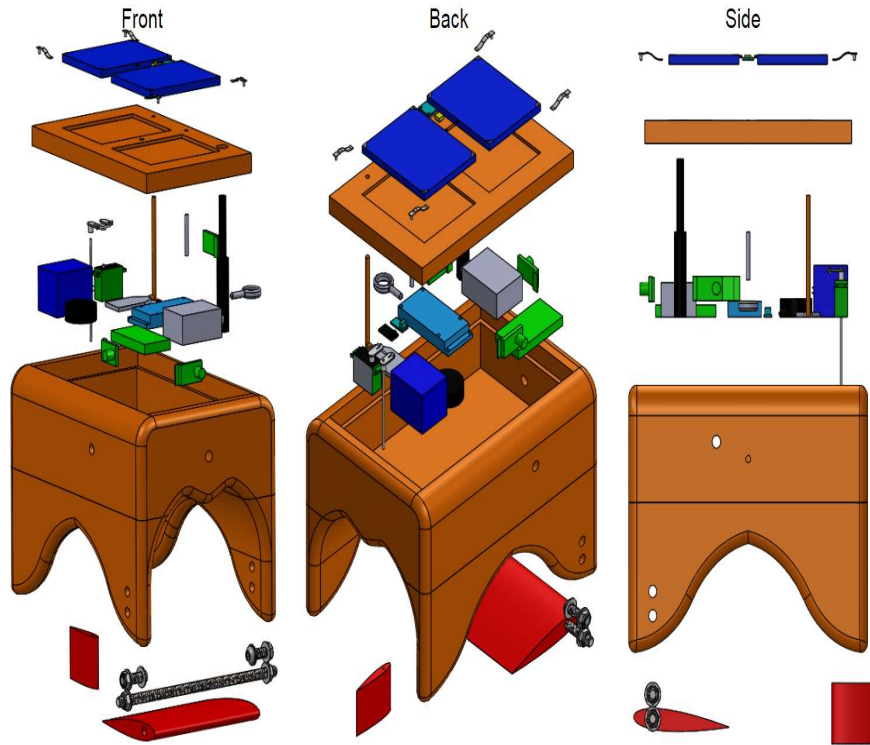


Figure 10: Exploded View of Recovery Vehicle

In Figure 10 exploded views from the front, back, and side of the recovery vehicle are shown, all components from the avionics to the propulsion system can be seen.

2.3.1.5 Performance Analyses

[AQ]

In order to prove that the UHABS-6 system will meet the given requirements multiple tests and analysis were conducted for each component. The latex weather balloon was analyzed to verify if a 1200g balloon could reach a maximum altitude of 100,000 feet. The parachute was analytically calculated for a diameter large enough to decrease the descent velocity to 15 ft/s. The hull structure and avionics were modeled in SolidWorks with alike materials and weights to verify that the module would weigh less than 6 pounds. Avionics were assembled in the internal structure of the hull to make sure all components could fit and that all image capturing devices were facing their respective angles. Solar cells were analyzed to determine power collection and charging capabilities to the battery. An FTM analysis was calculated to show what type of nichrome wire would be used to be able to detach the balloon and parachute. Radio frequency analysis was tested to determine the reliability of the signal connection. A COSMOS architecture was developed to show how our avionics system would interact with each other.

2.3.1.6 System FMECA

[JK]

Table 2: System FMECA

Process	List of Failure modes	Potential Effects	Severity of Effects	Probability of Failure	Invisibility of Failure	Criticality	RPN	Rank
Pre-Launch	Recovery vehicle cannot autonomously propel itself to designated recovery site	Cannot launch	9	5	3	1	135	2
	Hull Water Leakage	Cannot launch	9	3	3	1	81	6
	Weight Limit Failure	Cannot launch without weight approval by FAA	7	3	3	1	63	7
	Unfavorable predicted winds and ocean currents	Mission Delay	3	5	3	1	45	8
Flight	GS loses GPS signal	Unable to recovery BalloonSat module	10	5	5	1	250	1
	GS does not receive images & sensor data or live video	Dissatisfied customer	5	5	5	1	125	3
	Parachute Deployment Failure	Balloon descends faster than the specified limit and can cause harm to payload, people, or property	10	3	4	1	120	4
	FTM failure	Balloon ascends than max altitude or parachute will be stuck during recovery phase	7	3	5	1	105	5
	Frozen Avionics	Leads to lost communications and BalloonSat module cannot perform desired task.	9	3	3	1	81	6
Recovery	GS loses GPS signal	Unable to recovery BalloonSat module	10	5	5	1	250	1
	Hull, propeller/fins, or rudders break on landing impact.	BalloonSat module will not be able to function properly and will result not be able to travel to recovery site	9	3	3	1	81	6
	Failure to detach parachute for ocean landings	The propulsion system will not operate effectively, and can block solar cells from charging the batteries.	7	3	3	1	63	7

2.3.1.7 Safety Engineering

[AQ]

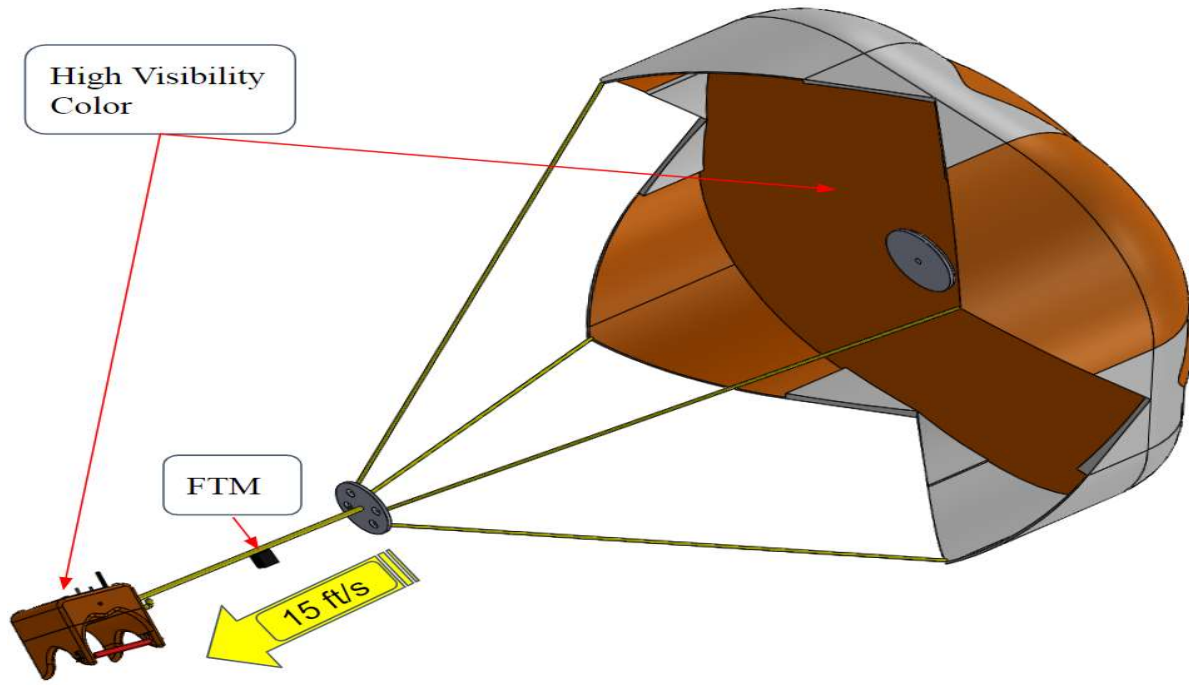


Figure 11: System Level Safety Engineering

In Figure 11 the safety engineering implemented in the UHABS-6 system showcases high visibility colors for long range visibility. Two FTM's to disconnect the balloon or detaching the recovery vehicle in case the system enters a no-fly zone area. Descending at a velocity of 15 ft/s will reduce the impact force of landing.

2.3.1.8 Fabrication Plan

[RT]

The fabrication plan of UHABS-6 mainly involves the manufacturing and assembly of the recovery vehicle. Therefore, production functional flows and manufacturing considerations will primarily be focused on the RVP subsystem. Since manufacturing will take place in Holmes Hall 140, the initial steps will be to obtain Mechanical Engineering machine shop training and acquire special training for hazardous material. To manufacture the hull, 3D parts will be printed to create a female mold of the hull for foam casting. The inner walls of the mold will be lined with packing tape and mold release will be applied to make the removal process more efficient and prevent damage to the hull. For the foam casting process, the syntactic foam and polyurethane foam will be created separately by mixing the 2-part mixture for both types of foams. First, the syntactic foam mixture will be poured into the bottom half of the hold and partially cured for 1-2 hours at room temperature before filling the remaining mold with the polyurethane mixture. The total curing time before removal will be approximately 24 hours. Finally, a wet layup process will be conducted to create the composite shell that comprises of epoxy resin and Kevlar 49

fabric. For propulsion, the fins and rudders will be manufactured using high quality PLA filament material and utilize the higher quality 3D printer than what was used for prototyping.

2.3.1.9 Integration & Test Plan

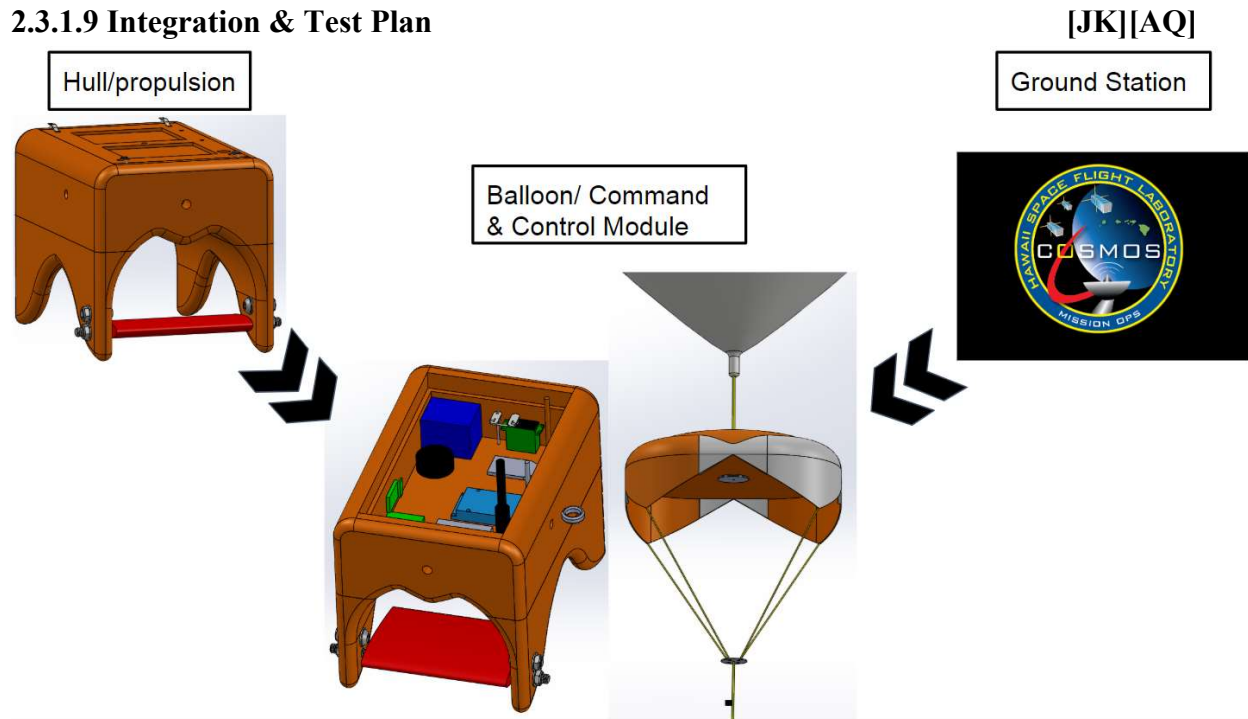


Figure 12: System Level Integration Plan [17]

The system level integration seen in Figure 12 details which order the subsystems will be compiled in. The RVP must be fabricated and the GS must have the COSMOS code finished before integration with the BCCM can be done. Once the RVP is finished, installation of the avionics can be implemented, at the same time the COSMOS software can be installed onto the avionics hardware. After all components in the recovery vehicle are installed, connection of the parachute and weather balloon will take place.

Table 3: System Test Plan for Autonomous Recovery Vehicle

Test	Location	Procedure	Success Criteria
Submergence	Lab	<ol style="list-style-type: none"> 1. Check watertight connection on vehicle. 2. Submerge vehicle into 2-3 ft of water. 3. Hold the vehicle submerge for 3-5 minutes. 4. Observe for air bubbles. 5. Inspect vehicle for water leakage. 6. Repeat 3 times. 	<ul style="list-style-type: none"> - No signs of air bubbles - No water leakage
Navigation	Beach	<ol style="list-style-type: none"> 1. Determine & upload GPS coordinates of wave currents. 2. Program designated recovery site. 3. Place vehicle into ocean approximately 30-50 yards away from designated location. 4. Activate autonomous system. 5. Repeat 3-5 times. 	<ul style="list-style-type: none"> - Vehicle returns to designated recovery site. - Navigation properly uses uploaded GPS wave current coordinates.
Weight	Lab	<ol style="list-style-type: none"> 1. Check that vehicle is fully assembled. 2. Power-on weight scale & tare weight. 3. Place vehicle onto scale and record weight. 	<ul style="list-style-type: none"> - Vehicle weighs under 6 lbs.

Table 4: System Test Plan for Data Transmission

Test	Location	Procedure	Success Criteria
Short Range Data Gathering (100 yards)	UHM Football Field	<ol style="list-style-type: none"> 1. Setup GS 100 yards from BalloonSat. 2. Gather sensor/image data & live stream video. 3. Monitor data & video acquisition for 1 hour. 4. Activate BCCM beacons from GS. 5. Check beacons. 	<ul style="list-style-type: none"> - GS successful data and video acquisition - Beacons activate from GS.
Long Range (2.31 miles)	GS: POST Rooftop BalloonSat: Magic Island	<ol style="list-style-type: none"> 1. Setup GS on POST rooftop. 2. Telemetry check with BalloonSat before departure. 3. BalloonSat team drives out to a location. 4. Gather sensor/image data & live stream video. 5. Monitor data & video acquisition at Ground Station for 1-hour mins. 6. Activate BCCM beacons from GS. 7. Check beacons. 	<ul style="list-style-type: none"> - GS successful data and video acquisition - Beacons activate from GS.

2.3.1.10 Human Factors Engineering/Accessibility & Maintainability

[AQ]

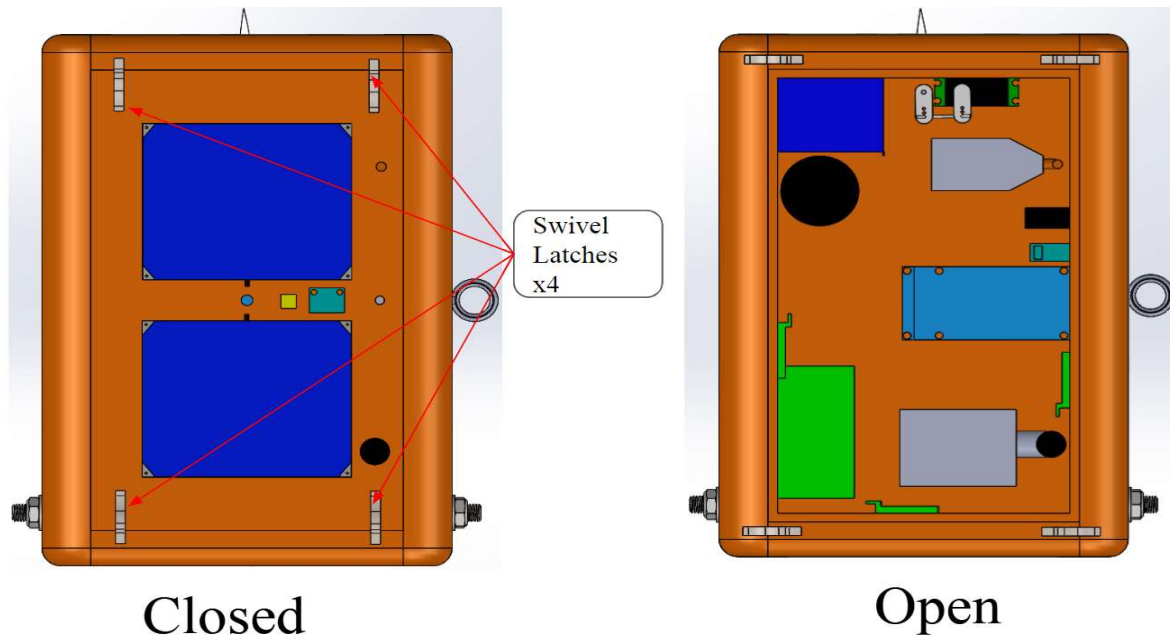


Figure 13: System Accessibility/Human Factor Engineering

The accessibility of the system only applies to the recovery vehicle as seen in Figure 13. Four swivel latches were implemented for the user to easily access all the avionics. The cover is fully detachable to account for antennas and wires connections.

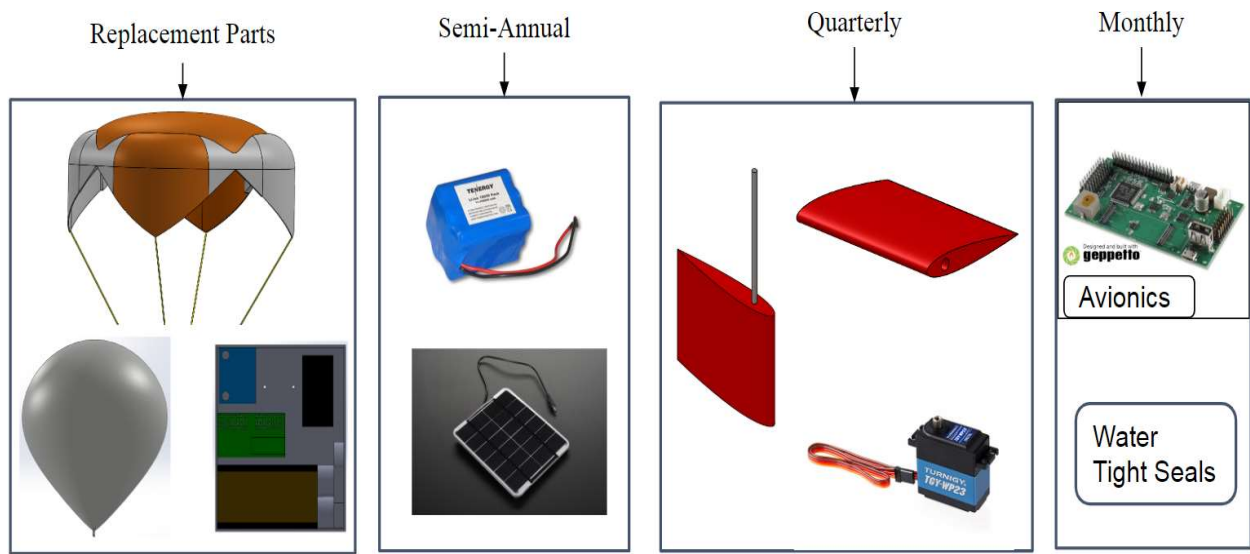


Figure 14: System Maintainability [19][20][21][22]

The system maintenance entails the components shown in Figure 14, monthly components will be the avionics and the water tight seals. Quarterly maintenance is the propulsion system including the rudder, glider, and the servo motor. Semi-Annual maintenance is subjected to the

power system, including the battery and the solar panels. Replacement parts will be needed for each operation as they will be lost, including a 6 feet parachute, a 1200g latex weather balloon, nylon cord, and two FTMs.

2.3.1.11 System Weight & Volume Budgets

[JK]

Table 5: System Weight & Volume Budget

Subsystem	Mass (lbs)	Volume (in ³)
Balloon C&C Module	0.75	25.16
Recovery Vehicle & Propulsion	4.93	12.44
Ground Station	N/A	N/A
Subtotal	5.68	37.60
20% Margin	1.136	7.52
Total	6.82	45.12
Allocation	6	240

2.3.1.12 System Level Power Budget and Power Profile

[AY][JK]

Table 6: Power Budget

Subsystems	Power (W)	Energy (Wh)
Balloon/C&C Module	22.47	67.23
Recovery Vehicle & Propulsion System	0	0
Ground Station	N/A	N/A
Total	22.47	67.23

Power Profile During Operation

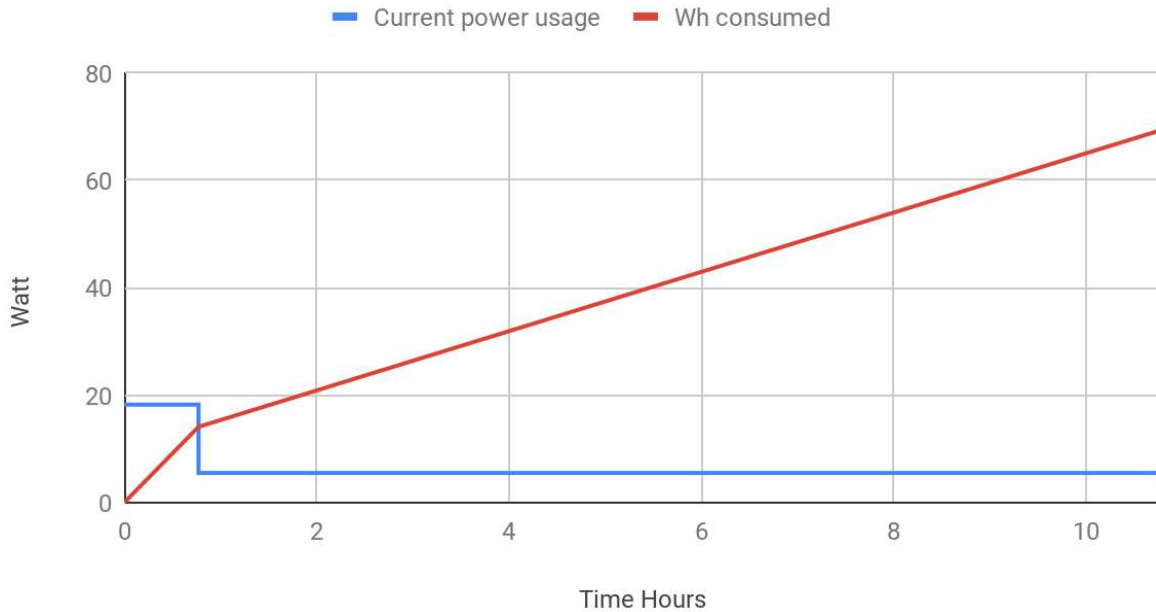


Figure 15: Power Profile of UHABS-6

The power profile of UHABS-6 varies greatly depending on the balloon release or burst altitude and landing distance from the designated recovery site. There are two operational phases: flight and recovery phase. From Figure 15, the power usage starts constant during the flight phase, approximately 18 watts. The time (in hours) of this constant watt usage can become longer depending on the time that BalloonSat ascends and descends the desired altitude. When the BalloonSat module lands, the recovery phase begins and the constant 18 watts usage decreases to a power of 5 watts until the BalloonSat is recovered. The shorter the flight phase, the less energy (Wh) consumed.

2.3.2 Subsystems

2.3.2.1 Balloon and Command & Control Module Subsystem

2.3.2.1.1 Subsystem Team Roles & Responsibilities

[AQ][AY]

Subsystem Lead - Akira Yokoyama

- Responsible for communicating subsystem plans with the project manager and avionics development for C&C module.

Subsystem Member - Austin Quach

- Responsible for developing the flight system.

2.3.2.1.2 Changes in subsystem design since PDR

[AY]

There are 5 changes to the BCCM subsystem since the PDR. The changes and the cost, power, mass, and volume are shown in Table 7. The Aerocore was added to the design due to the fact that the Arduino is not capable of housing and running COSMOS. The IMU and GPS were removed because the Aerocore has both of these components integrated inside the board. The sound beacon was changed to an Adept Rocketry SB40 due to the fact that it is self-powered and does not use the main battery and can last 24 hours. The wireless RF transceivers allow the C&C module to send commands to the FTM to have a failsafe incase the FTM fails to self-trigger. The voltage regulator was removed because the Arduino can regulate the voltage from the battery.

Table 7: Changes in BCCM Subsystem Design Since PDR

Changes	Cost	Power (W)	Weight (lbs)	Volume in ³
Add Aerocore 2 DuoVero	+\$149	+1.65	+0.08	+3.74
Remove IMU & GPS	-\$60	-0.03	-0.041	-3.5
Change audio beacon to Adept Rocketry SB40	+\$30	-1	-0.13	0
Add wireless RF transceivers	+\$12	+0.001	+0.01	+0.035
Remove voltage regulator	-\$2	-0.01	-0.002	-0.05
Total	+\$129	+0.61	-0.083	+0.225

2.3.2.1.3 BCCM Functional (Flow) Block Diagram

[JK]

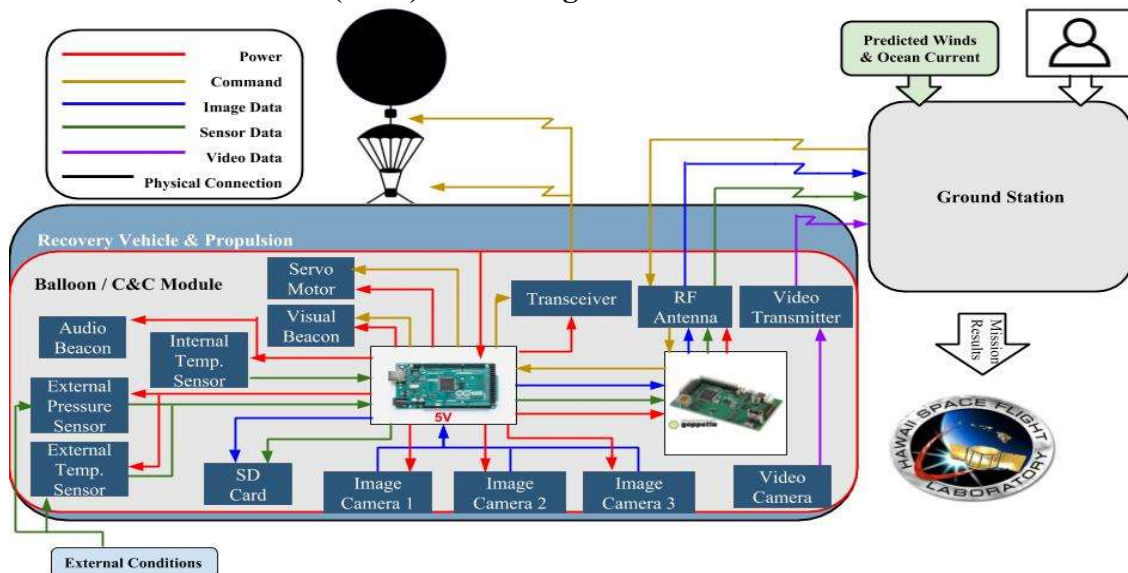


Figure 16: BCCM Functional Flow Block Diagram [17]

2.3.2.1.4 Subsystem Weight & Volume Budgets

[AY]

Table 8: BCCM Mass and Volume Budget.

C&C Module			
Item	Quantity	Total Mass(lbs)	Total Volume(in ³)
Pressure Sensor	1	0.003	0.06
Temp. sensor	2	0.2	1.74
Arduino	1	0.08	4.95
SD Card	1	0.008	0.19
Aerocore	1	0.1	3.75
Image / Video Camera	3	0.06	0.48
Visual beacon	1	0.0002	0
Audio beacon	1	0.01	2.98
Servo motor	1	0.05	1.96
RF Transceiver	1	0.05	6.61
Video transmitter	1	0.1	9.25
Voltage sensor	1	0.01	0.06
Wireless RF Transceiver	1	0.07	0.04
BCCM Total		0.75	25.16
BCCM Allocated		1	140

2.3.2.1.5 Subsystem Power Budget

[AY]

The BCCM has two operations modes, flight and recovery. During flight the C&C will be gathering data, streaming video, and sending data back down to the GS. The flight mode has a higher power requirement at 18.25 W compared to recovery at 5.32 W. This is because during the flight more electrical components are active. During the recovery phase the C&C module needs to use the navigation program to autonomously steer itself back to a designated location while taking advantage of currents if possible. Table 10 shows the power and energy during each phase.

After the recovery vehicle makes landfall the audio beacon and visual beacon are turned on. The audio beacon has an independent power source that lasts for 24 hours. The visual beacon has a power usage of 4.2 W with an energy consumption of 0.7 Wh with it blinking once every 10 seconds. The visual beacon is a luxury item and is not critical to operations. It would also activate after autonomous recovery has ended. As a result, it is not factored into the power profile in Figure 17.

Table 9: BCCM Power Requirements

C&C Module		
Item	Quantity	Power (W)
Pressure Sensor	1	0.06
Temp. sensor	2	0.79
Arduino	1	2
SD Card	1	0.75
Aerocore	1	1.65
Image / Video Camera	3	3.15
Visual beacon	1	4.2
Audio beacon	1	N/A
Servo motor	1	0.02
RF Transceiver	1	3.65
Video transmitter	1	6
Voltage sensor	1	0.2
Wireless RF Transceiver	1	0.001
BCCM Total		22.47
Allocated		22.47

Power Profile During Operation

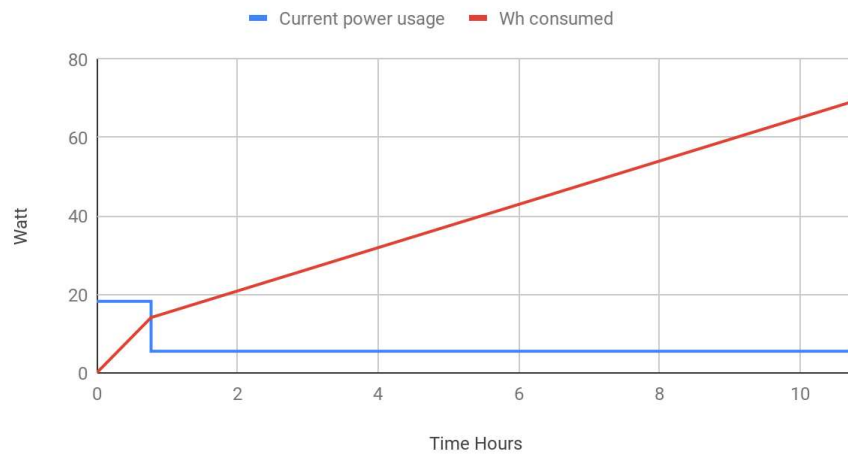


Figure 17: Power and energy usage for flight and recovery during a simulated operation.

Table 10: BCCM Break down of Power, Energy, and Duration of Simulated Operation.

Phase	Power (W)	Energy Used (Wh)	Duration (hr)
Flight	18.253	14.11	0.77
Recovery	5.32	55.17	10
Total		69.28	10.77

2.3.2.1.6 Description

[AQ][AY][JK]

2.3.2.1.6.1 Parts Description

[AY]

Table 11: Parts list for C&C

C&C Module		
Part Description	Component	QTY
Arduino	Arduino Mega 2560	1
Pressure Sensor	Adafruit BMP388	1
Temp. Sensors	T-PRO DS18B20	2
Camera/Video	Arducam Mini Module Camera Shield with OV2640 2 Megapixels	3
Voltage Sensor	Diymall Voltage Sensor De0-25v	1
Audio Beacon	Adept Rocketry SB40	1
Visual Beacon	Cree XLamp XHP35	1
RF Transceiver	Xtend 900	1
Video Transmitter	Mini 5000mW Wireless Video Transmitter	1
SD Card	MicroSD card breakout board+	1
Hand Warmers	HotHands Hand Warmers	2
Aerocore	AeroCore 2 DuoVero	1
Wireless RF Transceiver	Arduino NRF24L01+ 2.4GHz Wireless RF Transceiver Module	1
Servo Motor	Turnigy TGY-WP23	1

The Arduino is used to connect the pressure and temperature sensors, camera/video, voltage sensor, wireless RF transceiver, SD card, servo motor, and RF Transceiver. The Arduino will

control the mentioned parts, supply power to them, and store any data gathered from the parts onto the SD card.

The pressure sensor is used to gather atmospheric data and determine what altitude the system is currently at. The temperature sensor is used to gather atmospheric data and monitor internal temperature as state of health data. The voltage sensor is used to monitor the voltage of the battery and gather it as state of health data. The cameras will take pictures in the down, side, and up facing directions as dictated by the requirements. The video camera and video transmitter will be used to stream video down to the GS. The wireless RF transceiver is used as a failsafe to trigger the FTM if the FTM fails to self-trigger. The RF transceiver is used to send data to the GS and to receive commands from the GS. The servo motor will be used to control the rudder.

The Aerocore is to install and run COSMOS. The Arduino is incapable of running COSMOS. The Aerocore also has an IMU and GPS built into the board. The IMU is to determine heading during navigation. The GPS is to determine location for tracking, navigation and as a backup for altitude if the pressure sensor fails. The audio and visual beacons are to help in manual recovery when the recovery vehicle reaches land. The hand warmers are to keep the internal temperatures within ranges that the electrical components can operate in.

Table 12: Parts List for Flight System and FTM

Flight System		
Part Description	Component	Quantity
Balloon	Kaymont 1200g	1
Parachute	Rocketman HAB Parachute 6'	1
Nylon Cord	½" Nylon Rope	1
Shroud Disk	3D Printed Disk for Parachute	1
Flight Termination Mechanism		
Part Description	Component	Quantity
Nichrome Wire	TEMCo Nichrome 80 series wire 20 Gauge 25 FT	1
9V Battery	Duracell 9V	2
Arduino Mini	Arduino Pro Mini 328 - 5V/16MHz	2
Pressure Sensor	Adafruit BMP388	2
Wireless RF Transceiver	NRF24L01+ 2.4GHz Wireless RF	2
FTM Casing Protection	3D Printed Case	1

The balloon is the method in which the BalloonSat will ascend. The parachute will slow the descent of the payload so that it has a lesser chance to injure a person and break. The shroud disk is to prevent the nylon cord from tangling when used to tether the balloon, parachute, and payload together.

The nichrome wire is to be heated by the 9V battery to cut the nylon cord. The Arduino mini will be programmed to heat the nichrome wire when the pressure sensor detects a maximum or minimum altitude. The wireless RF transceiver is used as a failsafe to receive the trigger command from the C&C module in case the Arduino mini fails. The FTM casing is to house the above-mentioned parts.

2.3.2.1.6.2 Component layout

[AQ]

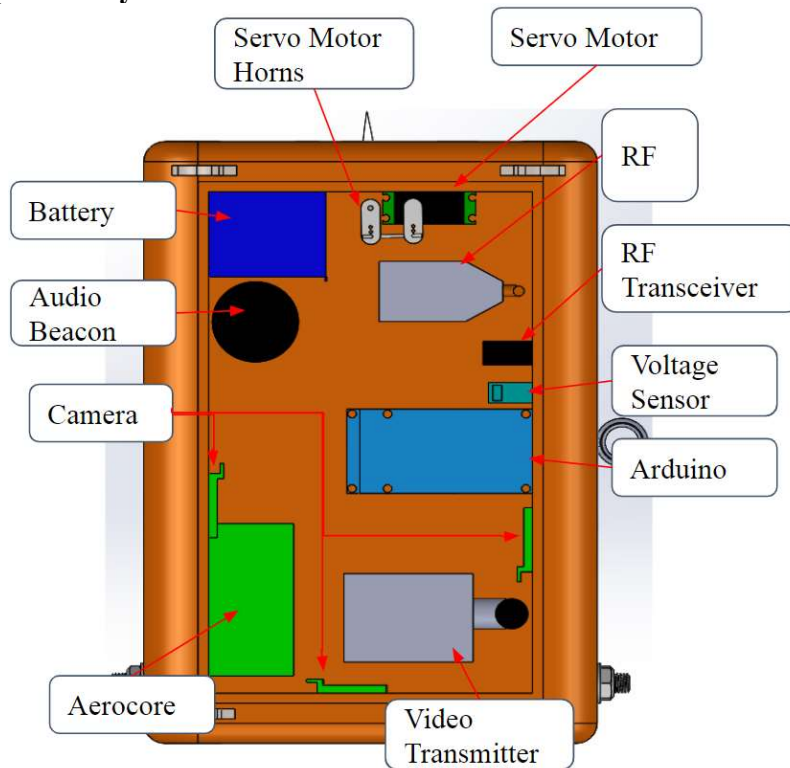


Figure 18: Internal layout of C&C module inside the recovery vehicle.

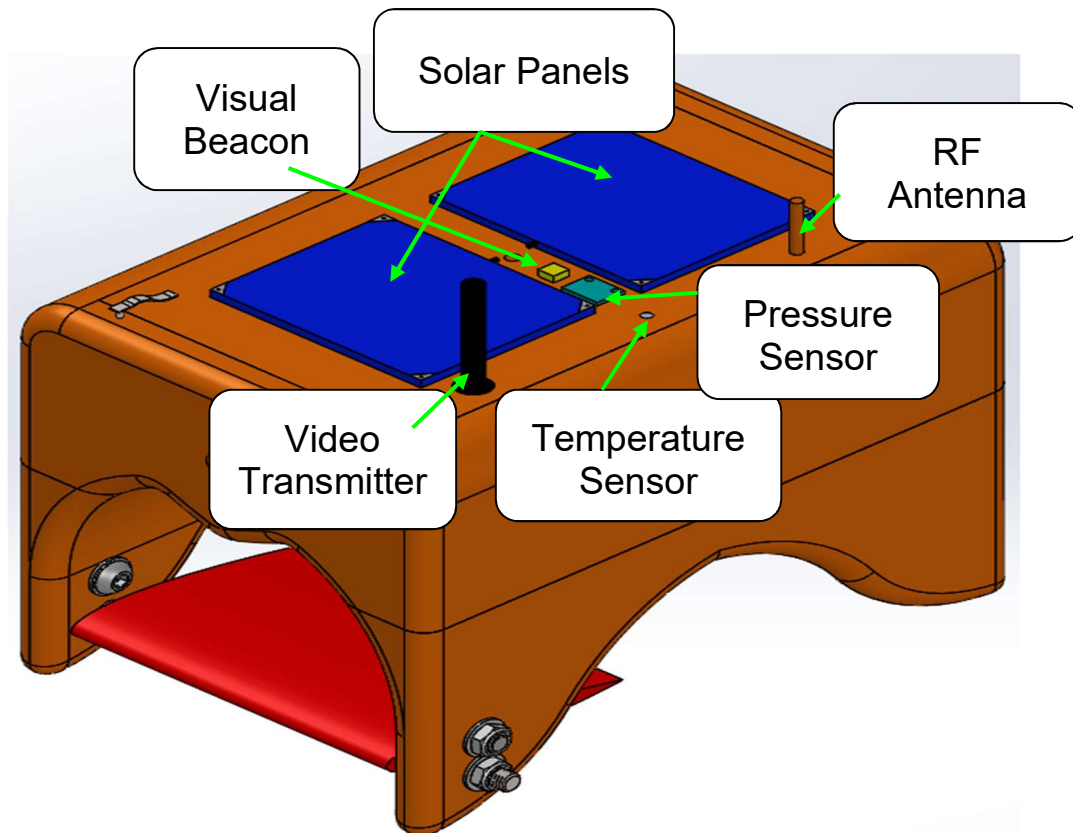


Figure 19: External view of C&C parts on the recovery vehicle

2.3.2.1.6.3 Software Description

[JK][AY]

The BCCM programming has two main parts to it, flight and recovery. During flight data, video, pictures, and location is being gathered and transmitted to the GS. Pressure and temperature sensors and cameras are turned off when landing occurs. During the flight the pressure is being checked, when the pressure corresponding to the maximum altitude is reached the C&C module sends a command to the balloon FTM to cut the nylon rope. At this point the descent phase of the flight has begun. When the pressure corresponding to the minimum altitude is reached a check is done using the GPS to see if system is above land or water. If the system is above land the program moves to the recovery section and the audio and visual beacons are triggered and other components are turned off. If the system detects that it is above water then a command is sent to the parachute FTM to cut the nylon rope. Once landing is confirmed the recovery phase begins.

The recovery phase for a water landing starts with checking current GPS location then creating a path to the designated recovery site. The path is created to minimize pathing going against the currents and to maximize pathing going with the currents. Once the path is set, the heading is determined using the IMU. If the current heading does not match the correct heading to the next location the rudder is turned to change the heading. This continues until the system detects that it is at the designated recovery site. When the designated recovery site is reached the beacons are turned on and other electrical components are turned off.

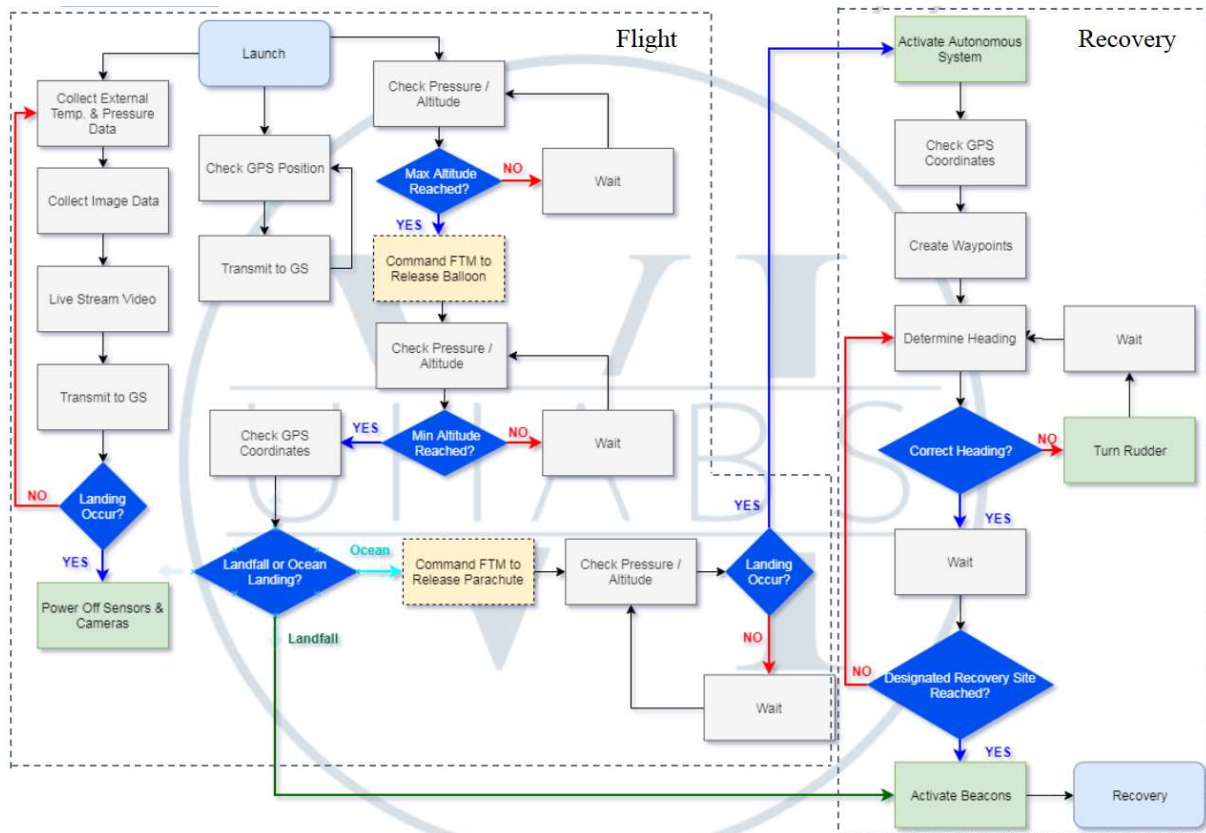


Figure 20: C&C Module Programming Flow Diagram

The programming for the balloon FTM is shown in Figure 21. The FTM has its own pressure sensor to ensure that it can still function if the wireless connection to the C&C fails. The FTM will trigger the nichrome wire to cut the nylon rope if the maximum altitude is reached.

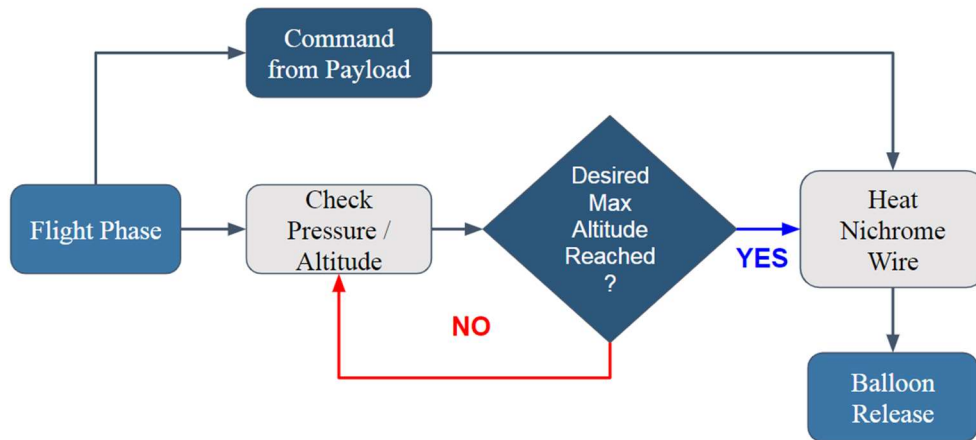


Figure 21: Programming Flow of Balloon Release FTM

The parachute FTM programming is shown in Figure 22 and is slightly different from the balloon FTM. The program must check that maximum altitude has been reached before it can move on. When minimum altitude has been reached a check is done to see if the system is above

land or water. If the system is above land the program ends. If the system is above water then the nichrome wire is triggered to cut the nylon rope to separate the parachute from the payload. The nichrome wire can also trigger if a command is received from the C&C module.

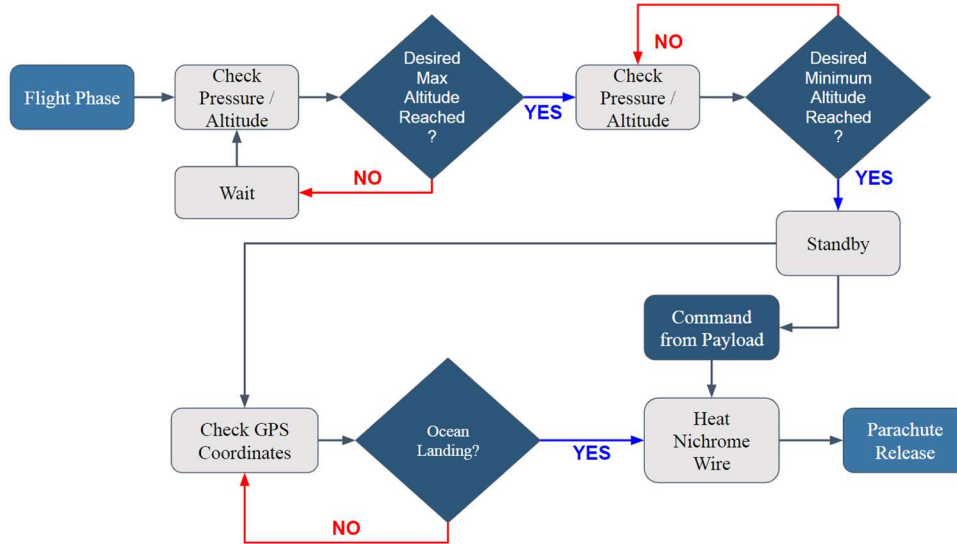


Figure 22: Programming Flow of Parachute Release FTM

2.3.2.1.7 Results of Technical Analyses

2.3.2.1.7.1 High Altitude Balloon Analysis

[JK]

To obtain the correct balloon type & size for the UHABS-6 mission, a kinematic analysis was conducted. The balloon burst altitude equation is shown in Equation (1) [23].

$$\text{Burst Altitude} = 23748 \ln \left(\frac{V_0}{V_b} \right) \quad (1)$$

Where the standard air density model (in feet) is 23748, V_0 is the initial volume of the balloon before launch, and V_b is the volume at balloon burst.

To determine if the initial with volume of balloon will generate enough lift force to carry the payload, the ascent velocity must be calculated. The ascent velocity (v_{ascent}) can be derived from the drag equation, as shown in Equation (2).

$$v_{ascent} = \sqrt{\frac{F_{lift}}{0.5(C_d)(\rho_{air})(A_c)}} \quad (2)$$

Where F_{lift} is the free lift force, C_d is the balloon drag coefficient (obtain from manufacturer), ρ_{air} is the density of air, and A_c is the area a circle (frontal face of a sphere). F_{lift} can be derived from Equation (3).

$$F_{lift} = (V_0)(\rho_{air} - \rho_{helium})(g) - [(W_b - W_p)(g)] \quad (3)$$

Where ρ_{helium} is the density of helium, g is gravity, W_b is the weight of the balloon, and W_p is the weight of the payload.

After contacting the Kaymont manufacturer, they were able to provide their balloon specifications and burst parameters, as shown in the Appendix. Each Kaymont balloon size was analyzed to determine their maximum burst altitude at minimum initial volume to generate F_{lift} . Assuming a payload weight (including FTM, parachute, & tethers) of 7 lb, the results show that to reach an altitude up to 100,000 feet, the BalloonSat must use a Kaymont 1200g Balloon. The initial volumes of the 1200g balloon was plotted versus both burst altitude (ft) and ascent velocity (ft/s), as shown in Figure 23 and Figure 24.

Balloon Burst Altitude (ft) vs. Initial Volume (ft³)

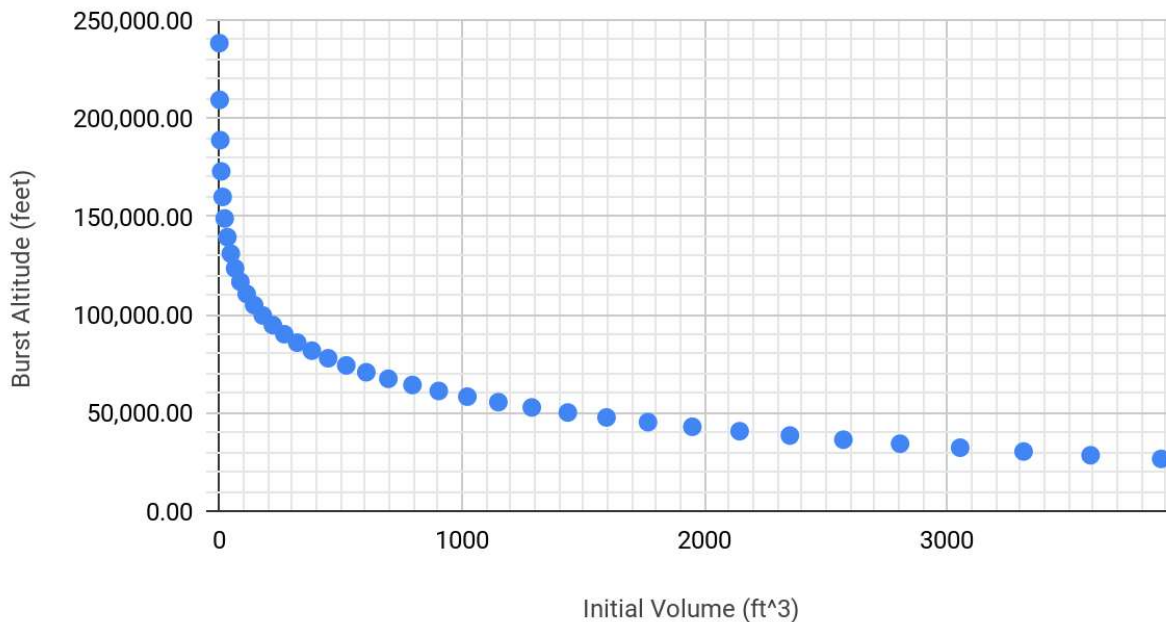


Figure 23: Kaymont 1200g Initial Volume to Burst Altitude

Balloon Ascent Velocity (ft/s) vs. Initial Volume (ft³)

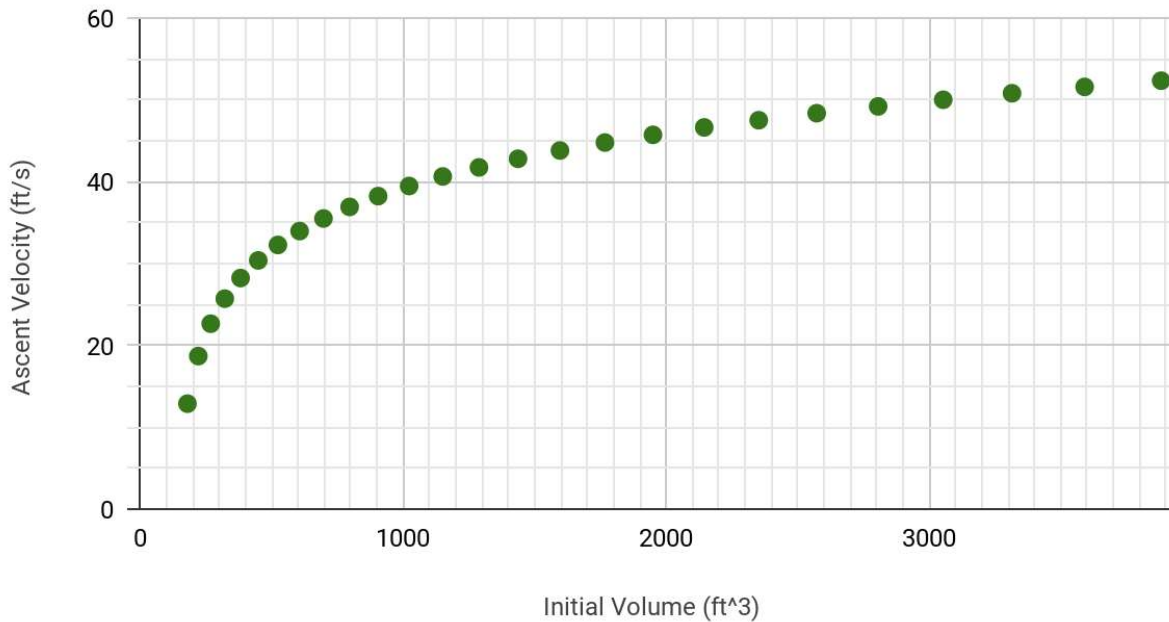


Figure 24: Kaymont 1200g Initial Volume to Ascent Velocity

From Figure 23 and Figure 24, the minimum volume of 180 ft³ will get the Kaymont 1200g Balloon to ascend to a height of 99,558 ft at a speed of 12.88 ft.

2.3.2.1.7.2 Parachute Size Analysis

[JK]

The parachute size, in diameter (D), needed to descend a max velocity of 15 feet per second can be derived from the drag equation. Equation (4) shows the drag equation.

$$F_d = \frac{1}{2} \rho_{air} C_d A v_{max}^2 \quad (5)$$

Where F_d is the drag force, C_d is the drag coefficient of the parachute, ρ_{air} is the density of air, A is the frontal area force on the parachute (circle), and v_{max} is the max velocity.

Rearranging the Equation (4), the minimum parachute size can be solved using Equation (5) and Equation (6).

$$A = \frac{2F_d}{\rho_{air} C_d v_{max}^2} \quad (5)$$

$$A = \left(\frac{\pi}{4}\right) D^2 \quad (6)$$

At terminal velocity, or max velocity, the drag force (F_d) is equal to the weight of the payload (including FTM & tethers) which is assumed to be 6.5 lb. The BalloonSat will use a high-altitude

balloon parachute from Rocketman Parachutes which have a C_d of 0.99 [24]. The result of calculations determines that the BalloonSat will need a minimum parachute size of 6 feet.

2.3.2.1.7.3 FTM Analysis

[AQ]

The FTM analysis is based on an online program [25]. To validate the program, testing was done with parameters set at 0.5in length nichrome wire that was 40 gages, connected to an 8-voltage battery, the temperature calculated using the program was that the nichrome wire itself would melt. Testing verified that the nichrome wire indeed melted, validating the online program. With the program validated, the final system will be using a 20 gage, 4in long nichrome wire with a 5-voltage connection.

2.3.2.1.8 Risk Analysis

[AY]

Table 13: BCCM Subsystem Risk Management

Identification	Consequence	Probability of Occurrence	Risk Rank	Risk Mitigation (Reactive , Proactive)
Lack of electronic knowledge hindering progress	4	3	Medium	-Start electronics systems early -Ask for assistance from people outside of the project
Avionics freezes	5	2	Medium	-Install heating system -Install insulation -Wait for system to warm up
Parachute detachment failure	4	2	Medium	-Ensure detachment unit works in all possible environmental conditions -Multiple detachment methods
Flight termination mechanism failure	3	2	Medium	- Integrate autonomous release when at desired altitude - Integrate manual release from ground station when above the desired altitude -Have a backup command sent from C&C
Air traffic interference with BalloonSat flight trajectory	5	1	Medium	-Research sites and find optimal site per FAA regulations -Reschedule launch
Parts do not arrive on time	3	1	Low	-Order parts early -Buy parts locally or rush order

2.3.2.1.9 Subsystem FMECA and Fault Tree

[AY]

Table 14: FMECA of BCCM subsystem.

Process	List of Failure modes	Potential Effects	Severity of Effects	Probability of Failure	Invisibility of Failure	Criticality	RPN	Rank
Flight	Video Transmitter Failure	Loss of video stream	5	5	5	3	125	3
	Parachute Failure	Payload will be damaged on impact. Recovery may fail.	10	3	4	1	120	4
	RF Transceiver Failure	Loss of communication with GS	10	5	2	1	100	5
	Parachute FTM Failure	Parachute will not detach and cause increased drag in recovery	7	3	3	1	63	7
	Early Balloon Burst	Landing location will be wrong.	5	3	4	1	60	8
	Balloon FTM Failure	Payload will ascend to higher altitude than planned causing error in landing location.	7	3	2	1R	42	9
	Pressure Sensor Failure	Precise altitude will be unknown. FTM may trigger at incorrect altitude	5	2	3	1R	30	10
	Camera Failure	Unable to take pictures or video	5	1	5	3	25	11
Autonomous Recovery	GPS Failure	Navigation will be incorrect	10	5	5	1	250	1
	Navigation Code Failure	Payload will be unable to navigate to correct destination.	10	7	3	1	210	2
	RF Transceiver Failure	Loss of contact and ability to send commands.	10	3	1	2	30	4
	Motor Servo	Steering loss	10	4	2	1	80	6
Manual Recovery	Audio Beacon Failure	Will no longer have an audio cue to find payload	3	1	2	3	6	12
	Visual Beacon Failure	Will be less visually perceivable	2	1	2	3	4	13

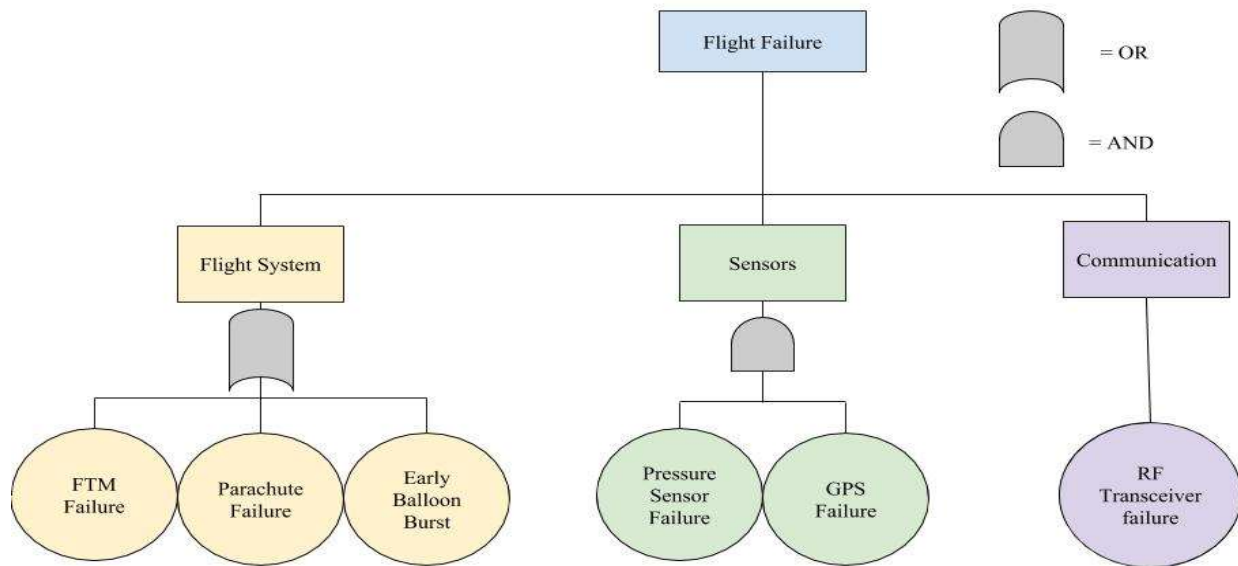


Figure 25: BCCM Flight Fault Tree

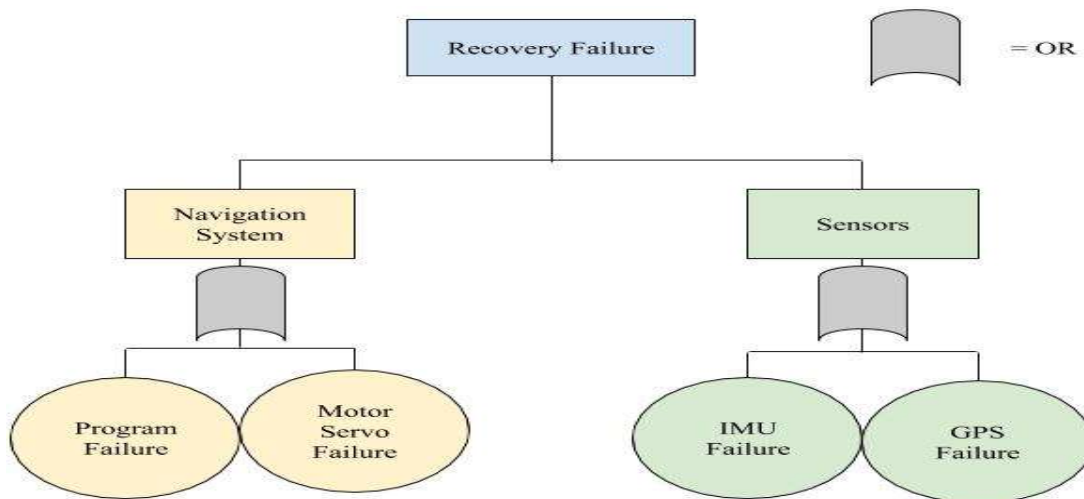


Figure 26: BCCM Recovery Fault Tree

2.3.2.1.10 Detailed Test Plan

[AQ][AY]

The parachute, FTM, and avionics will need to be tested in the BCCM to identify problems and to ensure that the subsystem can function during the operation.

To test the parachute a velocity test will be conducted. To perform the test a 6 lbs weight with an accelerometer will be attached to the parachute. The parachute and weight will be dropped from the 3rd floor of Holmes Hall and repeated 3 times. If the accelerometer still shows that the weight is accelerating, the drop will need to be tested at a higher height. Based off the acceleration data the velocity of the weight can be determined. The success criteria for this test is if the parachute descent does not exceed 15 ft/s.

The FTM will have a burn test to determine the time required to burn through the nylon rope and if it can occur under expected environmental conditions. To perform the test a section of nylon rope under 6 lbs of tension will be cut with 4 inches of 20-gauge nichrome wire. The nichrome wire will be connected to a 9V battery. Three burn tests will be conducted at different temperatures and pressures. The first test is at -70°F at 1 psi which are conditions at 60000 ft [26]. Another burn test will be conducted at -35°F at 5.4 psi which are conditions at 25000 ft [26]. The last burn test will be at 75°F at 14.7 psi which are conditions expected at sea level. The tests will be conducted in a thermal vacuum chamber. The success criteria for this experiment is if the burn can occur under the expected conditions.

The temperature and pressure sensors and cameras will be tested to see if data can be gathered successfully. The test will be to see if the sensors can gather data continuously for one hour. The camera will be tested to see if it can take pictures and video for one hour. The success criteria are if the sensors and camera can operate with the Arduino without errors and if the sensor data is no more than 5% off of expected values.

The hand warmers will need to be tested to determine if it can generate enough heat to prevent the electrical components from freezing. To perform the test the completed C&C system will need to be placed inside the recovery vehicle. The vehicle is then tested in conditions similar to those at 60000 ft and 25000 ft in a thermal vacuum chamber. Success criteria is if the internal temperature of the recovery vehicle does not fall below 0°F for 1 hour.

The GPS in the Aerocore will be tested to see if function is not affected when on the ocean. To conduct the test the Aerocore will be placed in a buoyant and waterproof container. The container will be placed on the ocean at least 50 ft from shore. The Aerocore will be left to gather location data for 15 minutes. After 15 minutes the container will be towed in while still gathering data. The success criteria are if the GPS can maintain connection during the test and if the gathered locations is no more than 15m off of expected locations.

The programming for the C&C module will be tested to ensure that it can run without errors. To perform the test the C&C module will be fully assembled but not placed into the recovery vehicle. The program will be run with all parts of the subsystem active. Success criteria is if the code can run for 1 hour without having errors and if the agents can communicate successfully between themselves.

2.3.2.1.11 Subsystem WBS

[RT]

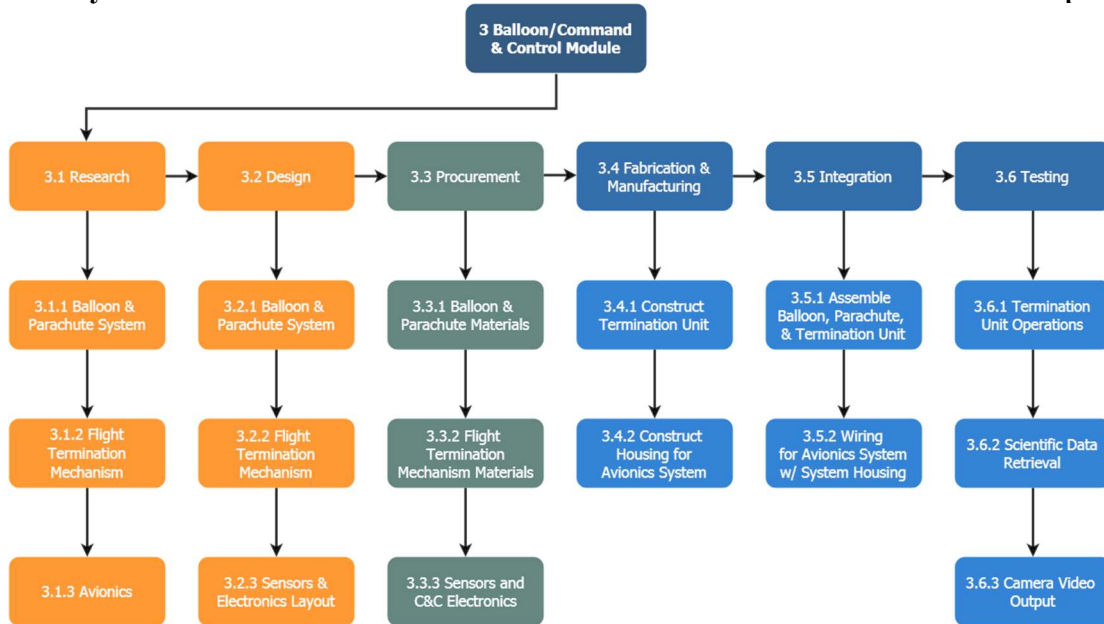


Figure 27: WBS of BCCM

2.3.2.1.12 Subsystem Schedule WBS and Gantt Chart

[RT][AY]

In Figure 28, the vertical line indicates the current date and the progress that the subsystem should be at. Currently the subsystem is in the procurement phase. For the rest of December and into part of January procurement of parts will continue. The current progress shows that the subsystem is behind schedule, however the procurement is only counted if the parts have already arrived. Parts in transit are not counted towards completion. The start of fabrication and manufacturing will be at the beginning of next semester. Testing of individual parts will be conducted as soon as the order is received. Testing the subsystem will begin as soon as all the parts are verified to operate accordingly with one another.

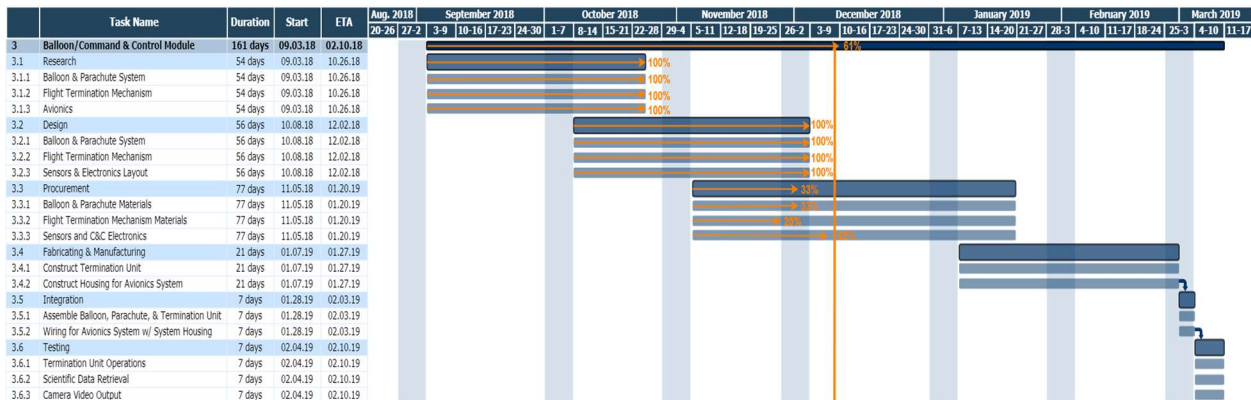


Figure 28: BCCM Combined WBS and Gantt Chart with progress.

2.3.2.1.13 Requirements vs. Implementation

[JK][AY]

ID	Requirements	Parent ID	Implementation	Status
SSDR-24	BalloonSat system shall be capable of releasing the balloon and/or parachute by command of BalloonSat module.	TLSR-03 TLSR-15	FTM to release the balloon and the parachute. RF Transceiver will allow GS to send release commands.	
SSDR-25	BalloonSat module shall collect state-of-health data during the entire flight phase.	TLSR-05	Voltage sensor will check the power level. COSMOS will report if agents are working.	
SSDR-26	BalloonSat module shall collect atmospheric temperatures and pressures during the entire flight phase.	TLSR-05	Temperature sensor and pressure sensor	
SSDR-27	BalloonSat module shall take images pointed in the upwards, downwards, and side directions.	TLSR-05	Cameras in the required directions will be able to take pictures	
SSDR-28	The BalloonSat system shall use flight termination mechanisms to release to the balloon and parachute	TLSR-03 TLSR-15	Two FTMs will be used.	
SSDR-29	The BalloonSat module shall activate autonomous propulsion system only if ocean landing occurs.	TLSR-14	Code will be able to determine if an ocean landing has occurred.	
SSDR-30	The location beacon shall activate when the BalloonSat module makes landfall or, if ocean landing occurs, reaches designated recovery site.	TLSR-12	Code will have beacon activate if landfall occurs. Code will activate beacon when last waypoint is reached.	
SSDR-31	The BalloonSat module shall be capable of powering on/off (recharge state) to recharge batteries via solar cells.	TLSR-16	System will enter power save mode when voltage sensor detects low battery.	
SSDR-32	The BalloonSat module shall end all image, video, and atmospheric data collection once landfall is made.	TLSR-05	Elements not in use for navigation will be turned off by code when flight phase is over.	
SSDR-33	The autonomous navigation system shall be programmed to navigate through pre-designated areas determined by predicted current and weather forecasts.	TLSR-14	Designated areas will be uploaded to the code the day before launch. Weather and current will be uploaded the day before launch.	

2.3.2.1.14 Remaining Issues and Concerns

[AQ][AY]

The remaining issues and concerns are integrating COSMOS on the Aerocore and programming the C&C module and the navigation program. Determining which type of balloon (350g,600g,1200g) to use. The different balloons have different burst altitudes and ascent rates. The weather prediction for the day will determine which balloon to use. Procuring the remaining electrical components is still a remaining issue. Finalizing the connection between the parachute and recovery vehicle to minimize turbulence that the payload experiences. The last concern is

that and the amount of time -required to cut through the nylon rope with the FTM is currently unknown as the configuration will change depending on the tethering plan.

2.3.2.2 Recovery Vehicle and Propulsion

2.3.2.2.1 Subsystem Team Roles & Responsibilities

[TS]

Subsystem Lead - Trevor Shimokusu

- Responsible for communicating subsystem plans with the project manager, and designing the propulsion and steering systems.

Subsystem Member - Reginald Tolentino

- Responsible for the external hull design and materials selection.

Subsystem Member - Christian Feria

- Responsible the designs of the vehicle's internal housing and insulation.

2.3.2.2.2 Changes in subsystem design since PDR

[TS]

Since PDR, the hull design and propulsion system have significantly changed. First, the hull geometry has changed from a flat bottom to a catamaran to stabilize heading control and increase maneuverability. The idea behind a flat bottom hull was to ensure the vehicle remains at the water surface during all instances of a wave in order to extract the most heave motion, and thus generate the most thrust. However, after considering our system is small enough to ride waves regardless of its geometry, the marginal gain in heading stability from a catamaran design was realized to far outweigh that of extra thrust. Moreover, the catamaran also functions to protect the rudders and fin from impact during landing.

Another change since PDR involved the hull material selection. We have decided to use a combination of two hull materials, in a two-part structure consisting of a polyurethane top section and a syntactic foam bottom. Syntactic foam has density of 15 lbs/ft³, which is much higher than that of polyurethane, 2 lbs/ft³, which will thus aid in lowering the system's center of mass to increase roll stability and mitigate the risk of capsizing.

The final notable change since PDR is the removal of an auxiliary propulsion system. After conducting analyses and preliminary testing on the oscillating fin propulsion we proposed during PDR, it was ultimately deemed sufficient for our mission's needs. Thus, to reduce weight, cost and power requirements, the motor and propeller assembly required by the auxiliary propulsion was taken out of the system design.

2.3.2.2.3 RVP Functional (Flow) Block Diagram

[JK][TS]

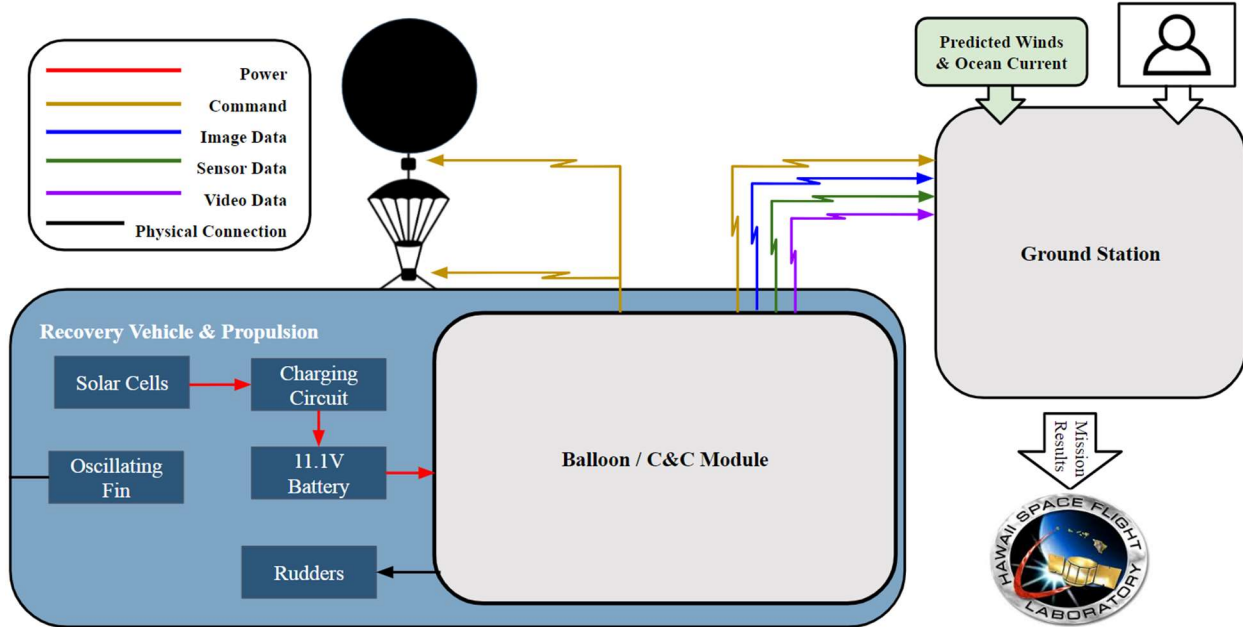


Figure 29: RVP Functional Flow Block Diagram [17]

2.3.2.2.4 Subsystem Weight & Volume Budgets

[CF]

Table 15: Mass and volume budget for RVP

Hull/Structure			
Item	Quantity	Mass (lbs)	Volume (in ³)
Hull	1	2.36	N/A
Propulsion/Steering System			
Item	Quantity	Mass (lbs)	Volume (in ³)
Oscillating Fin	1	0.52	N/A
Steel Connecting Rod	1	0.53	N/A
Rudder	1	0.04	N/A
Rudder Shaft	1	0.02	0.03
Nuts	4	0.09	N/A
Washers	6	0.06	N/A
Stoppers	2	0.14	N/A
Servo Connecting Rod	1	0.01	0.01
Servo horns	2	0.01	0.12
Electrical components			
Item	Quantity	Mass (lbs)	Volume (in ³)

11.1V Battery	1	0.63	12.28
Charging circuit	1	0.08	0.1664
Solar cells	2	0.38	N/A
RVP Total		4.86	12.44
RVP Allocated		4.93	100

The total mass and volume budget for the recovery vehicle along with its structure, propulsion, and electrical components came out to be 4.86 lbs and 12.44 in³, respectively. Both mass and volume budget fall under the allocated budget which means we have little room for adjustments.

2.3.2.2.5 Subsystem Power Budget

[TS]

To simplify power budgets and consolidate all electric powered components together, we have removed the servomotor from the RVP subsystem and placed it into the BCCM subsystem. Therefore, no component in the RVP subsystem requires power input.

2.3.2.2.6 Description

[CF][JK][TS]

Table 16: Parts list for RVP

Part Description	Model/Material	Quantity
Top Hull Section	AeroMarine Polyurethane 2# Foam	1 Gallon kit
Bottom Hull Section	SynFoam SG-15 Castable Syntactic Foam	1 Gallon kit
Hull Seal - 1	Kevlar 49	1 yd Roll
Hull Seal - 2	Loctite Marine Epoxy	0.85 fl. oz.
Fin	PLA Filament	1.75 mm (1kg)
Rudder		
Connecting Rod	High Strength Steel Threaded Rod	1
Fin Stoppers	Alloy Steel Thread-Locking Button Head Hex Drive Screws	2
Nuts	High-Strength Steel Thin Nylon-Insert Locknut	4
Washers	Zinc-Plated Steel Washer for Soft Material	6
Servo Horns	2F/25T Spline Super-Duty Servo Arm	2
Servo Connecting Rod	Uxcell 2mm Dia 100mm Length Stainless Steel Solid Round Shaft Rod	1

Rudder Shaft	Hillman 0.125-in Cold-rolled Weldable Steel Metal Round	1
Solar Panel	Medium 6V 2W Solar Panel	2
Charge Circuit	USB / DC / Solar Lithium Ion/Polymer charger - v2	1
Batteries	Li-ion 18650 Batteries	1

Table 16, above, is a list of parts that make up the recovery vehicle and propulsion system. The top section of the hull will be made out of AeroMarine Polyurethane #2 foam and the bottom section will be made out of SynFoam SG-15 Castable Syntactic foam. Kevlar 49 will be used to act as an external layer for extra protection from impact and Loctite Marine Epoxy will be used for structural reinforcement and to seal off water from getting in the hull. The fin and rudder will be 3D printed using PLA filaments. The propulsion system will consist of connecting rods, fin stoppers, nuts, washers, servo horns, servo connecting rods, and rudder shaft. The recovery vehicles' power system will consist of solar panels, charging circuit, and batteries.

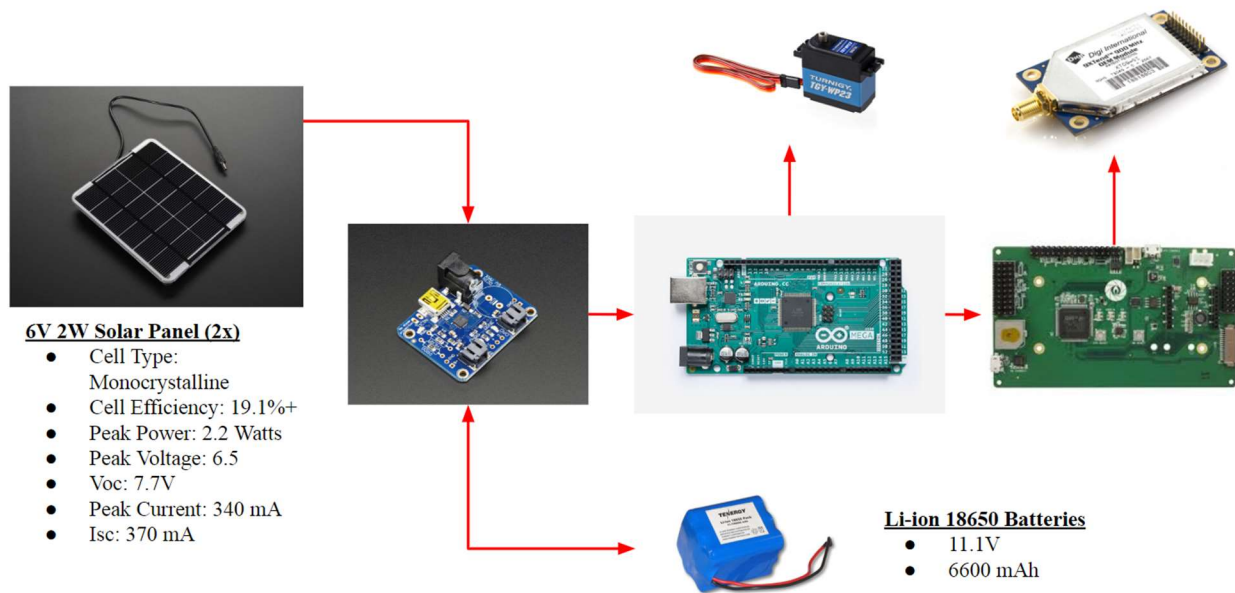


Figure 30: Power System Diagram [19] [20] [21] [22] [27] [28] [29]

The power system diagram (Figure 30) shows how power will be distributed throughout the recovery vehicle, and identifies the main source of power consumption: Arduino, servo motor, AeroCore, and RF Transceiver. Starting from the left, two 6V 2W solar panels will be connected in series to the maximum power point tracking (MPPT) solar charger. The MPPT solar chargers allows the 11.1V 6600mAh battery to both charge by solar panels, and discharge power to the

Arduino. The Arduino Mega 2560 regulates the 11.1V to 5V and provides power to the sensors, cameras, servo motor (for steering the rudder), and Aerocore. From the Aerocore, the RF Transceiver receives power to send signals to the Ground Station.

2.3.2.2.7 Results of Technical Analyses

2.3.2.2.7.1 Hull Thermal Analyses

[TS]

To approximate the heat input required to maintain the hull’s internal temperature at 0°C, a 1-D heat transfer problem was solved, considering each surrounding wall of the internal housing volume as a flat insulative wall. This simplified approach was executed to obtain a conservative result of heat input, higher than what we anticipate will actually occur.

By considering the coldest flight temperature, -55 C, as the external temperature along with an internal temperature of -20 C which gives most of the electronics a 20 C buffer from their low operating limit temperature of -40 C, we have calculated the heat loss for all 6 rectangular faces of the internal volume through with equation 7.

$$q = -kA \frac{dT}{dx} \quad (7)$$

Here, q represents the heat rate, A represents the heat transfer area, and $\frac{dT}{dx}$ is the temperature gradient across the walls of each side. Since only the top section of the hull is only made of polyurethane, the the thermal conductivity is given as 0.03 W/mK [30]. Table 17 summarizes the heat rates through each side of the internal housing.

Table 17: Summary of maximum heat losses during flight

Direction	Thermal Conductivity (W/mK)	Area (in ²)	Area (m ²)	Internal temp (C)	External Temp (C)	Wall Thickness (in)	Wall Thickness (m)	Heat Loss (W)
Top	0.030	96.640	0.062	-20.000	-55.000	0.950	0.024	2.713
Bottom	0.030	106.524	0.069	-20.000	-55.000	1.000	0.025	2.841
Front	0.030	19.150	0.012	-20.000	-55.000	1.250	0.032	0.409
Back	0.030	19.150	0.012	-20.000	-55.000	1.250	0.032	0.409
Side	0.030	30.000	0.019	-20.000	-55.000	1.500	0.038	0.533
Side	0.030	30.000	0.019	-20.000	-55.000	1.500	0.038	0.533
Total								7.438

Considering much of this heat loss can be compensated with the heat output from all of the avionics, a heat input lower than this value will actually be required. Moreover, there is a multitude of available heating sources on the market that can easily meet this heating requirement such as lightweight USB heating pads or hand warmers.

2.3.2.2.7.2 Hull Stability

[TS] [RT]

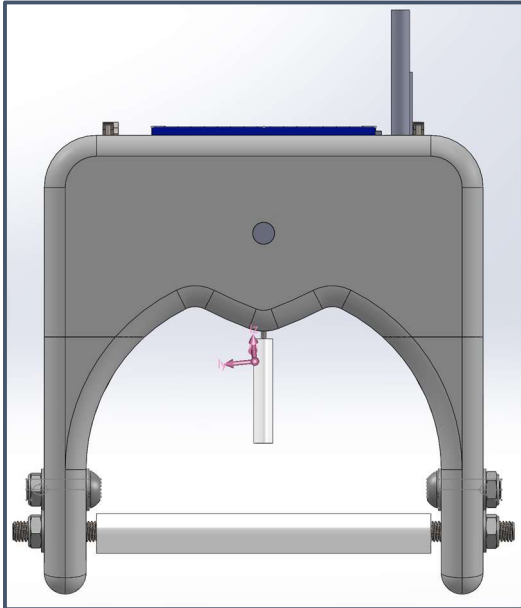


Figure 31: Center of gravity location on recovery vehicle

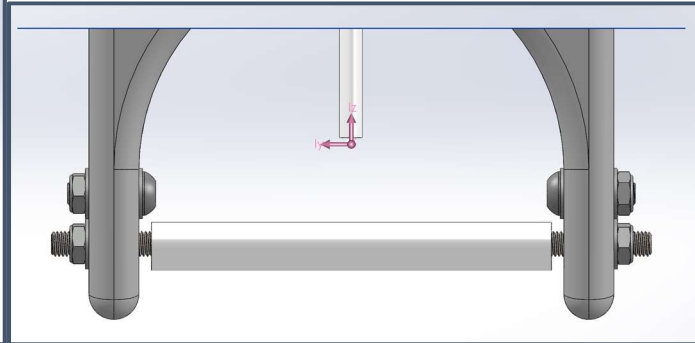


Figure 32: Center of buoyancy location on recovery vehicle with water-line indicator

As a key feature of the recovery vehicle to self-right upon undesired water landing, the hull stability was numerically analyzed utilizing the buoyant force equation below in Equation 8:

$$F_{df} = \rho_{H_2O} g V_{df} \quad (8)$$

where F_{df} is the force of the displaced fluid, ρ_{H_2O} is the density of water, g is gravity, and V_{df} is the volume of the displaced fluid. From the SolidWorks model, Figure 31 was captured to visually illustrate the location of the center of gravity (CoG) of the entire module, which includes the propulsion and avionic components. The water-line in Figure 32 was determined by rearranging the buoyant force equation to solve for V_{df} , which was calculated at 166.2 in³. Therefore, all components above the water-line were removed to obtain the center of buoyancy (CoB) located in Figure 32. By comparing the two figures, it is evident that the CoG is greater than the CoB. From this analysis, this means that our system in this configuration will not be able to self-right itself in the event that it lands unconventionally. However, current action is being taken to make the necessary adjustments to elevate the CoB and lower the CoG. For instance, shortening the leg appendage on the bottom will result in the CoB rising on the hull due to the volume displaced increasing. In addition, adjusting the ratio between the polyurethane and syntactic foam to decrease the syntactic foam percentage will lower the center of gravity due to syntactic foam having approximately 8 times the mass density than polyurethane foam. These adjustments would then make the CoB greater than the CoG to make our system self-righting.

2.3.2.2.7.3 Hull Stability

[RT]

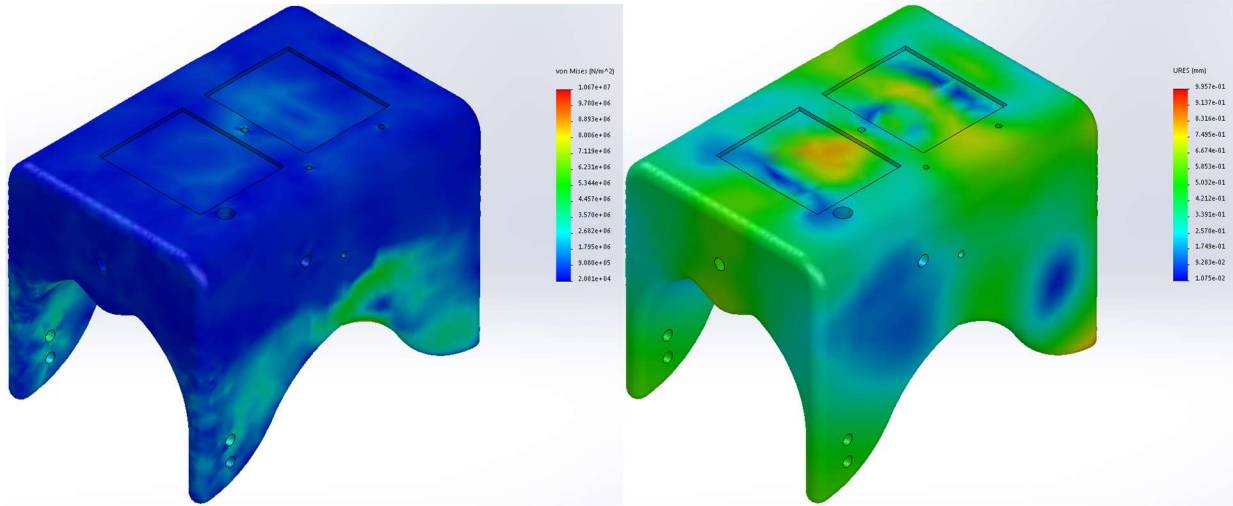


Figure 33: FEA Drop Test Simulation on Front Face

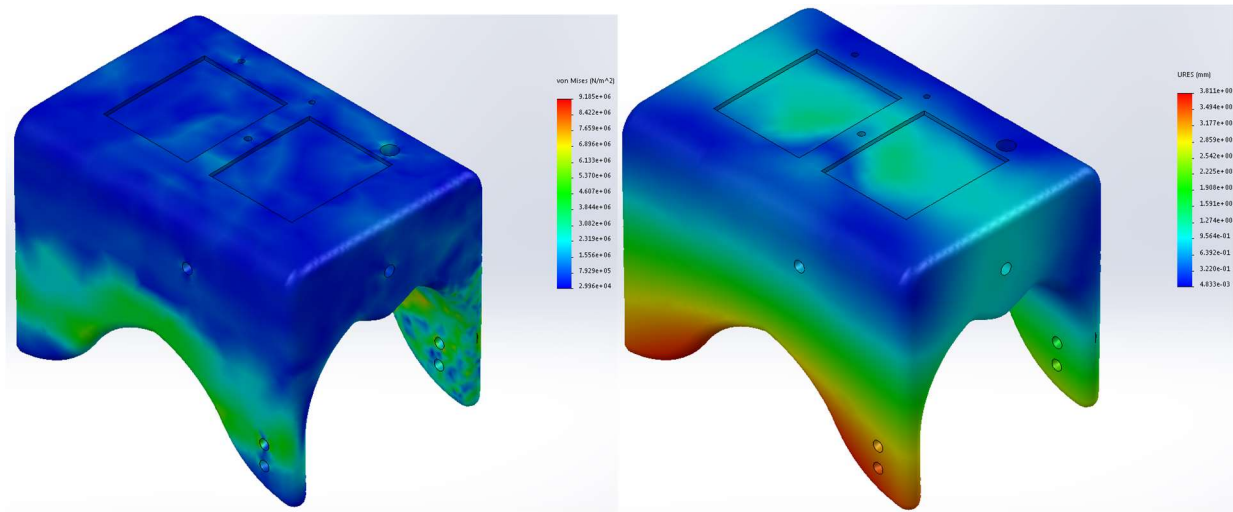


Figure 34: FEA Drop Test Simulation on Side Face

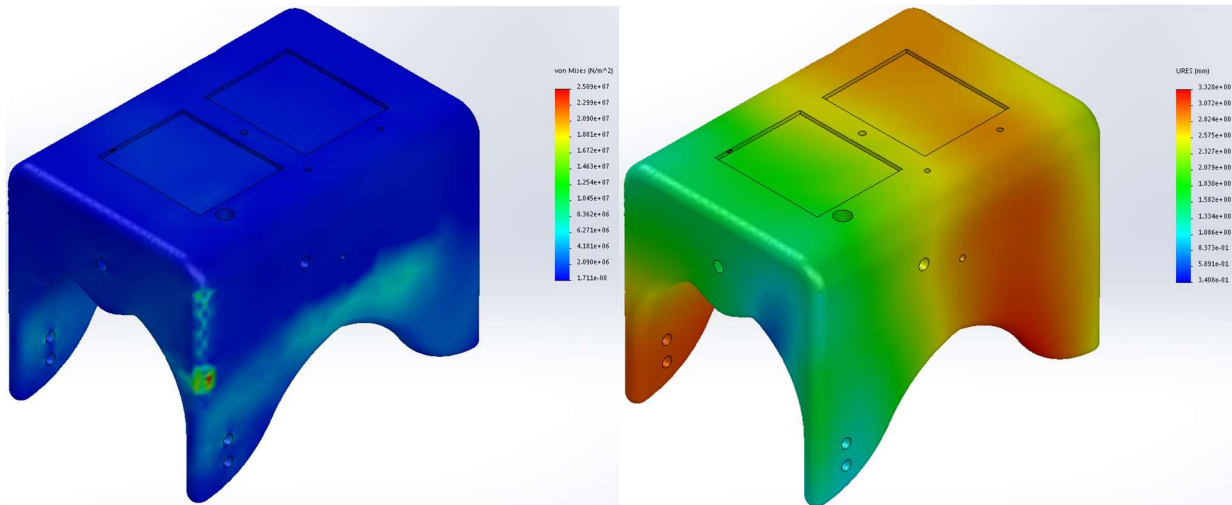


Figure 35: FEA Drop Test Simulation on Corner Face

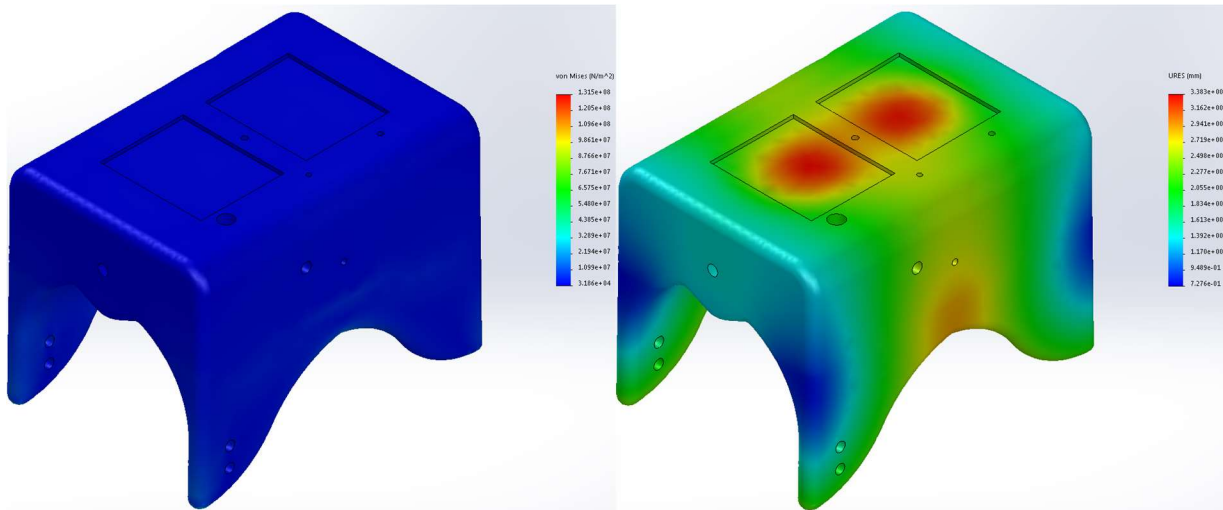


Figure 36: FEA Drop Test Simulation on Bottom Face

Table 18: Von Mises Stress and Displacement Summary from FEA Drop Test Simulation

Scenario	Front Face	Side Face	Corner Face	Bottom Face
Von Mises Stress [lb_f/in^2]	1,547.55	1,332.17	3,639.00	19,072.46
Displacement [in.]	0.039	0.150	0.131	0.133

Further analysis was conducted on the hull structure utilizing the Finite Element Analysis (FEA) Drop Test simulation on SolidWorks. A total of four tests were conducted with results displayed above in Figures 33 to 36, which differ based on the direction of the velocity in each scenario: perpendicular to the front, side, corner, and bottom faces respectively. The setup parameters in each scenario had the direction of gravity in the same direction as its velocity with the velocity having a magnitude of 30 ft/s (twice the amount expected). Since just the hull structure was analyzed, which excluded the internal and external components, the total weight of the system

was approximately 2 lbs. (3 times less than the expected weight of the system); however, to account for the lack of mass, the velocity was doubled. By doing so, this would result in a much greater force than expected as doubling velocity results in a factor of times four due to the square relationship in Equation 9. Comparing all four scenarios in Table 18, the greatest maximum Von Mises stress was determined to be on the bottom face with stress recorded at $1.907 \cdot 10^{-4}$ lb_f/in² and greatest maximum displacement on the side face at approximately 0.15 inches. From these results, there are no immediate signs of catastrophic failure of the hull structure despite the impact force being greater than what the hull will be expected to experience, which suggests that the current state of the hull will not fail due to water landing as conservative measures were taken with the target surface being assumed to be rigid. Additionally, it is important to note that this analysis only took into account the foam materials without the epoxy resin and Kevlar fibers on the hull surface which will add reinforcement to the structure upon impact, thus lowering the displacement in all four scenarios.

As a comparative study, we have conducted FEA tests on the fin to analyze the difference in stress distributions developed when dropped on its side and on its face. The force used in these simulations was obtained by considering the all of the kinetic energy of a 15 ft/s impact speed converting to a deformation of 0.5 inch with no heat dissipation. This is illustrated in equation 9,

$$F = \frac{mV^2}{2d} \quad (9)$$

where F is the calculated impact force, m is the mass of the system taken to be 6 lbm, V is the 15 ft/s descent speed, and d is the impact deformation assumed to be 0.5 inches. These inputs yield a force of 503 lbf, which was used in the static studies performed on the fin. It should be emphasized that since the fin and rudder are going to be made out of 3D printed PLA plastic materials, Solidworks simulations were not used to identify factors of safety and failure rates due to material input limitations that don't accurately capture the nonlinear nature of 3D printed materials. Therefore, these simulations were only used to determine the best configuration for impact. Figures 37 and 38 display the results of these simulations.

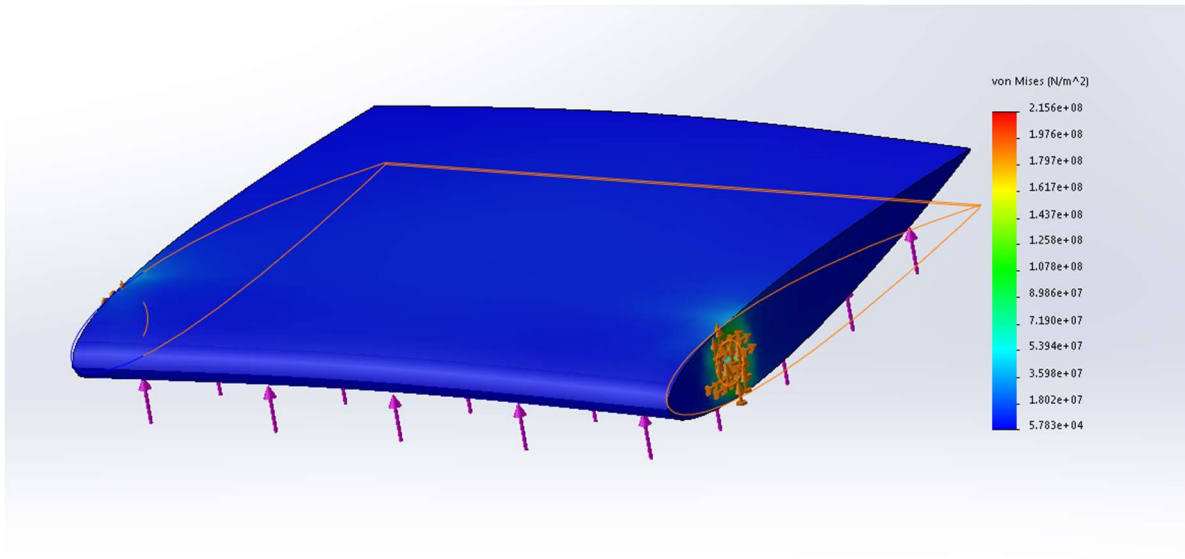


Figure 37: FEA results of the fin during a bottom impact

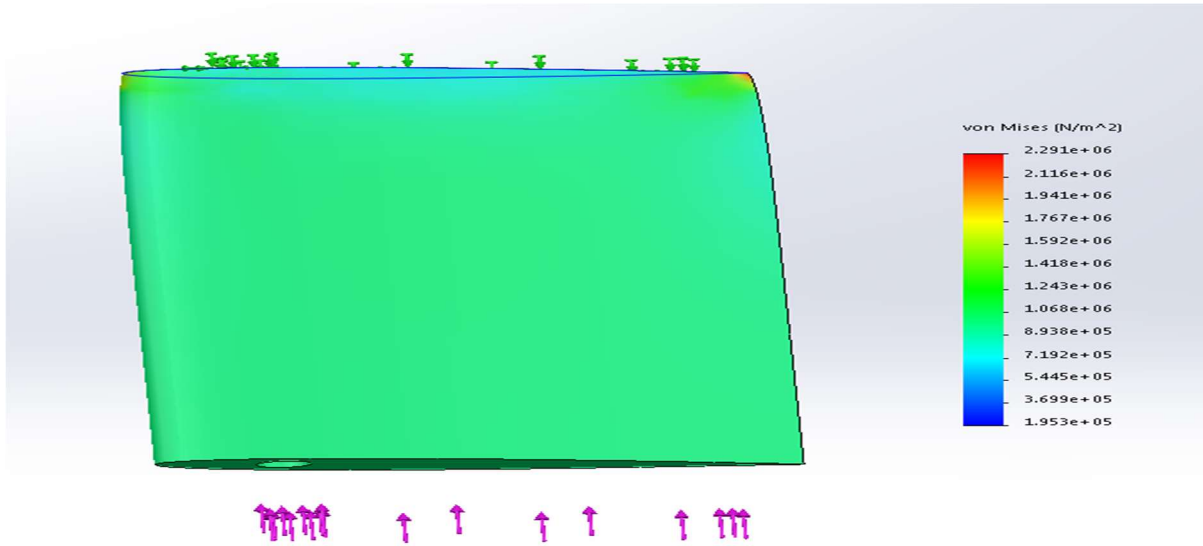


Figure 38: FEA results of the fin during a side impact

As seen above the side impact yields a much lower maximum von Mises stress, 2.29 MPa than that of the bottom impact, 216 MPa. Therefore, to minimize the risk of fracture to the fin, a side impact is preferred.

A failure rate for the rudder was similarly not found due to the material limitations in Solidworks. We thus plan to conduct testing on all 3D printed parts to observe how they behave over time when subjected to impacts. Moreover, given their low cost and quick time to manufacture, multiple parts can be made readily available to exploit the safest possible landing assembly.

2.3.2.2.7.3 Propulsion and Steering Analysis

[TS]

To analyze the performance of the oscillating fin propulsion, simple harmonic motion was assumed to model the heaving motion of waves. The heave was thus assumed to be given by equation 10,

$$h(t) = A\sin(\omega t) \quad (10)$$

where, h represents the surface vehicle's vertical position above the flat waterline, A represents the wave amplitude, and ω represents the wave frequency. The wave heave velocity can then be obtained to from equation 11.

$$v(t) = \frac{dh}{dt} = A\omega\cos(\omega t) \quad (11)$$

These values of heaving velocity, along with a guessed horizontal velocity value for different wave conditions given by the root mean square of the wave heave velocity function, can be used to determine the angle that relative flow makes with the horizontal. The difference between this angle and the angle between the fin and the horizontal, assumed to have a maximum value of 45 deg and time varying behavior similar to the heaving velocity, is the angle of attack, given by equation 12.

$$\alpha(t) = \tan^{-1} \frac{u_0}{v(t)} - \frac{\pi}{4} \cos(\omega t) \quad (12)$$

Stoppers will be placed above the fin such that the maximum angle between the fin and the horizontal is 45 deg. Figure 39, below, displays the angle of attack for the fin during an instant where the system is heaving up.

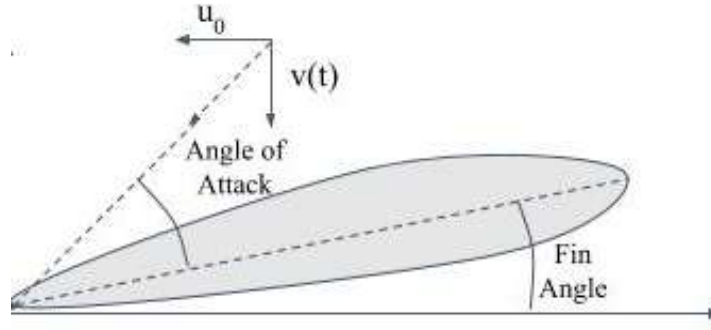


Figure 39: Illustration of the oscillating fin during a wave upstroke

By limiting the angle between the fin and horizontal to 45 deg, small angles of attack are achieved for a wide range of sea states. Approximations for coefficients of drag and lift for any instant of time can then be obtained through equations 13 and 14, respectively [31]

$$C_L(t) = 2\pi\alpha(t) \quad (13)$$

$$C_D(t) = 1.28\sin(\alpha(t)) \quad (14)$$

These coefficients can then be used to calculate the net thrust, F_T , which is the difference between the horizontal components of lift and drag generated by the fin. This is given by equation 15, below.

$$F_T(t) = \frac{1}{2}\rho cb(u^2 + v^2(t))\left[C_L \sin\left(\tan^{-1}\frac{v(t)}{u_0}\right) - C_D \cos\left(\tan^{-1}\frac{v(t)}{u_0}\right)\right] \quad (15)$$

Here ρ is the density of water, c is fin chord length, b is the fin span, and u is the speed of advance. To find the speed of advance, u , this net thrust can then be equated to the total drag on acting on the system, D_{Hull} , which is a function of the speed of advance, given by equation 16.

$$D_{Hull} = 0.074Re^{-1/5}\frac{1}{2}\rho LWu^2 + 2\left[C_{D,l}\frac{1}{2}\rho(1.5c)W_l u^2\right] + C_{D,r}\frac{1}{2}\rho c_r b_r u^2 \quad (16)$$

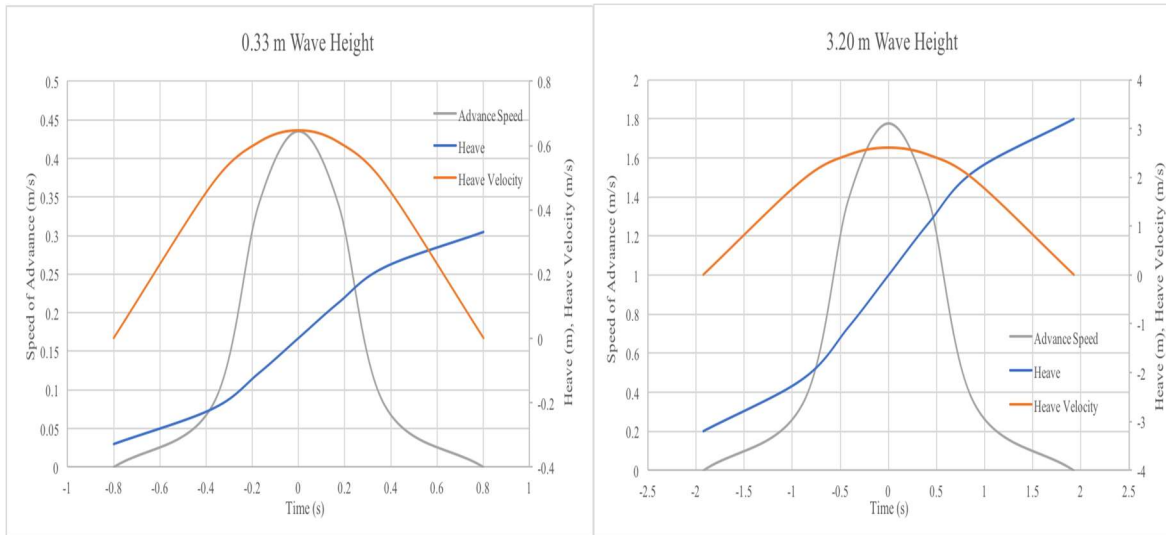
Here, Re is the Reynolds number assumed to be constant with u_0 , L is the hull length, W is the hull width, W_l is the hull leg width, $1.5c$ is the distance from the bottom of the hull leg to waterline, $C_{D,l}$ is the coefficient of drag for c-shaped frontal section of the hull length, $C_{D,r}$ is the

coefficient of drag of the rudder with zero attack angle, c_r is the rudder chord length, and b_r is the rudder span. The first term in this equation represents the drag on the hull bottom, which can be approximated as turbulent drag over a flat plate [32], the second term represents the drag on the hull legs, and the third represents the drag on the rudder. We have not accounted for forces due to currents in this equation because the currents flow in the shore direction at the north side of the island, which is where we are planning to launch our system. Therefore, neglecting this force term can be considered conservative, since there will likely be assisting current forces during the mission.

After equating the net thrust and total hull drag, the speed of advance can be obtained through equation 17, assuming $C_{D,l} = 1.2$ [32] and $C_{D,r} = 0.007$ [33].

$$u = \sqrt{\frac{-\frac{1}{2}cbv^2(t)[C_L \sin(\tan^{-1} \frac{v(t)}{u_0}) - C_D \cos(\tan^{-1} \frac{v(t)}{u_0})]}{\frac{1}{2}cb[C_L \sin(\tan^{-1} \frac{v(t)}{u_0}) - C_D \cos(\tan^{-1} \frac{v(t)}{u_0})] - 0.037Re^{-1/5}LW + 1.8cW_t + 0.0035c_r b_r}} \quad (17)$$

This speed of advance was plotted, shown in figures 40, for two different sea states representative of the calm and rough operating limits we anticipate the system being subjected to.



Figures 40: Predicted speeds of advance for a sea state 2 (left) and sea state 6 (right)

For sea state 2 oceanic conditions, which represent calm waters, the average predicted speed of advance is 0.195 m/s, while for a sea state of 6, which represents very rough conditions, the average predicted speed is found to be significantly higher at 0.798 m/s. Since these sea states represent the lower and upper limits of anticipated operating conditions, an averaged advance speed can be calculated as 0.497 m/s which would allow the recovery segment to be completed

in roughly 4.5 hours. However, due to unpredictable factors such as competing forces due to currents and other environmental factors, we are allowing for a total recovery time of 10 hours.

Steering will be accomplished by supplying full power from the charging circuit to the servo motors in order to turn the rudder left or right depending on heading data acquired by the IMU. The servo linkage used for steering will involve two servo horns connected by a Z-bar link that are attached to the servo motor and rudder rod. This linkage assembly is shown in figure



Figure 41: Image of the servo linkage that will control steering

The left servo horn in the figure will be mounted onto the servo motor shaft, while the right servo horn will be attached to the rudder connecting rod, which will be fixed to the rudder with an adhesive. Rotational motion transmitted to the rudder, driven by the servo motor, will be accomplished by ensuring both servo horns and parallel at all times, with the Z-bar connecting rod always parallel to the axis on which the servo motor and rudder shaft lie. With the rudder rotated relative to incoming flow, a lift force generated will act perpendicular to the heading of the boat, thus generating a moment about the system's longitudinal center of gravity to alter the system's heading. Moreover, due to the nonlinear equations of motion governing this type of rotation, testing will be conducted to determine optimal angles for turning rather than analysis.

2.3.2.2.7.4 Battery Operation Time

[JK]

The operation time of the BalloonSat, using Li-ion 18650 11.1V 6600mAh battery pack, can vary depending on the time spent in each operation phase: ascent flight, descent flight, and recovery. The BalloonSat will ascend and descend the balloon burst altitude at different speeds. Furthermore, the time spent in the ascend and descend phase will be different. The recovery time will vary depending on the distance between the landing location and the designated recovery site. To approximate the average battery operation time, the BalloonSat will only drain the battery capacity to 20% before going into a recharge state and the average wattage from the three phases will be used to calculate operation time. Table show the electrical components in operation during each phase with the power consumed.

Table 19: Electrical Power Consumption During Each Operational Phase

Component	Ascent Flight Phase Power Usage (W)	Descent Flight Phase Power Usage (W)	Recovery Phase Power Usage (W)
Pressure Sensor	0.06	0.06	0
Temp. sensor	0.792	0.792	0
Arduino	2	2	2
SD Card	0.75	0.75	0
Aerocore	1.65	1.65	1.65
Image / Video Camera	3.15	3.15	0
Audio beacon	N/A	N/A	N/A
Servo motor	0	0	0.020835
RF Transceiver	3.65	3.65	3.65
Video transmitter	6	6	0
Voltage sensor	0.2	0.2	0.2
Wireless RF Transceiver	0.001	0.001	0
Total	18.253	18.253	5.52

With the known power used during each phase, the average battery operation time (in hours) can be calculated using Equation (18) and (19).

$$\text{Energy Capacity to Charge @20\%} = (11.1V)(6600mAh)(80\%) \quad (18)$$

$$\text{Average Battery Operation Time} = \frac{\text{Energy Capacity to Charge @ 20\%}}{W_{\text{ascent}} + W_{\text{descent}} + W_{\text{Recovery}}} \quad (19)$$

Where W_{ascent} is the power used during the ascent flight phase, W_{descent} is the power used during the descent flight phase, and W_{recovery} is the power used during the recovery phase.

The results of the calculation show that the average operation time of the Li-ion 11.1V 6600mAh battery will be approximately 5 hours. When the burst altitude and the landing location is known with the flight predictor, the time spent in each phase can be calculated using the ascent velocity, descent velocity, and average recovery vehicle speed using Equation (20).

$$\text{Time} = \frac{\text{distance}}{\text{velocity}} \quad (20)$$

With the exact phase times, the exact operation time of the Li-ion 11.1V 6600mAh battery can be determine using Equation (21) and Equation (22).

$$Power\ Consumption = \frac{W_{ascent}(T_{ascent})+W_{descent}(T_{descent})+W_{recovery}(T_{recovery})}{T_{ascent}+T_{descent}+T_{recovery}} \quad (21)$$

$$Battery\ Operation\ Time = \frac{Energy\ Capacity\ to\ Charge\ @20\%}{Power\ Consumption} \quad (22)$$

2.3.2.2.7.5 Solar Panel Analysis

[JK]

The BalloonSat will consumes less power with no electrical propulsion. Furthermore, to reduce weight, the BalloonSat will use two 6V 2W solar panels (series) to recharge the battery. The battery will be charged by the solar cells and discharged to the system using the Solar Lithium Ion/Polymer Charger version 2 by Adafruit. To determine the time for the Li-ion 11.1V 6600mAh battery to be charged by the solar panels, the efficiency of the Solar Lithium Ion/Polymer Charger will be assumed to be 95%, similar to other maximum power point tracking solar chargers [34]. In addition, the assumption that each solar panel will generate full 2 watts will be made to simplify analysis. The power generated by the solar panel to the battery can be calculated using Equation (23).

$$Solar\ Power = n_{panels}W_{solar}\eta_{MPPT} \quad (23)$$

Where n_{panel} is the number of the solar panels used, W_{solar} is the watts generated by each solar panel, and η_{MPPT} is the efficiency of the maximum power point tracking solar charger.

The results show that the two 6V 2W solar panels will generate 3.8 watts to the battery. The time to recharge the battery at 20% capacity can be calculated using Equation (18) and Equation (24).

$$Battery\ Charge\ Time\ @20\% \ Capacity = \frac{Energy\ Capacity\ to\ Charge\ @20\%}{Solar\ Power} \quad (24)$$

The results show that the two 6V 2W solar panels will charge the Li-ion 11.1V 6600mAh at 20% capacity within 15 hours. However, Hawaii has only 6 sun hours per day on average [35]. Furthermore, the percent of charge expected in one day can be approximated using Equation (25).

$$\%Charge = \frac{Solar\ Power(Sun\ Hours)}{Energy\ Capacity\ to\ Charge\ @20\%} \quad (25)$$

The results show that the two 6V 2W solar panels will charge the Li-ion 11.1V 6600mAh at 20% capacity by 38.7% within 6 sun hours.

2.3.2.2.8 Risk Analysis

[CF][TS]

Table 20: Risk Analysis for RVP

Identification	Consequence	Probability of Occurrence	Risk Rank	Risk Mitigation (Reactive , Proactive)
Recovery system is unable to overcome ocean conditions	5	4	High	<ul style="list-style-type: none"> - Optimize the vehicle hull design to reduce drag - Implement a fail-safe propulsion system - Obtain stronger motors to provide required thrust to overcome drag
Recovery vehicle capsizes	4	4	High	<ul style="list-style-type: none"> - Optimize the distribution of weight in the module
System breaks upon landing	5	3	High	<ul style="list-style-type: none"> - Reinforce structural supports connecting fin and hull - Conduct FEA simulations to locate and reduce high local stress concentrations
Hull leaks causing water damage to electronics	4	2	Medium	<ul style="list-style-type: none"> - Conduct waterproof tests to ensure the hull is watertight
Vibration damaging electronic components or hull	3	3	Medium	<ul style="list-style-type: none"> - Ensure tight and secure fittings and connections between motors and propellers/rudders

2.3.2.2.9 Subsystem FMECA

[CF][TS]

Table 21: FMECA for RVP

Process	Potential Failure Mode	Potential Effects	Severity of Effects (SEV)	Probability of Failure (OCC)	Invisibility of Failure (DET)	Criticality	RPN	Rank
Recovery Phase	Hull fracture	Breaking upon landing will cause the recovery vehicle dysfunctional	8	5	3	1	120	3
	Hull leakage	Water entering the recovery vehicle will damage avionics and will sink into the ocean	10	3	3	1	90	4
	Propulsion component failure	A broken propulsion system will not provide enough thrust	9	5	3	1	135	2
	Steering component failure	A broken steering system will not provide turning	9	5	3	1	135	2
	Capsize	An overturned recovery vehicle will be dysfunctional and irretrievable	9	5	5	1	225	1

The FMECA shown in Table 21 above, identifies all the potential failure modes of the RVP subsystem and the effects that these failures modes can have on our RVP subsystem during the recovery phase. Severity, Occurrence, and Detection are rated from a scale of 1 through 10 with 1 being least likely and 10 being very likely. As can be seen, highlighted in purple are the top four potential failure modes that pose the most threat to the success of our mission. All failure modes have a criticality rating of 1, meaning that should any of these failure modes occur, total loss of the vehicle or total failure of the mission would occur.

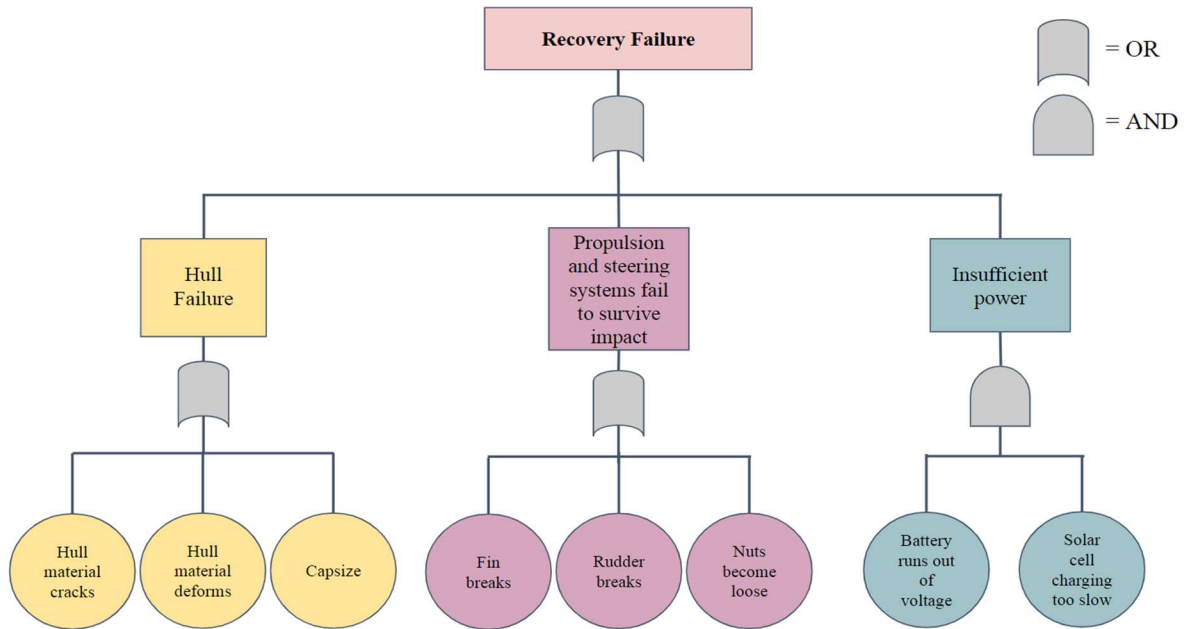


Figure 42: Fault tree analysis for RVP

Figure 42 shows a fault tree analysis of the RVP subsystem. The purpose of a fault tree analysis is to help identify potential causes of system failures, similar to FMECA. As shown above, the lower level events can cause the middle events to happen which can cause the main event to happen resulting in a recovery failure.

2.3.2.2.10 Detailed Test Plan

[TS]

Table 22: Detailed testing plan for RVP

Test	Location	Procedure	Success Criteria
Waterproof	Lab with tank access	<ol style="list-style-type: none"> 1. Fill tank of water with volume larger than that of the vessel 2. Submerge vehicle fully in water 3. Hold the vehicle submerge for 3-5 minutes. 4. Observe for air bubbles 5. Inspect vehicle for water leakage. 6. Repeat 3 times. 	<ul style="list-style-type: none"> - No signs of air bubbles - No water leakage
Drop Test	Beach	<ol style="list-style-type: none"> 1. Drop the hull in water and land from height a of 5 ft to simulate drops with 2x the maximum allowable kinetic energy 2. Retrieve vehicle 3. Repeat 3 times. 	<ul style="list-style-type: none"> - Hull structure and control surfaces do not fracture - Electronic components remain fully functional
Insulation	HSFL Thermo-vacuum	<ol style="list-style-type: none"> 1. Connect thermocouples to DAQ system 2. Apply thermocouples and hand warmers in internal housing 3. Place the system into thermal vacuum chamber at -50°C for one hour 4. Monitor temperature over time 	<ul style="list-style-type: none"> - The internal hull temperature remains within electronic operating limits
Self-righting	Pool, Holmes Hall 142, or Beach	<ol style="list-style-type: none"> 1. Place system in water upside down 2. Wait and observe the system's behavior 3. Place system on its side 4. Wait and observe the system's behavior 	<ul style="list-style-type: none"> - System returns back to vertical position
Thrust	Holmes Hall 142, Beach	<ol style="list-style-type: none"> 1. Place system in water 2. Allow the system to heave up and down with waves 3. Record distance traveled over 30 second intervals for different wave heights 	<ul style="list-style-type: none"> - System advances in forward direction with an average speed of 0.15 m/s
Steering	Holmes Hall 142, Beach	<ol style="list-style-type: none"> 1. Advance the system in its forward direction by subjecting the system to waves 2. Supply power to servo motor 	<ul style="list-style-type: none"> - System turns in correct direction (left when rudder turns CW and right when rudder turns CCW from top view)

2.3.2.2.11 Subsystem WBS

[RT]

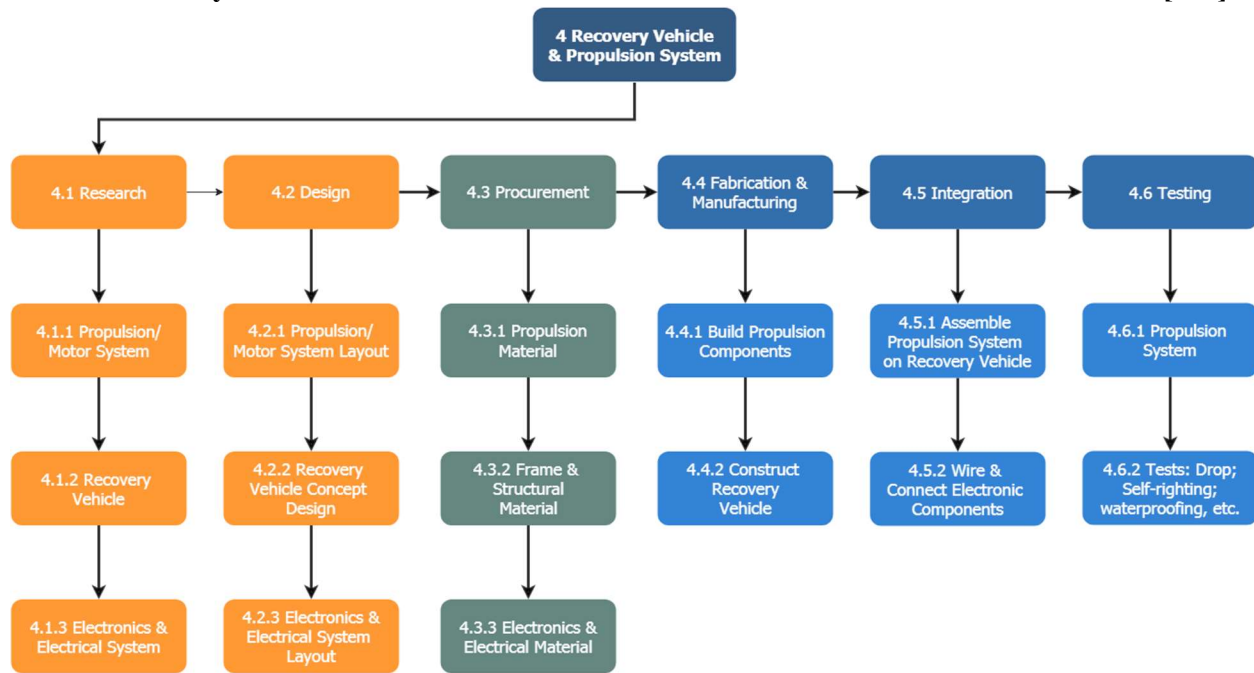


Figure 43: WBS for RVP

Figure 43 shows the work breakdown structure of the RVP subsystem. Once all parts are ordered, received, and tested we will begin the fabrication and manufacturing of the hull as well as assembling the propulsion system.

2.3.2.2.12 Subsystem Schedule WBS and Gantt Chart

[RT]

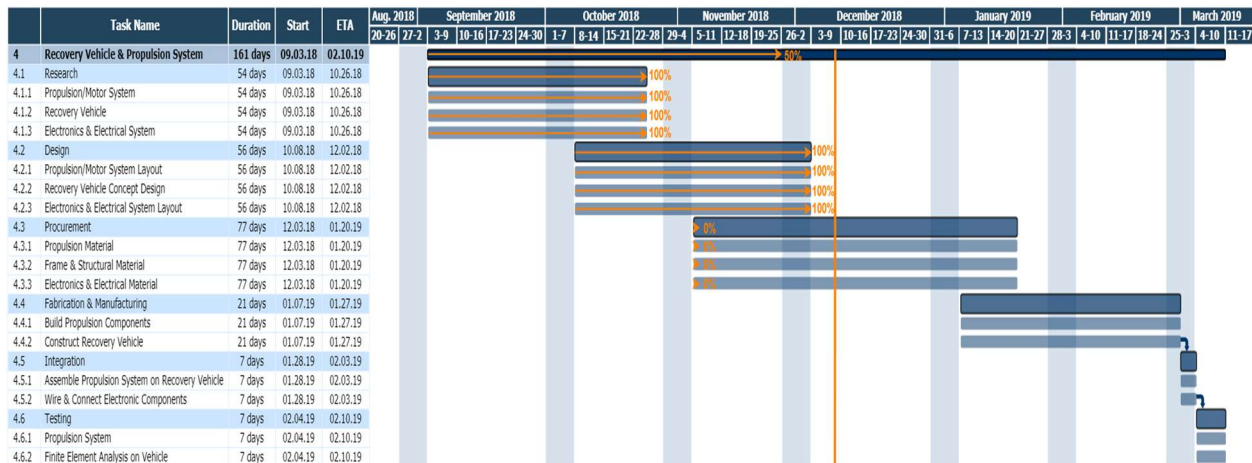


Figure 44: Gantt Chart with integrated WBS

As shown in Figure 44, we are currently finalizing all parts that needs to be purchased for each subsystem. All parts will be ordered during the winter break and hopefully we receive them by early January. As soon as all parts are received, we will test every part to make sure they are not

defective and are fully functional. Once the testing of every part is clear, we will begin fabrication and manufacturing of the hull, assembly of the propulsion system, and configure the avionics within the hull.

2.3.2.2.13 Requirements vs. Implementation

[CF][JK]

ID	Requirement/Constraint	Implementation	Status
SSDR-34	The BalloonSat recovery module structure/hull shall maintain the temperature of the payload within its operating limits 0°C to 70°C.	<ul style="list-style-type: none"> ● Hand warmers as temporary heat source ● Insulative hull material 	Yellow
SSDR-35	The BalloonSat recovery module structure/hull shall provide a Factor of Safety of at least 2.0 when subjected to landing impact.	<ul style="list-style-type: none"> ● Durable hull material ● Design with minimal stress concentration 	Yellow
SSDR-36	The BalloonSat recovery module structure/hull shall return back to its vertical position in no more than 5 seconds in the event of capsize.	<ul style="list-style-type: none"> ● Design with center of gravity lower than center of buoyancy 	Yellow
SSDR-37	The BalloonSat module shall utilize its location and orientation data to provide power and actuate the steering system.	<ul style="list-style-type: none"> ● GPS and IMU data input to microcontroller 	Red
SSDR-38	The propulsion system shall provide sufficient thrust to advance the at an average speed of at least 0.15 m/s.	<ul style="list-style-type: none"> ● Oscillating fin 	Yellow
SSDR-39	The BalloonSat module structure/hull shall protect electronic components from water exposure.	<ul style="list-style-type: none"> ● Waterproof epoxy resin ● Waterproof adhesives between parts 	Red

2.3.2.2.14 Remaining Issues and Concerns

[CF]

The biggest issue we need to address involves the center of buoyancy and center of gravity of the recovery vehicle. Currently the center of gravity of our recovery vehicle is greater than the center of buoyancy, which means our recovery vehicle won't be able to self-right if it capsizes. To resolve this issue, we will be lowering the center of gravity by finding the right ratio of polyurethane and syntactic foam. Also, we will elevate the center of buoyancy by shortening the leg appendage.

Another issue we need to address is the unavailability of 3D printing materials in the Mechanical Engineering Department. Although we have access to the 3D printers, we will have to purchase

our own filaments to 3D print the fin and rudder for our propulsion system. The last issue we need to address is safety training to properly handle epoxy and foam during the manufacturing stage of our project. The recovery vehicle and propulsion subsystem members must be well trained and knowledgeable when using epoxy and foams because may be complicated to use and contain hazards that may be detrimental to our health.

2.3.2.3 Ground Station

2.3.2.3.1 Subsystem Team Roles & Responsibilities

[BI]

Subsystem Lead - Bryson Inafuku & Subsystem Member - Ian Fujitani

- Responsible for communicating with PM on subsystem plans, monitoring and assigning subsystem tasks, and sharing updates/statuses on subsystem at team meetings.
- Responsible for all COSMOS programming and keeping track of all hardware that will be used for the ground station such as the antenna, computer, modem, video receiver, LCD monitor, and the external battery source.
- Responsible for selecting a launch site, predicting the flight path of the C&C module, and obtaining flight permissions.

2.3.2.3.2 Ground Segment Architecture

[BI]

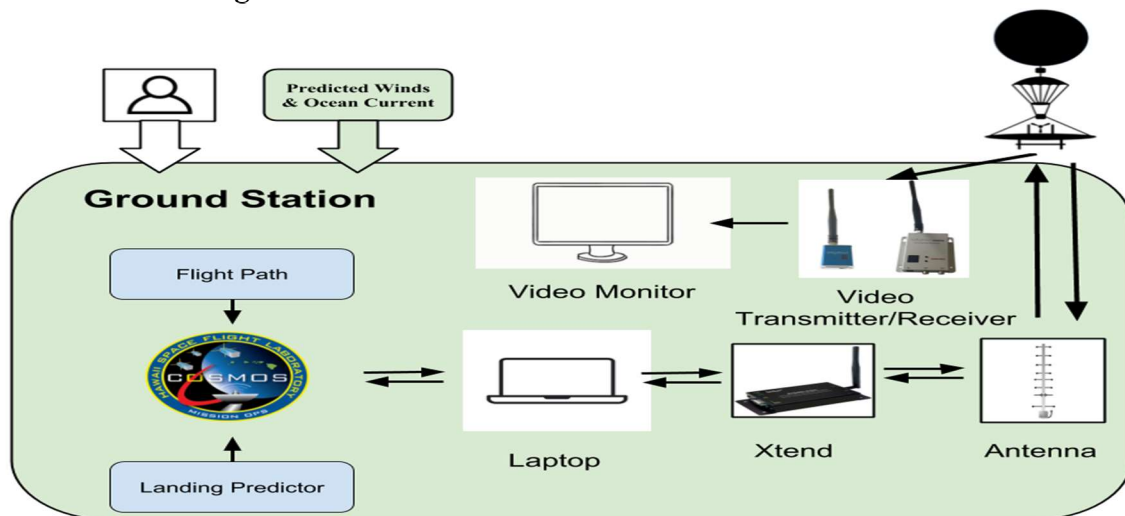


Figure 45: Ground Segment Architecture [17]

In the figure above is the ground segment architecture. It's very similar to the functional flow block diagram. Data will be sent to and from the Balloon/C&C Module to the antenna at the ground station, then through the Xtend modem, and to the laptop to display. Video data will be sent from the Balloon/C&C Module to the video receiver at the ground station and then sent to the video monitor to display a live stream video. The two external interfaces are the user and the predicted winds and ocean currents. The difference from the functional flow block diagram is that COSMOS is shown being integrated. There are two different programs that will be associated with COSMOS which is the landing predictor and flight path software.

2.3.2.3.3 Changes in subsystem design since PDR

[IF]

For ground station, the single item that has changed is the video transmitter. The specifications of the video transmitter presented in PDR was insufficient for covering the 100,000 feet of distance for the UHABS-6 mission. With new knowledge and expectations of data transmission and its capabilities, the ground station has selected a new video transmitter-receiver set. The most notable difference between the old and new transmitters is that the old transmitter had a transmission power of 700 mW, while the newly selected transmitter has a transmit power of 7000mW [36,37]. The justification for this change may be easier understood after reviewing the analyses performed, but greater power generally results in greater transmission distance. The new transmitter is also light, as to preserve the weight allowance of the BalloonSat. This is the reasoning behind the selection of the new video transmitter for the mission.

2.3.2.3.4 GS Functional (Flow) Block Diagram

[BI][IF]

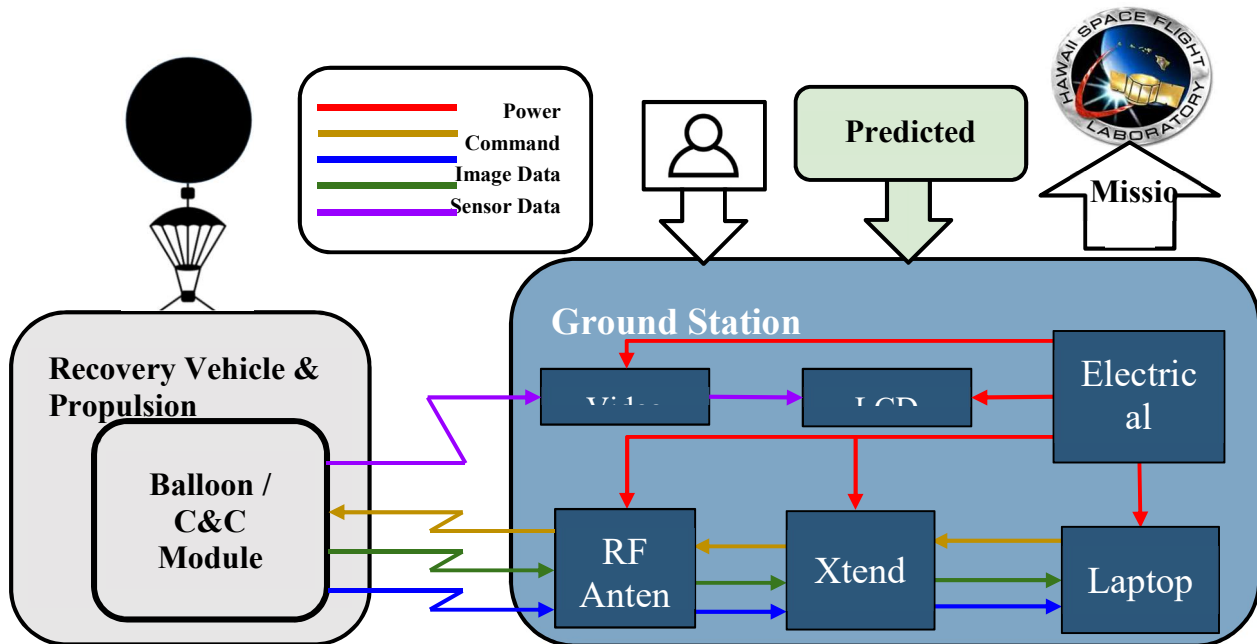


Figure 46: Ground Station Functional Flow Block Diagram [17]

In the Figure above is the functional flow block diagram for the ground station. As shown, image and sensor data will be sent from the Balloon/C&C Module to the Yagi antenna at the ground station, then the image and sensor data will be transferred to the Xtend modem and then to the laptop to display. We will be able to send specific commands from the laptop through both the Xtend modem and the Yagi antenna to the Balloon/C&C Module. The Balloon/C&C Module will also send video data to the video receiver on the ground station and from the video receiver the video data will be transferred to the LCD monitor to display a live stream video. The ground station will have an electrical generator to power the laptop, Xtend modem, Yagi antenna, video receiver, and the LCD monitor throughout the whole mission. Lastly, there are two external interfaces that affect the ground station operations. These two external interfaces are the user and the predicted winds and ocean currents. All of our mission results will be given to the Hawaii Space Flight Laboratory (HSFL).

2.3.2.3.5 Detailed description

[IF]

Table 23: Parts list for Ground Station

Component	Function
Inspiron 15 7000 Laptop	Ground station operations
Xtend 900 RF Transceiver	Long distance data transmission
Video transmitter	Transmission of live video
LCD Display Monitor	Display live video
Yagi Antenna	Extend transmission range
Power Generator	Power Source

Table 23 lists the parts needed to operate the BalloonSat Ground Station. The Inspiron Laptop will house COSMOS and provide a medium for user interface, as well facilitate the last step in data collection. The Xtend RF Transceiver will serve to supplement the data connection between the GS and the BCCM subsystems. The video transmitter will facilitate the transmission of the live video feed from BalloonSat to ground station, and the Display Monitor will display the video received. The connections mentioned here will both be completed through the use of Yagi Antennas to provide extra gain to the GS connection modules. The ground station will operate off of power provided by the Power Generator. These are the parts used in GS operations.

2.3.2.3.6 Subsystem Integration Plan

[BI][IF]

The system level integration plan for the ground station involves complete integration of COSMOS. For this to occur, the ground station will first become immersed in the operational abilities of COSMOS. Once further understanding of the software is obtained, the ground station will begin testing COSMOS with the relevant components throughout procurement. Upon completion of successful integration testing, COSMOS will be fully integrated with the assembled BCCM.

2.3.2.3.7 Software flowchart

[BI][IF]

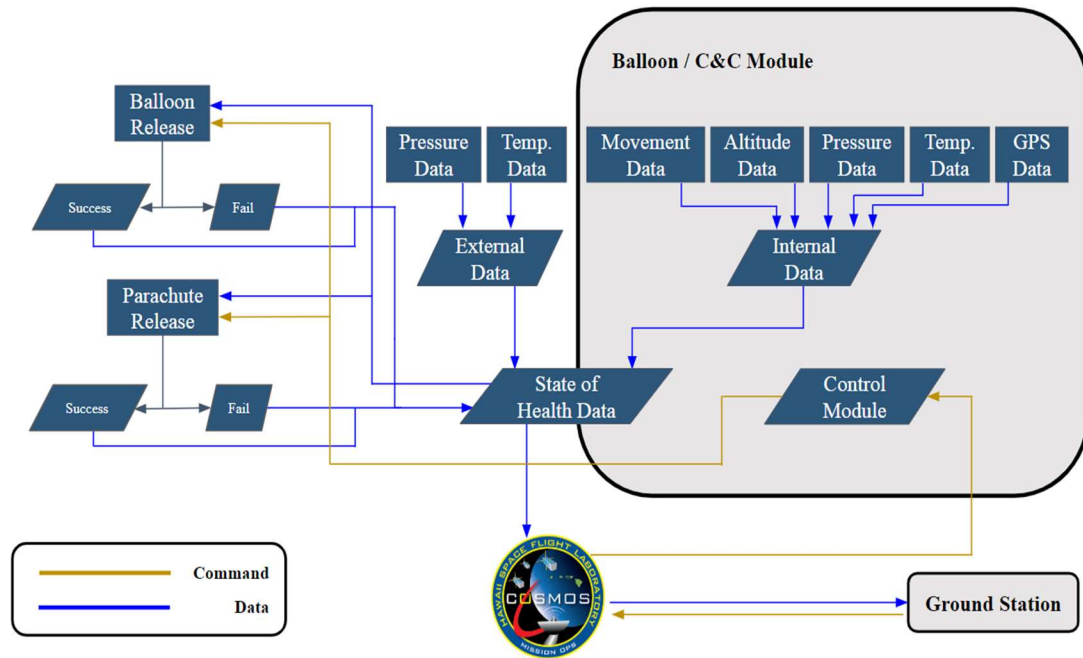


Figure 47: Ground Station Software Flowchart [17]

In the Figure above is the ground station software flow diagram. Starting with the Balloon/C&C Module, there will be movement, altitude, pressure, temperature, and GPS data. All this data will be combined, stored, and transmitted as internal data. This internal data will be relayed as state of health data to the ground station. The Balloon/C&C Module will also have external pressure and temperature data that will be relayed as state of health data to the ground station. The software flow also includes the command flow of releasing the balloon and parachute. The ground station will receive data and information regarding if the balloon and parachute release is successful or a failure.

2.3.2.3.8 COSMOS Architecture

[BI]

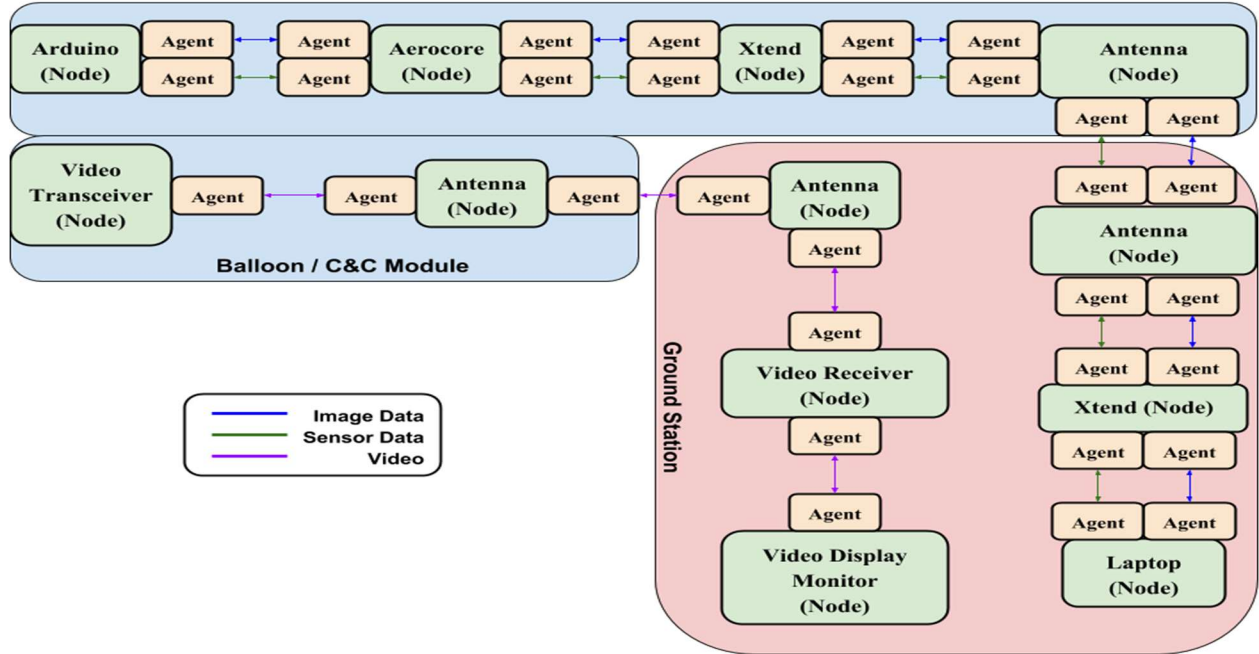


Figure 48: Ground Station COSMOS Architecture

In the Figure above is the ground station COSMOS architecture. Starting with the Balloon/C&C Module, it includes an Arduino, an Aerocore, a Xtend modem, two antennas, and a video transceiver. The ground station consists of two antennas, a video receiver, a video display, a Xtend modem, and a laptop. Each of these components is called a Node within COSMOS and we assign agents to each node. These agents allow data to be transferred between the different components within the software COSMOS.

2.3.2.3.9 Results of Analyses - Signal Reliability

[IF]

To analyze the capabilities of signals and connections used during the mission, a multitude of factors were considered. In understanding the abilities of propagating radio frequency (RF) waves, signals were first analyzed for their various characteristics. Essential characteristics of RF signals are; wavelength, frequency, bandwidth and power. Wavelength and frequency hold an inverse relationship, and increasing wavelength or decreasing frequency increases signal reception [38]. Decreasing frequency, however, results in lower bandwidth and lower rates of data transmission capabilities. With higher transmit power, greater frequency and greater distance may be achieved.

Other factors that affect RF signals are antenna selections. Antennas are usually omnidirectional or directional. Directional antennas have been selected for use in this mission as they have the most desirable characteristics. Directional antennas provide increased gain in a specific direction, and as a result greater range. This greater signal in a single direction, as opposed to the multidirectional distributed signal of omnidirectional antennas, provides a situation ideal for the BalloonSat mission. Lastly, it is important to raise the antenna to a subjective height above the ground, to ensure the most welcoming environment for signal propagation.

Taking into account the information presented above, it is possible to estimate signal capabilities in a highly ideal, theoretical situation. This calculation is possible through the use of the Friis Equation, otherwise known as Friis Transmission Formula. This equation has three basic derivations as follows:

$$P_R = \frac{P_T G_T G_R \lambda^2}{(4\pi R)^2} \quad (26) [39]$$

$$P_R = \frac{P_T G_T G_R C^2}{(4\pi R f)^2} \quad (27) [39]$$

$$P_R = (PLF) * \frac{P_T G_T G_R C^2}{(4\pi R f)^2} \quad (28) [39]$$

These equations exhibit the relationships explained above. An important thing to note about these equations is the relationship provided between power transmitted, (P_T) and power received (P_R). It is because of this relationship, provided by Friis equation, that a theoretical estimate of the mission signal reliability may be generated. This type of estimate has been generated for the Xtend and video transmission modules, to find GS receiving capabilities. Under ideal connections, connection capabilities are as follows:

Table 24: XTend 900 RF Signal Reliability Under Ideal Conditions and Ideal Gain [40,41]

Power Transmitted, P_T [mW]	Distance, R [ft]	Frequency, f [MHz]	Ideal Gain, G_T, G_R [dB, dB]	Power Received, P_R [mW]	> -110? [dBm]
1000	25,000	900	42,70	$3.563 \cdot 10^{-5}$	-44.48
1000	50,000	900	42,70	$8.907 \cdot 10^{-6}$	-50.50
1000	100,000	900	42, 70	$2.227 \cdot 10^{-6}$	-56.52

Table 25: Video Transmitter Signal Reliability Under Ideal Conditions and Ideal Gain [37]

Power Transmitted, P_T [mW]	Distance, R [ft]	Frequency, f [MHz]	Ideal Gain, G_T, G_R [dB, dB]	Power Received, P_R [mW]	> -100? [dBm]
5000	25,000	1080	2,8	$6.732 \cdot 10^{-7}$	-61.72
5000	50,000	1080	2,8	$1.683 \cdot 10^{-7}$	-67.74
5000	100,000	1080	2,8	$4.208 \cdot 10^{-8}$	-73.76

Analysis of the results in tables 24 and 25 above show that strong connections over the length of the mission are to be expected.

The last factor that affects signal propagation is any obstacle or hindrance to the signal transmission. As a signal propagates through the atmosphere, it will encounter multiple regions of varying properties. These properties are described for signals as indices of refraction. An index of refraction may be calculated using the following estimation:

$$n = 77.6 * 10^{-6} \left(\frac{P}{T}\right) - 5.6 * 10^{-6} \left(\frac{e}{T}\right) + 3.73 * 10^{-1} \left(\frac{e}{T^2}\right) + 1 \quad (29) [42]$$

Indices of refraction account for general properties of separate media, however, they do not describe a relationship for propagation between the media. This relationship is described by Snell's Law shown below.

$$n_1 \sin(\theta_1) = n_2 \sin(\theta_2) \quad (30) [42]$$

Further investigation into Snell's Law will provide further insight on the refractions that occur in signals, and provide greater estimations on signal reliability.

2.3.2.3.10 Risk Analysis

[BI]

Table 26: Risk Analysis for Ground Station

Identification	Consequence	Probability of Occurrence	Risk Rank	Risk Mitigation (Reactive, Proactive)
Failure to track the location of the BalloonSat module	5	4	High	- Ensure GPS data can be received when propulsion system is in the water and tested over various ranges.
Failure of receiving permission for a launch site	5	3	High	- Research possible launch sites in advance.
Failure to integrate COSMOS	4	5	High	- COSMOS workshops and additional assistance from HSFL mentors.
Failure to land in the ocean within five miles of Oahu	5	4	High	- Use landing predictor program.
Failure of receiving image and sensor data	3	3	Medium	- Ensure transceiver onboard C&C module can send image and sensor data over long distances.
Failure of receiving a live-stream video from the C&C module	3	3	Medium	- Ensure transceiver onboard C&C module can send a live-stream video to the Ground Station.
Receive poor video quality	2	5	Medium	- Integrate a receiver that can receive a live-stream video with good quality.

2.3.2.3.11 Results of FMECA and Reliability Analysis

[BI][IF]

Table 27: FMECA for Ground Station

Process or Link in process	List all potential failure modes	Potential effects	Severity of effects	Probability of failure-effect	Invisibility of failure	Criticality	RPN	Rank
Xtend 900 Connection	Obstruction of Signal	Weakness or loss of signal. Loss of status info and command on system.	9	9	5	1	405	1
Video Transmitter	Obstruction of Signal	Loss of, or low-quality display of live video.	5	9	5	3	225	2
Video Transmitter	Power Loss	Loss of, or low-quality display of live video.	7	5	5	3	175	3
Xtend 900 Connection	Antenna Failure	Weakness or loss of signal. Loss of status info and command on system.	9	5	3	1	135	4
Xtend 900 Connection	Power Loss	Weakness or loss of signal. Loss of status info and command on system.	9	5	3	1	135	4
Inspiron 15 7000	Software Crash	Loss of status info and command on system.	9	5	3	2	135	4
Inspiron 15 7000	Power Loss	Loss of status info and command on system.	9	3	5	2	135	4
LCD Display	Power Loss	Loss of, or low-quality display of live video.	5	3	5	3	75	5
LCD Display	Video Loss	Loss of, or low-quality display of live video.	5	1	3	3	15	6

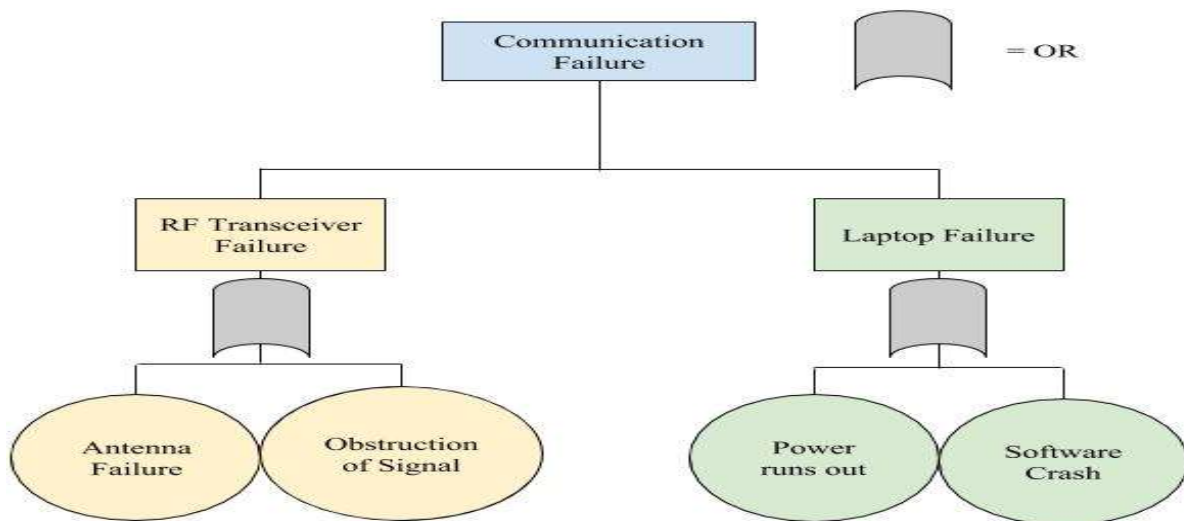


Figure 49: Ground Station Fault Tree

2.3.2.3.12 Site Selection

[BI]



Figure 50: Possible Site Selections [43]

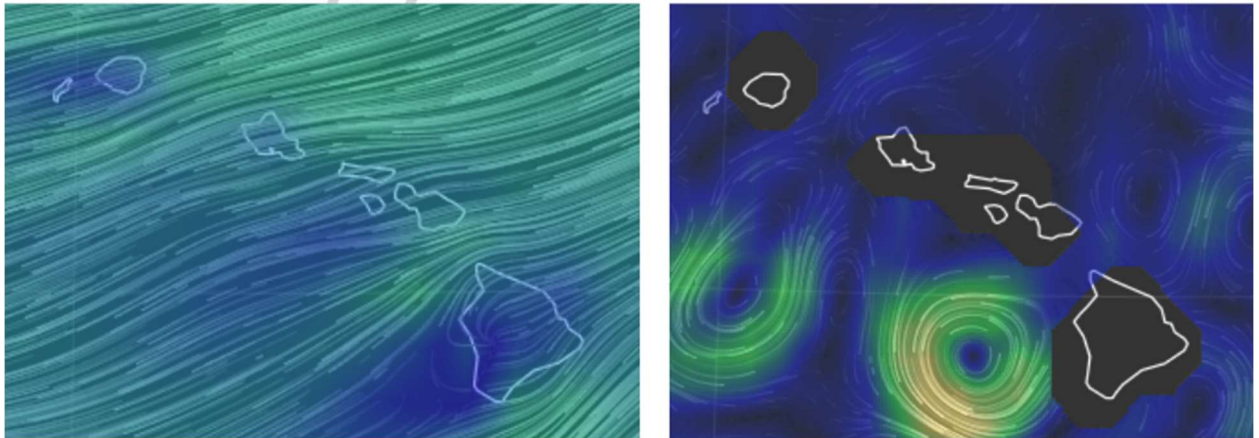


Figure 51: Possible Wind & Ocean Current Simulator [44]

In the figures above are wind patterns, ocean current patterns, and possible site selection spots. We have a possible wind and ocean current simulator that we will use as the launch date approaches. This simulator is called Earth and it has the capability to display wind and ocean currents. If the user selects a specific location on the map, the program displays the coordinates and the current speed of the wind and ocean currents. Our launch date will be in April of 2019. We have to also determine weather factors as the launch date approaches such as precipitation. It's also vital that we follow FAA & FCC regulations. Our possible site selections are, Kokololio Beach Park, Hukilau Beach Park, and Swanzy Beach Park.

2.3.2.3.13 Flight Path Estimations

[BI]

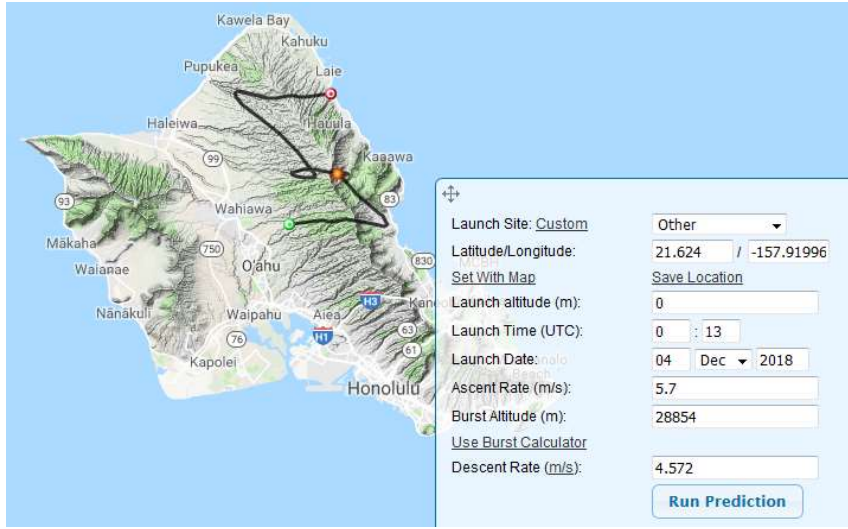


Figure 52: Flight Path Estimation for Kokololio Beach Park [44]

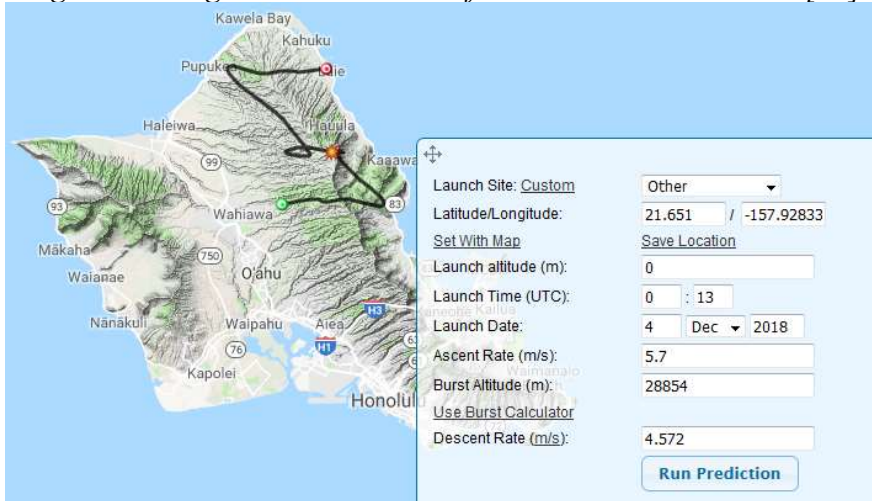


Figure 53: Flight Path Estimation for Hukilau Beach Park [43]

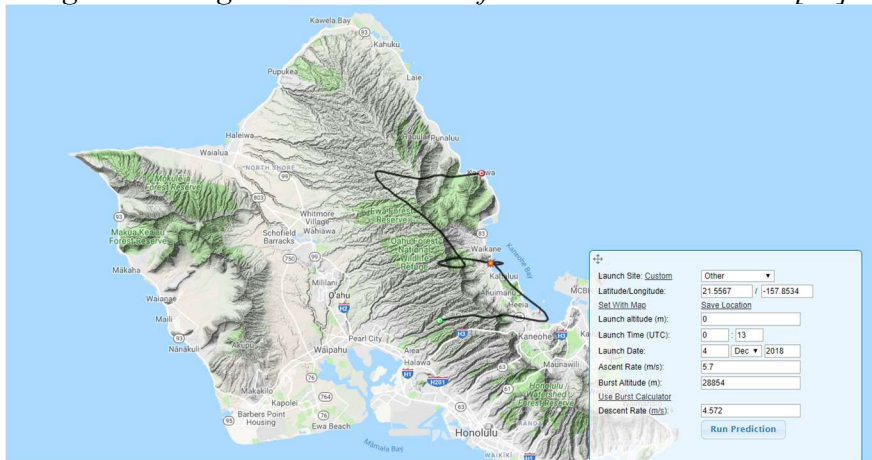


Figure 54: Flight Path Estimation for Swanzy Beach Park [43]

In the three figures above are the flight path estimations from the three possible launch sites. The program that was used is called the CUSF Landing Predictor 2.5. The program allows the user to select any location and the program displays the latitude and longitude of that specific location. The only downside with the program is that the user can select a launch date up to only 180 hours in the future. An ascent rate of 5.7 m/s, burst altitude of 28854 m, and descent rate of 4.572 m/s was used to calculate the flight paths. As shown in the three figures above, the estimated landing spots are all on land.

2.3.2.3.14 Detailed Testing Plan

[BI]

Table 28: Detailed Testing Plan for Ground Station

Component	Testing	Success Criteria
Xtend 900 RF Transceiver	<ul style="list-style-type: none"> - Test connection to antenna - Send sensor data from Arduino to computer 	<ul style="list-style-type: none"> - Receive image and sensor data
Yagi Antenna	<ul style="list-style-type: none"> - Test connection over an unobstructed distance - Determine a data rate 	<ul style="list-style-type: none"> - To determine a viable data rate
Video Transmitter	<ul style="list-style-type: none"> - Test connection over an unobstructed distance - Determine possible video quality 	<ul style="list-style-type: none"> - Receive live video feed
GPS	<ul style="list-style-type: none"> - Test connection with Xtend and determine if GPS data can be received 	<ul style="list-style-type: none"> - Receive GPS coordinates

2.3.2.3.15 Requirements vs Implementation Table

[BI][IF]

ID	Requirements	Implementation	Status
SSDR-33	Shall be able to send commands to the BalloonSat module to: release balloon at desired altitude, release parachute before ocean landing occurs, and activate autonomous recovery system.	<ul style="list-style-type: none"> Transceiver aboard the payload module and the antenna at the ground station will have constant communication and connection between each other until the end of the mission. Programmed COSMOS code to initiate an emergency release of the balloon just in case. 	
SSDR-34	Shall integrate COSMOS into both Ground Station & BalloonSat module.	<ul style="list-style-type: none"> COSMOS software will be set up on a windows laptop. 	
SSDR-35	Shall collect and report state-of-health (SOH) data of the BalloonSat module throughout the entire mission.	<ul style="list-style-type: none"> Using programmed COSMOS code to collect and report SOH data and also making sure the connection between the transceiver aboard the payload module and the antenna at the ground station will not fail. 	
SSDR-36	Shall receive images and display a live-stream video from the BalloonSat module during the flight phase.	<ul style="list-style-type: none"> Transceiver will send images and a live-stream video to the antenna at the ground station. 	
SSDR-37	Shall be able to monitor and track the location of the BalloonSat module during the recovery phase.	<ul style="list-style-type: none"> Transceiver will send coordinate data to the antenna at the ground station from the GPS on the payload module. 	
SSDR-38	Shall be able to receive sensor data from the BalloonSat module during the flight phase.	<ul style="list-style-type: none"> Transceiver will send sensor data to the antenna at the ground station. 	
SSDR-39	Shall be able to predict the flight path of the BalloonSat module.	<ul style="list-style-type: none"> Use a landing predictor program. 	

2.3.2.3.16 Subsystem WBS

[RT][IF]

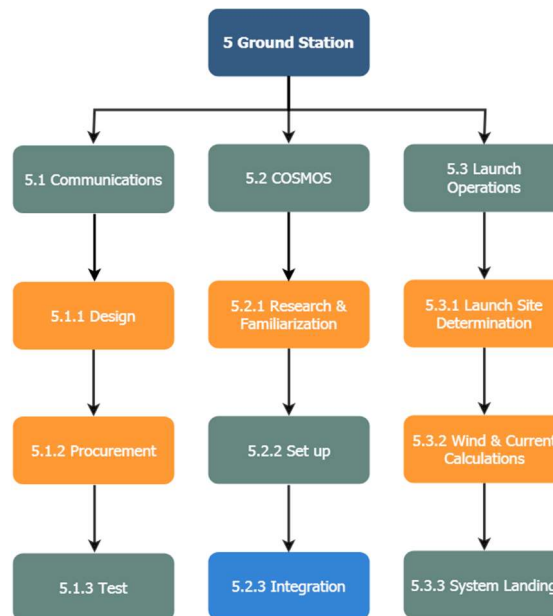


Figure 55: Ground Station WBS

Figure 55 above shows the work breakdown structure for the GS subsystem. Once all the necessary parts are procured, testing may be performed on ground station components. Set up of communications will then be complete. Progress in terms of software currently involves further familiarization with COSMOS, and further analysis into weather conditions for launch.

2.3.2.3.17 Subsystem Schedule WBS and Gantt Chart

[RT][IF]

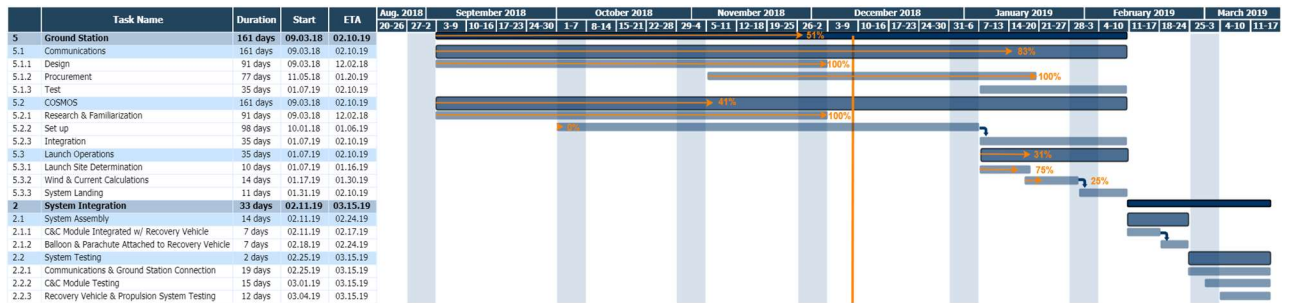


Figure 56: Gantt Chart with integrated WBS

Shown in Figure 56 is current progress within the GS operations. The main groups being worked on now are Communications and COSMOS. In terms of communications, the ground station has completed the overall design behind mission communications, and is currently waiting on attainment of parts by other subsystems to initiate the testing of individual communications systems. On the COSMOS side, the ground station has begun familiarization, but is still working on a basis for set up.

2.3.2.3.18 Remaining Issues and Concerns

[BI]

The remaining issues and concerns are seeking additional help from HSFL mentors regarding COSMOS, selecting an official launch site, conducting research for a RockBlock which is a secondary GPS, and lastly performing further analysis on signal loss.

3.0 Management and Cost Overview

3.1 Team Organizational Chart

[RT]

UHABS-6 is led by the Project Manager (PM), Jacob Keomaka, who oversees all mission objectives, requirements, and final decisions. He is responsible for team progression; communication with Dr. Sorensen and TA, Saeed Karimi; announcing and scheduling meetings; promoting a safe, productive, and enjoyable working environment; and developing and applying the project management process. Under the PM, the Project Administrator (PA), Reginald Tolentino, is responsible for the financial aspect of the project from budgeting and acquiring funding; planning system and subsystem level tasks; assisting the PM; and communicating between upper management and subsystem leads. The System Integrator (SI), Austin Quach, is responsible for facilitating communication between subsystems; integrating the subsystems; managing system testing; and meeting with the PM and PA. Under the higher-level management

team, the team is broken into three main subsystems which include the BCCM, RVP, and GS. The subsystem leads are Akira Yokoyama, Trevor Shimokusu, and Bryson Inafuku respectively and are responsible for generating and communicating tasks to the PM; assigning subsystem tasks and ensuring completion within the required time frame; scheduling subsystem meetings; and sharing updates and statuses of subsystem during general team meetings. The members of the respective subsystems are as follows: Austin Quach (BCCM), Christian Feria (RVP), Reginald Tolentino (RVP), and Ian Fujitani (GS). The responsibilities for subsystem members include completing tasks assigned by the subsystem lead and attending all subsystem and system level meetings. The team’s organizational chart can be seen below in Figure #.

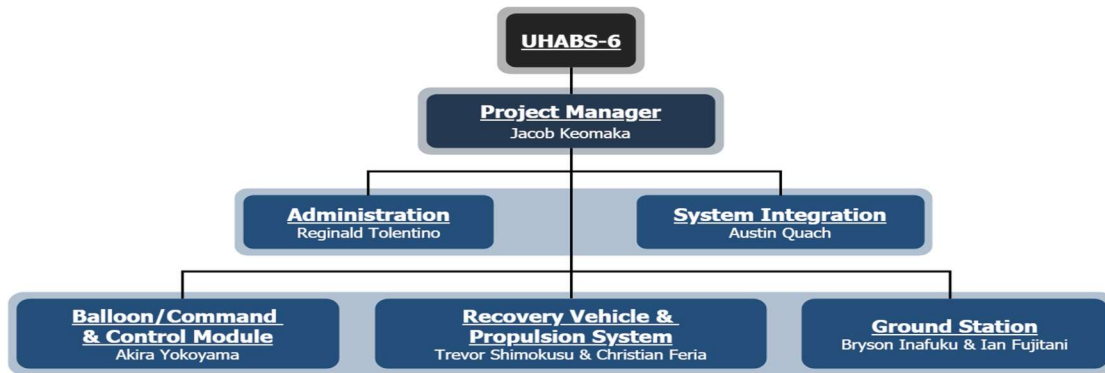


Figure 57: UHABS-6 Team Organizational Chart

3.2 Project Work Breakdown Structure

[RT]

The general Work Breakdown Structure (WBS) in Figure 58 displays the breakdown from Level 1 to Level 3. Level 2 which includes Administration, System Integration, and the three subsystems captures the system level assignments, while Level 3 overarches the tasks that will be accomplished, which were derived from Level 2. For instance, the BCCM will first undergo research, then design, procurement, fabrication and manufacturing, integration, and finally testing. However, since the UHABS-6 team is taking a Systems Engineering approach, iterations between each sequential task will be conducted in order to mitigate unforeseen problems and potential failures during the integration and testing phase. In addition, the majority of these tasks are not interdependent meaning that certain tasks are able to overlap and initiate parallel to the prior task even before it has been completed (see Figure 59). Refer to Appendix G for a more detailed WBS, which includes the Level 4 subtasks. This general WBS also illustrates the current progress of each subsystem with orange indicating completed Level 3 tasks, teal indicating in-progress Level 3 tasks, and unfilled boxes representing tasks that have not been started. These color indicators are also present on the overall system level WBS to also indicate the current progress in the Level 4 subtasks.

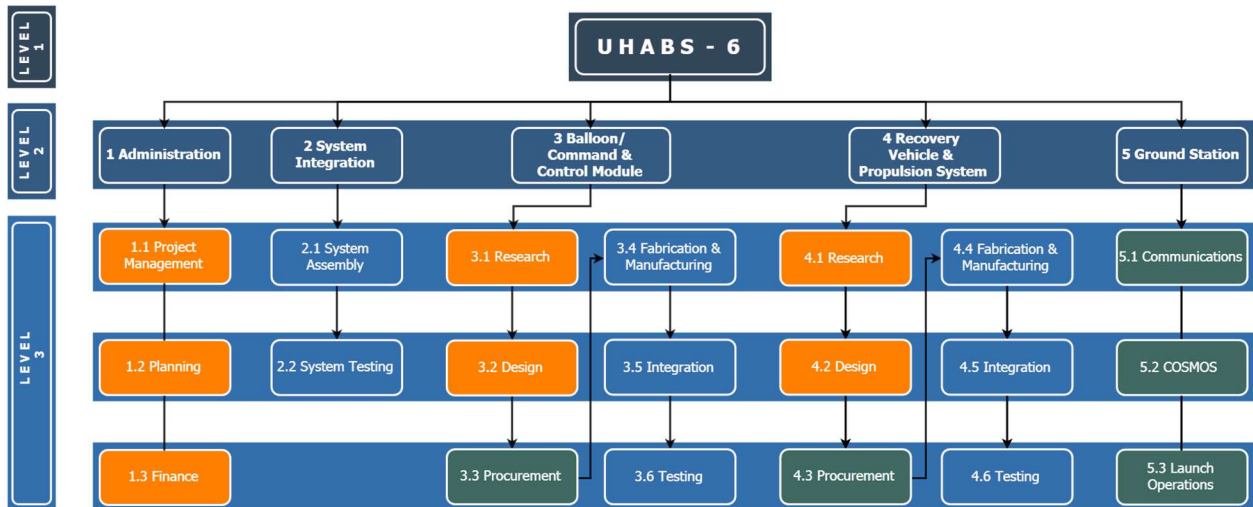


Figure 58: UHABS-6 General Work Breakdown Structure

3.3 System-level Schedule

[RT]

From the detailed WBS, the Gantt Chart in Figure 59 was generated. The UHABS-6 project started on August 20, 2018 and will have a completion date of all its tasks and operations by March 15, 2019 with a six-week buffer. From the system level, the first phase which includes the proposal, Preliminary Design Review, and Critical Design Review have been completed. With the orange line indicating the current status, the entire administration level tasks for the first phase have been accomplished with funding sources and project finances being finalized; the design phase for BCCM, RVP, and GS reaching 100% completion. The only tasks that are behind schedule are procurement for the BCCM and RVP subsystem and setup of COSMOS, which will have high priority throughout the month of December 2018 in order to remain on schedule for the second phase starting in January 2019.

Table 29: Component List Per Subsystem

BCCM Subsystem	RVP Subsystem
Pressure Sensor	Hull material 1
SD Card	Hull material 2
Aerocore	Mold Cast
Image / Video Camera	Fin material
Visual beacon	Rudder material
Audio beacon	Rudder Shaft
Servo motor	Connecting Rod
Video transmitter/receiver set	Nuts
Wireless RF Transceiver	Washers
Parachute	Stoppers
Nichrome Wire	Servo Connecting Rod
Balloon	Servo horns
Mini Arduino (FTM)	Solar panel
	MPPT Solar Charging Circuit
	11.1V Battery

3.5 Risks Management

[JK][RT]

Table 30: Project Management Risk Analysis

Identification	Consequence	Probability of Occurrence	Risk Rank	Risk Mitigation (Reactive , Proactive)
Late procurement of parts	4	4	High	-Buy emergency locally or reevaluate part selection. -Start procuring parts prior to Spring 2019.
Not meeting deadlines	4	4	High	-Host team meeting addressing issue and make adjustments. -PM host weekly team meetings to remind members of upcoming deadlines and check on statuses of each task relating to the deadline.
Lack of communication	4	2	Medium	-Team meeting addressing and correcting issue. -Top-level management meets weekly.
Significant change in design concept	4	2	Medium	-PM host meeting SE and Administration lead to make necessary adjustments. -PM ensures that the SE communicates effectively with subsystem leads.
Organization Deficiency	3	2	Low	-Top-level management meeting to address and correct issue. -Administration and PM coordinate with other and individually meet with SE and subsystem leads weekly.
Lack of funding	5	3	Low	-Apply for scholarships and reach out to aerospace companies for potential funding. -Fundraising and personal funds

3.6 Configuration and Change Management

[JK]

Table 31: Change Management Log

Subsystem	Change	Reason	Affected Subsystems	Date of Change	Approved By
RVP	Hull geometry	Improve resistance to capsizing.	BCCM	11/5/18	-Jacob Keomaka -Austin Quach
RVP	Increase mass budget to 5 lbs	Improve hull design of recovery vehicle.	BCCM	11/5/18	-Jacob Keomaka -Austin Quach
BCCM	Reduce mass budget to 1 lbs	Increase mass budget for RVP	RVP	11/5/18	-Jacob Keomaka -Austin Quach
BCCM	Add Aerocore 2 Duovero to C&C module	Integrate COSMOS into C&C module.	RVP	11/7/18	-Jacob Keomaka -Reginald Tolentino
GS	Add helium tank & electrical generator cost to Subsystem Budget	For launch preparations.	BCCM	11/26/18	-Jacob Keomaka -Reginald Tolentino
BCCM	Remove IMU & GPS from Subsystem Budgets	IMU are built into Aerocore 2 Duovero.	RVP	11/28/18	-Jacob Keomaka -Reginald Tolentino
RVP	Remove auxiliary propulsion	Proved the principle of the oscillating fin & reduce weight.	BCCM	11/28/18	-Jacob Keomaka -Austin Quach

3.7 Financial Budget

[RT]

Based off of the subsystems' major trade studies and component selections conducted in the PDR, the total financial budget with 20% margin came out to be \$2,370. With the current source of funding from UHM Mechanical Engineering Department at \$2000, the difference comes out to be \$370, which will be covered through personal funds. However, the remaining amount will only need to be covered if UHABS-6 goes over the allocated funding, since the \$2370 includes the 20% margin at \$395.00.

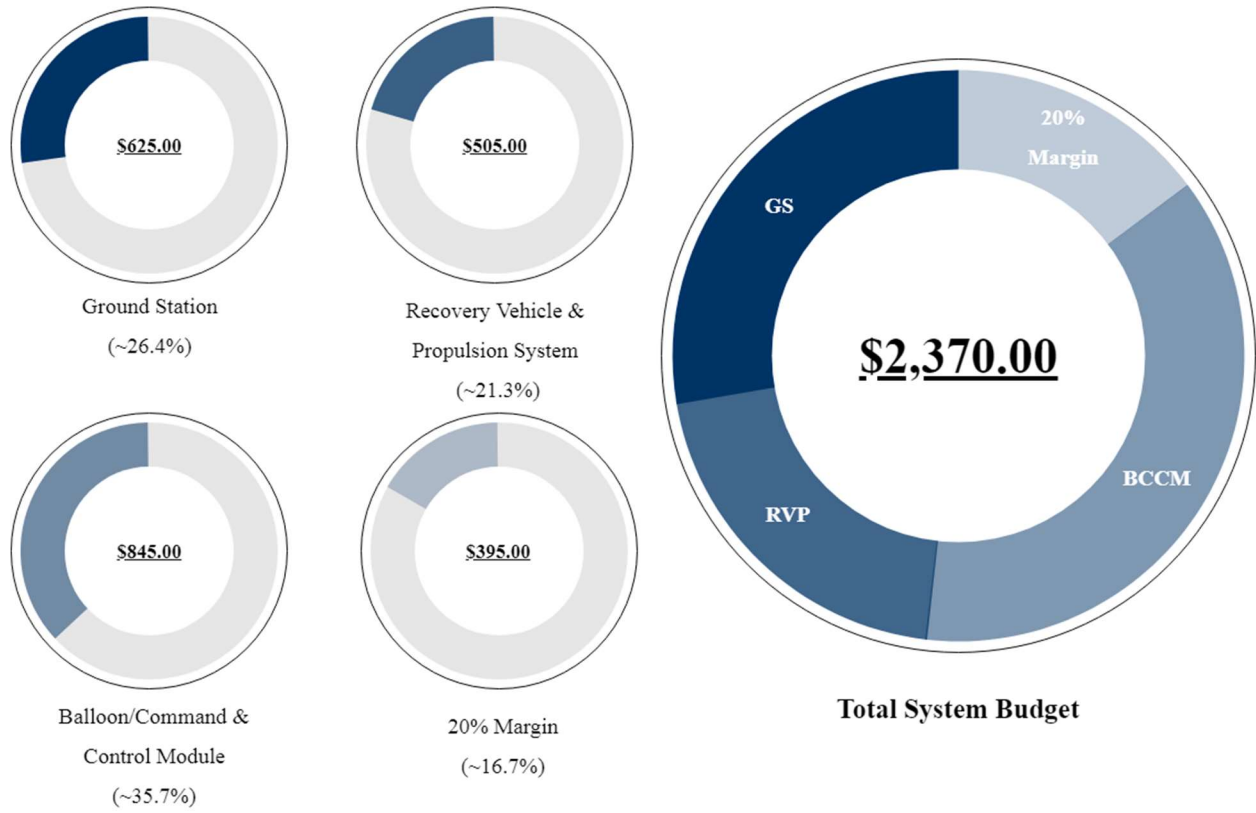


Figure 60: System Financial Budget

Table 32: Financial Summary

Total System Budget	\$2370.00
UHM Mechanical Engineering Department	- \$2000.00
Personal Funds	- \$370.00
Difference	\$0.00

3.8 Documentation List

[JK]

Documentation Title	Status
Phase A & B (Proposal to PDR)	
Project Management Plan (PMP)	
System Engineering Management Plan (SEMP)	
Configuration Management Plan	
Integrated Master Schedule	
Operations Concept Document	
Team Meeting Minutes	
Financial Spreadsheet & Tracking	
Mission Requirements Document	
System Specification Document	
PDR Package	
Phase C (PDR to CDR)	
Integration & Test Plan (ITP)	
System Acceptance Test Description	
Mission Operations Plan (MOP)	
Training Plan (TP)	
System Design Document (SDD)	
CDR Package	
Phase D (CDR to Launch)	
Operations & Procedures Document	
Flight Operations Handbook	
TRR Package	
MRR Package	

Phase E (Operations)	
Monthly Status Report	
Anomaly Report	
Phase F (Post-Mission)	
UHABS-6 Final Report	

3.9 Remaining Issues and Concerns

[JK][RT]

The UHABS-6 team needs to procure the rest of the electrical components for the C&C module, and procure the materials and hardware to begin manufacturing and assembling the recovery vehicle in January 2019. The RVP subsystem needs to get ME workshop training to use the facilities to develop the recovery vehicle.

The Project Manager, Jacob Keomaka, wants to plan more team meetings starting in January 2019 to ensure the subsystems to improve communications amongst subsystems and keep up with the project schedule.

4.0 Conclusion

[JK]

UHABS-6 has evolved and changed over the course of time from PDR to CDR. A notable change was the conceptual design of the autonomous recovery vehicle becoming more sustainable and mobile. The hull design has been changed from a flat-hull to a rounded catamaran hull to improve movement in the ocean, resistance to capsizing, and protection of the oscillating fin and rudder. The principles of the wave-powered thrust have been proven by testing a 3D prototype. Furthermore, the auxiliary propulsion (aircraft propeller and motor) was removed to reduce module weight and power consumption.

The BCCM subsystem has finalized their electrical components to meet the operational requirements during both flight and recovery phases of the mission. The BCCM subsystem team was able to determine the required high-altitude balloon and parachute size through kinematic analysis. The UHABS-6 team will use a Kaymont 1200g balloon to ascend up to 100,000 ft, and descend by a Rocketman 6 feet diameter high altitude balloon parachute to descend at a rate below 15 ft/s. The next step for the team is to finish procuring electrical components to begin assembling, programming, and testing in January 2019.

As mentioned above, the RVP subsystem have modified the hull and propulsion system to improve the overall performance of the recovery vehicle. The RVP subsystem team finalized the layout of internal and external C&C module components, and finalized hardware necessary to assemble the propulsion and steering system to the recovery vehicle. Also, the team conducted analyses on the oscillating fin, solar panels, batteries, rudder, and the hull. The kinematic analysis of the oscillating fin provides insight of how much forward thrust is produced base on wave amplitude. The energy analysis of the solar panel helps to determine the expected to time and percent charge during the sun hours of Hawaii. The battery energy analysis provides an approximation of the average battery operation time. The kinematic analysis of the hull stability proved that the hull design needs improvement to resist capsizing. The FEA analysis of the rudder, fin, and hull provides bench level approximations of how the recovery vehicle will handle landing impact. Lastly, a thermal analysis of hull proves that our avionics in the internal hull will protected from the extreme cold environment. The next step for the team is to finish procuring material and hardware to begin manufacturing, assembling, and testing in January 2019.

The Ground Station has finalized their components for their communications and identified how the COSMOS integrates and interacts with the BCCM subsystem. A RF analysis was conducted the proposed-on RF and video transmitter and receiver sets, and prove that in the perfect conditions, the Ground Station will be able to maintain communications with the BalloonSat during the entire mission. In addition, the Ground Station found programs to predict winds, ocean currents, and flight path. These programs will help to determine the balloon burst altitude and designated recovery site before launch day. The next step for the team is begin integration and programming of COSMOS in the Ground Station in January 2019 (all components already acquired).

The UHABS-6 team looks forward to January 2019. However, the team needs to communicate more effectively and stay organized if the UHABS-6 expects to launch and achieve mission success.

References

- [1] Code of Federal Regulations, 2018, “Electronic Code of Federal Regulations,” Title 14 Chapter I Subchapter F Part 101 Subpart D, Available: <https://www.ecfr.gov/cgi-bin/text-idx?SID=ce2fdebc9a188698e43b879eec03cf64&mc=true&node=sp14.2.101.d&rgn=div6> [Accessed 31 Oct. 2018].
- [2] Asada, M., Balderama, C., Culter, K., Nunes, M., and Stercho, A., 2009, “Theia 1 Payload Module Final Report,” University of Hawaii at Manoa College of Engineering, Hawaii, Honolulu.
- [3] Yoshimoto, D., De Leon, J., Domingo, J., Poon, M., Ha, A., Butay, K., Pitpit, T., Gershom, Y., Onodera, B., Alexander, Z., Rayno, M., Howard, M., Peters, K., Morrison-Fogel, D., Bisquera, C., Kim, K., Kaeo, W., Shay, E., Oshiro, C., Guyett, E., Reyes, P., and Ang, J., 2017, “UH Advanced BalloonSat System Mission #4,” University of Hawaii at Manoa College of Engineering, Hawaii, Honolulu.
- [4] Aragon, F., Geonzon, A., Hu, K., Nelson, J., and Prince, J., 2015, “BALLOONSAT PROJECT,” University of Hawaii at Manoa College of Engineering, Hawaii, Honolulu.
- [5] Aipa, L., Arine, D., Bui, A., Calaro, K., Clark, K., Liu, K., Paz, R., Tan, R., Torigoe, J., Valdez, E., Yamaguchi, J., and Yang, J., 2018, “Final Report for UHABS-5 Zeppelin,” University of Hawaii at Manoa College of Engineering, Hawaii, Honolulu.
- [6] Lee, S. J., 2014, “DEVELOPMENT OF OPTIMIZED PATH PLANNING AND AUTONOMOUS CONTROL FOR RETURN-TO-POINT VEHICLE OF HIGH-ALTITUDE BALLOONING,” Faculty of the Graduate College of the Oklahoma State University, Oklahoma.
- [7] Hu, G., Zwiebel, J., 2016, “BALLOONS,” Available: <https://stanfordssi.org/teams/balloons> [Accessed 31 Oct. 2018].
- [8] Space Hardware Club at the University of Alabama Huntsville, “BalloonSat High Altitude Balloon Payload Development,” Available: <http://space.uah.edu/BalloonSat.html> [Accessed 31 Oct. 2018].
- [9] Rainwater, S., 2012, “Platypus Cooperative Robotic Watercraft,” Available: <http://robots.net/article/3445.html> [Accessed 31 Oct. 2018].
- [10] Naval Technology, “Bluefin SandShark Micro Autonomous Underwater Vehicle,” Available: <https://www.naval-technology.com/projects/bluefin-sandshark-micro-autonomous-underwater-vehicle/> [Accessed 31 Oct. 2018].
- [11] Liquid Robotics, 2018, “How It Works”, from <https://www.liquid-robotics.com/wave-glider/how-it-works/>.
- [12] Terao, Y., Sakagami, N., 2012, “Application of Wave Devouring Propulsion System for Ocean Engineering”, Seoul, Korea.

[13] Atakins, E., 2018, “Flying Fish,” Available: <https://a2sys.engin.umich.edu/> [Accessed 31 Oct. 2018].

[14] DroneRafts, “Tech Specs WaterStrider,” Available: <https://www.dronerafts.com/tech-specs-waterstrider/> [Accessed 31 Oct. 2018].

[15] UHM College of Engineering. 2018. [image] Available: <https://www.facebook.com/University-of-Hawaii-at-Manoa-College-of-Engineering-129062940452318/> [Accessed 31 Oct. 2018].

[16] Matsunaga, E. 2011. Hawai'i Space Flight Laboratory aerospace engineer named AIAA Fellow University of Hawai'i at Mānoa. [image] Available: <https://manoa.hawaii.edu/news/article.php?afd=4637> [Accessed 31 Oct. 2018].

[17] Hawaii Space Flight Laboratory Logo. 2018. [image] Available: <https://www.hsfl.hawaii.edu/logos/> [Accessed 31 Oct-2018].

[18] Federal Aviation Administration. 2018. [image] Available: https://en.wikipedia.org/wiki/Federal_Aviation_Administration [Accessed 31 Oct. 2018].

[19] Tenergy 18650 6600mAh 11.1V Protected Lithium Ion (Li-ion) Bare Leads Battery, 2018, [image] Available: <https://www.batteryjunction.com/tenergy-111-6600-pcb.html> [Accessed 6 Dec. 2018].

[20] Medium 6V 2W Solar panel - 2.0 Watt, 2018, [image] Available: <https://www.adafruit.com/product/200> [Accessed 6 Dec. 2018].

[21] Turnigy TGY-WP23 Waterproof Metal Gear Digital Servo 23kg / 0.12sec / 24g, 2018, [image] https://hobbyking.com/en_us/turnigy-tgy-wp23-waterproof-metal-gear-digital-servo-23kg-0-12sec-75g.html [Accessed 6 Dec. 2018].

[22] AeroCore 2 for DuoVero, 2018, [image] <https://store.gumstix.com/aerocore-2-for-duovero.html> [Accessed 6 Dec. 2018].

[23] Belley, B., 2016, “Near-Space Balloon Burst Altitude Calculator - Science”, Available: <https://www.launchwithus.org/lwu-blog/2016/6/26/near-space-balloon-burst-altitude-calculator-science> [Accessed 6 Dec. 2018].

[24] Michaelson, B., 2018, “High Altitude Balloon Parachutes”, Available: <https://the-rocketman.com/recovery-html/>.

[25] Jacob's Online, 2018, “Nichrome Wire Resistance”, Available: <https://www.jacobs-online.biz/nichrome/NichromeCalc.html>

[26] “U.S. Standard Atmosphere,” The Engineering Toolbox. [Online]. Available: https://www.engineeringtoolbox.com/standard-atmosphere-d_604.html. [Accessed 6 Dec. 2018]

[27] ARDUINO MEGA 2560 REV3, 2018, [image] <https://store.Arduino.cc/usa/Arduino-mega-2560-rev3> [Accessed 6 Dec. 2018].

[28] USB / DC / Solar Lithium Ion/Polymer charger - v2, 2018, [image] <https://www.adafruit.com/product/390> [Accessed 6 Dec. 2018].

[29] XTend 900 1W RPSMA, 2018, [image] <https://www.sparkfun.com/products/retired/9411> [Accessed 6 Dec. 2018].

[30] Bergman, T. L., Lavine, A. S., Incropera, F. P., and Dewitt, D. P., 2011, *Fundamentals of Heat and Mass Transfer*, John Wiley & Sons, Danvers, MA, Appendix A.

[31] Hall, N., 2015, “National Aeronautics and Space Administration.” Available: <https://www.grc.nasa.gov/www/k-12/airplane/kiteaero.html>

[32] White, F. M., 2008, *Fluid Mechanics*, McGraw Hill, New York, NY, Chap. 7.

[33] 2018, “Airfoil Tools.” Available: <http://airfoiltools.com/polar/details?polar=xf-naca0015-il-50000>

[34] 2018, “All About Maximum Power Point Tracking (MPPT) Solar Charge Controllers,” Available: <https://www.solar-electric.com/learning-center/batteries-and-charging/mppt-solar-charge-controllers.html>.

[35] 2018, “Hawaii Sunlight Hours & Renewable Energy Information,” Available: <https://www.turbinegenerator.org/solar/hawaii/>

[36] Camecho Wireless Audio Video AV Transmitter Receiver Sender Set 16-ch 1.2Ghz 700mw (DC 12V) for CCTV Camera DVR FPV DVD, 2018, Available: https://www.amazon.com/Camecho-Wireless-Transmitter-Receiver-Sender/dp/B00MPDTUY2/ref=pd_sim_421_4?_encoding=UTF8&pd_rd_i=B00MPDTUY2&pd_rd_r=80ee76c6-db78-11e8-af33-013c6f83c3a6&pd_rd_w=aTPQ1&pd_rd_wg=FDkiU&pf_rd_i=desktop-dp-sims&pf_rd_m=ATVPDKIKX0DER&pf_rd_p=18bb0b78-4200-49b9-ac91-

f141d61a1780&pf_rd_r=M2WVN80RNSRQ5V7PRR4H&pf_rd_s=desktop-dp-sims&pf_rd_t=40701&pisc=1&refRID=M2WVN80RNSRQ5V7PRR4H [Accessed 6 Dec. 2018].

[37] Mini FPV Wireless Transmitter and Receiver 5000mW Lightweight Wireless AV Transmitter 70km from air Long Range Image Sender, 2018, Available: <https://www.aliexpress.com/item/UAV-Security-Camera-Transmitter-and-Receiver-5000mW-Lightweight-Wireless-AV-Transmission-5-8km-Long-Range-Image/32831467962.html?spm=2114.10010108.1000023.6.7cf73c86LJ2ogx> [Accessed 6 Dec. 2018].

[38] “Introduction to RF & Wireless Communications Systems,” National Instruments. [Online]. Available: <http://www.ni.com/tutorial/3541/en/> [Accessed 6 Dec. 2018].

[39] “The Friis Equation,” Antenna Theory. [Online]. Available: <http://www.antenna-theory.com/basics/friis.php> [Accessed 6 Dec. 2018].

[40] Digi XTend® 900 MHz, 2018, Available: <https://www.digi.com/products/xbee-rf-solutions/sub-1-ghz-modules/xtend-module#specifications> [Accessed 6 Dec. 2018].

[41] XTend® 900MHz RF Modems, 2018, Available: <https://www.digi.com/products/xbee-rf-solutions/boxed-rf-modems-adapters/xtend-900mhz-rf-modems#specifications> [Accessed 6 Dec. 2018].

[42] Mason, S. P., 2010, “ATMOSPHERIC EFFECTS ON RADIO FREQUENCY (RF) WAVE PROPAGATION IN A HUMID, NEAR-SURFACE ENVIRONMENT,” [Online]. Available: <https://apps.dtic.mil/dtic/tr/fulltext/u2/a518587.pdf> [Accessed 6 Dec. 2018].

[43] CUSF Landing Predictor 2.5, 2018, <http://predict.habhub.org/> [Accessed 6 Dec. 2018].

[44] Hawaii predicted ocean currents, 2018, [image] <https://earth.nullschool.net/> [Accessed 6 Dec. 2018].

Appendices

A - System Specifications Document

[JK]

Mission Statement		Priority	Status
The UHABS-6 team will successfully develop a high altitude BalloonSat system capable of carrying small payloads in a near-space environment, while flight testing the Comprehensive Solution for Mission Operations Systems (COSMOS) mission operations software, and return safely to Earth for intact recovery. A recovery system will be incorporated into the BalloonSat system that upon landing in the ocean will be programmed to autonomously propel itself to a designated recovery site for recovery		Mandatory	
ID	Primary Objectives		
OBJ-01	To develop a reliable, high-altitude BalloonSat system capable of carrying small payloads to a near-space environment.	Mandatory	
OBJ-02	To develop a recovery system which enables the BalloonSat module to safely land in the ocean or land.	Mandatory	
OBJ-03	To develop a recovery system able to autonomously propel the payload to a designated recovery site if an ocean landing occurs.	Mandatory	
OBJ-04	To utilize and test COSMOS as operation and software for the HSFL.	Mandatory	
ID	Secondary Objectives		
OBJ-05	To obtain images and video during the flight phase.	Desired	
OBJ-06	To collect atmospheric and state-of-health data during flight phase.	Desired	
ID	Top-level System requirements		
TLSR-01	BalloonSat system shall consist of a helium-filled latex weather balloon capable of carrying a payload to a near-space environment.	Mandatory	
TLSR-02	BalloonSat modules shall weigh no more than 6 lbs each, and the total combined weight of all modules to not exceed 12 lbs.	Mandatory	
TLSR-03	The BalloonSat system shall be capable of reaching an altitude up to 100,000 ft until the balloon burst or is released by command.	Mandatory	

TLRSR-04	The BalloonSat shall descend by parachute with a maximum design landing speed of 15 ft/s.	Mandatory	
TLRSR-05	During the entire flight, the BalloonSat shall take environmental and engineering measurements, images, and collect science data.	Mandatory	
TLRSR-06	Collected environmental and engineering measurements, images, and science data shall be stored on-board the BalloonSat and transmitted to Ground Station.	Desired	
TLRSR-07	The BalloonSat shall downlink telemetry of its position and speed to the Ground Station for the entire mission.	Mandatory	
TLRSR-08	The BalloonSat shall be capable of receiving uplinked commands from the Ground Station.	Mandatory	
TLRSR-09	During the flight phase, the BalloonSat shall live stream video pointed downward and is received by Ground Station.	Desired	
TLRSR-10	The team shall calculate the predicted track of the BalloonSat using prevailing winds.	Mandatory	
TLRSR-11	The team shall calculate the altitude at which the balloon should be released to ensure that the BalloonSat module lands in the ocean not more than five miles from Oahu.	Mandatory	
TLRSR-12	The BalloonSat recovery module shall be equipped with an audible and waterproof location beacon capable of functioning continuously for at least 24 hours and audible from distance of at least 100 yards in scrub.	Mandatory	
TLRSR-13	The BalloonSat recovery module shall be painted in a waterproof, highly visible color and have attached recovery contact information and an American flag that will not be affected by water or sunlight.	Mandatory	
TLRSR-14	The BalloonSat system shall incorporate a recovery system that will enable the BalloonSat module to land on the ocean, and autonomously propel itself to a designated location.	Mandatory	
TLRSR-15	If ocean landing occurs, the BalloonSat shall detach the parachute before landing in the ocean.	Mandatory	
TLRSR-16	The BalloonSat shall charge its batteries using solar cells.	Mandatory	
TLRSR-17	The BalloonSat shall remain fully functional and intact after recovery.	Mandatory	
TLRSR-18	The BalloonSat system shall utilize COSMOS software for mission operations.	Mandatory	

ID	Constraints		
TSLR-19	UHABS-6 design shall be completed by December 2018.	Mandatory	
TSLR-20	UHABS-6 shall be built, tested, launched, and recovered by April 2019.	Mandatory	
TSLR-21	UHABS-6 mission shall use and test COSMOS.	Mandatory	
TSLR-22	The following regulations from the Code of Federal Regulations (4) shall be followed: <ul style="list-style-type: none"> ● Modules cannot exceed a weight of 6 lbs ● Payload cannot exceed a weight of 12 lbs ● Avoid no-fly zones 	Mandatory	
TSLR-23	Shall notify FAA prior to launch.	Desired	
ID	Subsystem Derived Requirements	Parent ID	
SSDR-24	BalloonSat system shall be capable of releasing the balloon and/or parachute by command of BalloonSat module.	TLSR-03 TLSR-15	Mandatory
SSDR-25	BalloonSat module shall collect state-of-health data during the entire flight phase.	TLSR-05	Mandatory
SSDR-26	BalloonSat module shall collect atmospheric temperatures and pressures during the entire flight phase.	TLSR-05	Mandatory
SSDR-27	BalloonSat module shall take images pointed in the upwards, downwards, and side directions.	TLSR-05	Mandatory
SSDR-28	The BalloonSat system shall use flight termination mechanisms to release to the balloon and parachute	TLSR-03 TLSR-15	Mandatory
SSDR-29	The BalloonSat module shall activate autonomous propulsion system only if ocean landing occurs.	TLSR-14	Mandatory
SSDR-30	The location beacon shall activate when the BalloonSat module makes landfall or, if ocean landing occurs, reaches designated recovery site.	TLSR-12	Mandatory

SSDR-31	The BalloonSat module shall be capable of powering on/off (recharge state) to recharge batteries via solar cells.	TLSR-16	Mandatory	
SSDR-32	The BalloonSat module shall end all image, video, and atmospheric data collection once landfall is made.	TLSR-05	Mandatory	
SSDR-33	The autonomous navigation system shall be programmed to navigating through predesignated areas determined by predicted current and weather forecasts.	TLSR-14	Mandatory	
SSDR-34	The BalloonSat module structure/hull shall maintain the temperature of the payload within its operating limits.	TLSR-01 TLSR-03	Mandatory	
SSDR-35	The BalloonSat module structure/hull shall provide sufficient protection to internal components from impact damage.	TLSR-17	Mandatory	
SSDR-36	The BalloonSat module structure/hull shall be resistant to capsizing in the ocean.	TLSR-14 TLSR-17	Mandatory	
SSDR-37	The BalloonSat module shall utilize its location and orientation data to provide power and actuate the steering system.	TLSR-14	Mandatory	
SSDR-38	The propulsion system shall provide thrust to overcome oceanic conditions to traverse the distance between the BalloonSat module's landing position and shore.	TLSR-14	Mandatory	
SSDR-39	The BalloonSat module structure/hull shall protect electronic components from water exposure.	TLSR-14 TLSR-17	Mandatory	
SSDR-33	The Ground Station shall be able to predict the flight path of the BalloonSat module.	TLSR-10	Mandatory	
SSDR-34	The Ground Station shall collect and report state-of-health (SOH) data of the BalloonSat module throughout the entire mission.	TLSR-06	Mandatory	
SSDR-35	The Ground Station shall be able to monitor and track the location of the BalloonSat module during the recovery phase.	TLSR-07	Mandatory	
SSDR-36	COSMOS shall be integrated into both Ground Station & BalloonSat module.	TLSR-18	Mandatory	

SSDR-37	The Ground Station shall display a live-stream video from the BalloonSat module during the flight phase.	TLSR-09	Mandatory	
SSDR-38	The Ground Station shall be able to receive sensor data and images from the BalloonSat module during the flight phase.	TLSR-06	Mandatory	
SSDR-39	The Ground Station shall be able to send commands to the BalloonSat module to: release balloon at desired altitude, release parachute before ocean landing occurs, and activate autonomous recovery system.	TLSR-08	Mandatory	

B - Financial Budget

[JK]

Balloon / C&C Module		
Item	Quantity	Cost
Pressure Sensor	3	\$29.85
Temp. sensor	2	\$11.96
Arduino	1	\$38.50
SD Card	1	\$7.95
Aerocore	1	\$149.00
Image / Video Camera	3	\$77.97
Visual beacon	1	\$4.94
Audio beacon	1	\$29.95
Servo motor	1	\$40.00
RF Transceiver	We Have	
Video transmitter	1	\$259.00
Voltage sensor	We Have	
Wireless RF Transceiver	1	\$11.98
Subtotal		\$843
Parachute	1	\$55.50
Nichrome Wire	2	\$5.74
Balloon	1	\$85.00
9v Batteries	We Have	
Tether	We Have	
Mini Arduino (FTM)	3	\$25.98
Recovery Vehicle & Propulsion		
Item	Quantity	Cost
Hull material 1	1	\$56.00

Hull material 2	1	\$66.00
Mold Cast	8	\$160.00
Fin material	1	\$37.80
Rudder material	1	\$37.80
Rudder Shaft	1	\$2.73
Connecting Rod	2	\$11.36
Nuts	1	\$7.09
Washers	2	\$8.78
Stoppers	1	\$6.74
Servo Connecting Rod	1	\$4.49
Servo horns	1	\$13.50
Solar panel	2	\$58.00
MPPT Solar Charging Circuit	1	\$17.50
11.1V Battery	1	\$79.95
Subtotal		568
Ground Station		
Yagi Antenna	2	Owned
Xtend 900	We Have	
Video Transmitter	Included in BCCM	
Inspiron 15 7000 Laptop	1	Owned
LCD Display Monitor	1	Owned
Helium Tank	2	\$570
Power Generator	1	\$52
Subtotal		\$622
Total (Rounded Up)		\$1970
Total w/ 20% Margin		\$2,370
UHM Mechanical Engineering Dept.		\$2,000
UHABS-6 Personal Funding		\$370
Difference		\$0

C - Kaymont Balloon Burst Parameters

Balloon Weight (gr)	200	300	350	450	500	600	700	800	1000	1200	1500	2000	3000
Diameter at Release (cm)	117	123	125	130	133	142	146	150	157	179	185	195	212
Volume at Release (cu.m)	0.83	0.97	1.03	1.1	1.22	1.5	1.63	1.76	2.01	2.99	3.33	3.89	4.97
Gross Lift (gr)	960	1110	1185	1335	1405	1720	1870	2020	2310	3440	3830	4470	5720
Nozzle Lift (gr)	760	810	835	885	905	1120	1170	1220	1310	2240	2330	2470	2720
Payload (gr)	250	250	250	250	250	250	250	250	250	1050	1050	1050	1050
Recommended Free Lift (gr)	510	560	585	635	655	870	920	970	1060	1190	1280	1420	1670
Rate of Ascent (m/min)	320	320	320	320	320	320	320	320	320	320	320	320	320
Diameter at Burst (cm)	300	378	412	472	499	602	653	700	786	863	944	1054	1300
Volume at Burst (cu m)	14.1	28.3	36.6	55.1	65.1	114.2	145.8	179.6	254.3	336.5	440.5	613.1	1150.3
Bursting Altitude (km)	21.2	24.7	25.9	27.7	28.4	30.8	31.8	32.6	33.9	33.2	34.2	35.4	37.9

D - BCCM Reliability Analysis

Item	Reliability	MTBF (hr)
Arduino	>0.99	>8760*
Pressure Sensor	0.99	6.6 x 10 ⁷
Temp. Sensors	>0.92	>168*
Camera/Video	>0.98	>48*
Voltage Sensor	>0.92	>168*
Audio Beacon	Unknown	24 Hours*
Visual Beacon	0.99	5 x 10 ⁴ Hours
RF Transceiver	Unknown	Unknown**
Video Transmitter	Unknown	Unknown**
SD Card	Unknown	Unknown
Hand Warmers	0.78	8
Aerocore	Unknown	Unknown**
Wireless Transceiver	Unknown	Unknown**
Servo Motor	Unknown	Unknown**

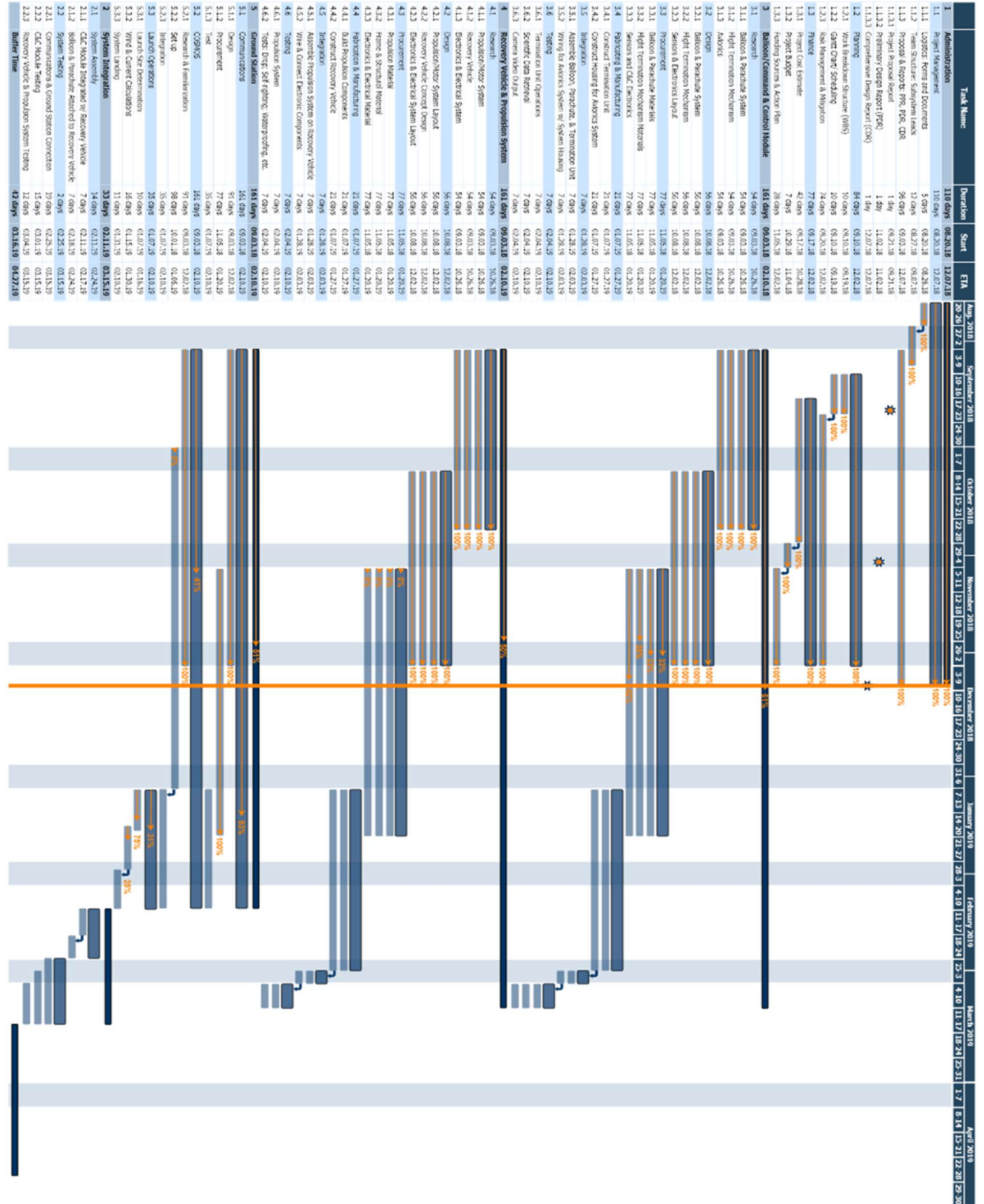
* Conservative estimate

** Still waiting on manufacture or manufacturer does not have information.

E - First Pugh Analysis of Conceptual Design UAV

Criteria	Weighting	Baseline (Airboat)	Submarine	Seaplane	Wave Power	Drone w/ Landing Pad
Lower Cost	1	0	-1	-1	-1	-1
Complexity of Code	5	0	0	0	0	-1
Power to Distance	3	0	-1	-1	1	-1
Weight	5	0	-1	-1	-1	1
Manufacturability	3	0	-1	-1	-1	-1
Time to Manufacture	5	0	-1	-1	-1	-1
Accessibility	3	0	-1	0	0	1
Travel Longevity	5	0	1	-1	1	0
Survival Impact	5	0	1	-1	0	-1
Avionic Protection	5	0	1	1	0	-1
Total:		0	-5	-22	-6	-19

F – Gantt Chart



G - WBS

